Final Report RSC-4598

DEVELOPMENT AND CHARACTERIZATION ANALYSIS OF A RADAR POLARIMETER

by

S. Bong

A. J. Blanchard

March 1984

Supported by

National Aeronautics and Space Administration
Goddard Space Flight Center
Greenbelt, Maryland 20771

Contract No. NAS 5-26686

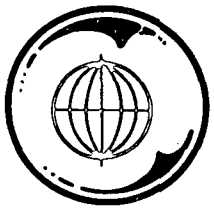

TEXAS A&M UNIVERSITY
REMOTE SENSING CENTER
COLLEGE STATION, TEXAS

Final Report RSC-4598

DEVELOPMENT AND CHARACTERIZATION ANALYSIS OF A RADAR POLARIMETER

by

S. Bong

A. J. Blanchard

March 1983

Supported by

National Aeronautics and Space Administration
Goddard Space Flight Center
Greenbelt, Maryland 20771

Contract No. NAS 5-26686

ABSTRACT

The interaction of electromagnetic waves with natural earth surface has been of interest for many years. A particular area of interest in controlled remote sensing experiments is the phenomena of depolarization. For this purpose, the Remote Sensing Center at Texas A&M University has designed an active radar system.

This report documents the development stages of the radar system. It also includes the laboratory procedures which provides some information about the specifications of the system. The radar system developed is termed the Radar Polarimeter System. The contents of this report will provide a better insight of the operation of the RPS in terms of the newly developed technique--synthetic aperture radar system. It will also provide system performance in terms of radar cross section, in terms of power, and in terms of signal to noise ratio. In summary, this report will provide a person with an overview of the RPS in terms of its operation and design as well as how it will perform in the field.

TABLE OF CONTENTS

TABLE OF CONTENTS (Continued)

TABLE OF CONTENTS (Continued)

LIST OF TABLES

LIST OF TABLES (Continued)

LIST OF FIGURES

LIST OF FIGURES (Continued)

LIST OF FIGURES (Continued)

INTRODUCTION

Controlled remote sensing experiments have been implemented for over a decade by the Remote Sensing Center of Texas A&M University. Many of these experiments are performed for scientific investigations relating to backscattered energy from natural scenes. In this regard, the Remote Sensing Center is currently developing a mobile radar system. The development of the radar system has been funded by contract with the NASA Goddard Space Flight Center.

There have been various radar systems built to investigate the physical interaction process related to electromagnetic energy backscattered from natural earth scenes [2]. Depolarization is an important phenomenon in regard to radar backscatter from natural scenes, especially as related to radar remote sensing. Depolarization measurements have not been adequately addressed in the past due to the limited capabilities of the measuring devices. With this in mind, the RSC has developed a radar system specifically to investigate depolarization phenomena. The radar design is a short pulse system with a front end similar to a synthetic aperture radar system [3]. The radar system being developed by the RSC is termed Radar Polarimeter System (RPS).

Problem Statement

The purpose of this research is to define the operational characteristics of the RPS and demonstrate its capability to make radar cross section measurements. Quantification of the measurement capability of the RPS is important since it is a short pulse, pulse compression system, while all other radar systems used to acquire backscatter measurements of a similar nature are frequency modulated continuous wave (FM-CW) systems [2], [1]. A relevant issue is to determine whether or not different system induced measurement effects exist for these two types of systems.

Approach

The RSC has developed an RPS for use in a research project at Texas A&M University. This system has been used to acquire some field measurements. The RSC is also constructing a second RPS for delivery to the NASA Goddard Space Flight Center. The duplicate RPS that will be delivered to NASA will be used for laboratory tests to verify the design criteria of the RPS. Specific measurements will be made to determine the minimum detectable signal, receiver saturation levels, power output, and system losses. Also, the internal calibration technique will be evaluated for sources of errors.

In addition to the laboratory performance evaluation, the field data acquired by the RPS that is being field tested will be evaluated. These raw data will be converted to radar cross section. An algorithm for converting the raw measurements to radar cross section will be

developed and implemented on a Digital Equipment Corporation (DEC) VAX-750 computer system. The algorithm will then be implemented in FORTRAN. The reduced data will be compared to values from theoretical calculations of the radar cross section in order to demonstrate the accuracy and validity of the RPS field measurements. Thus, the problems involved in the research may be divided into:

1. Characterization analysis of the RPS
2. Algorithm development to convert the acquired data into radar cross section
3. Verification of the acquired data by comparing it to ground truth and/or theoretical values

Scope of the Report

This report is to define the functional characteristics of the RPS and demonstrate that its operations are within the design specifications.

The second section will describe the general operation of the RPS in terms of its hardware. This section deals with background information pertaining to the RPS.

The third section will discuss the development of the radar equation and how it is applied in the operation of the RPS. Based on the modified radar equation, an algorithm to convert raw measurements to radar cross section values will be developed.

The fourth section reports on the operational analysis of the RPS. This is a laboratory procedure where the design criteria of the RPS is analyzed. System specification will then be defined in terms of the analysis result.

The fifth section concludes the report with a brief summary of the overall RPS performance as compared to design criterion and a discussion of recommendations for design improvements.

OPERATION OF RADAR SYSTEMS

Background

Radar technology that has been developed during the first half of the twentieth century, marked the greatest advance in the methods of sensing remote objects. Since it has its own well-controlled source of illumination, the radar made it possible to perform detection as far as measurement of accurate radial distance to target. Since radar systems utilize radio waves that are able to penetrate the atmosphere undisturbed, they are able to possess longer ranges and greater sensitivity than other systems operating in the visible portion of the electromagnetic spectrum.

Detection is a process by which the target is sensed in the presence of undesired noise occurring from the background radiation, other echoes, or noise that are generated in the radar system. A typical radar system-to-target geometry is presented in Figure 1. The target is sensed by the radar signal originally from the transmitter which then is reflected by the target. The transmitter is usually connected to transmit radar signals via an antenna. The antenna illuminates electromagnetic energy in the form of the solid angle ψ as indicated in Figure 1. The target at some distance which is commonly called the range, intercepts a fraction of the originally transmitted energy and scatters it in different directions. Some of the scattered energy is captured by the receiving antenna in the radar system.

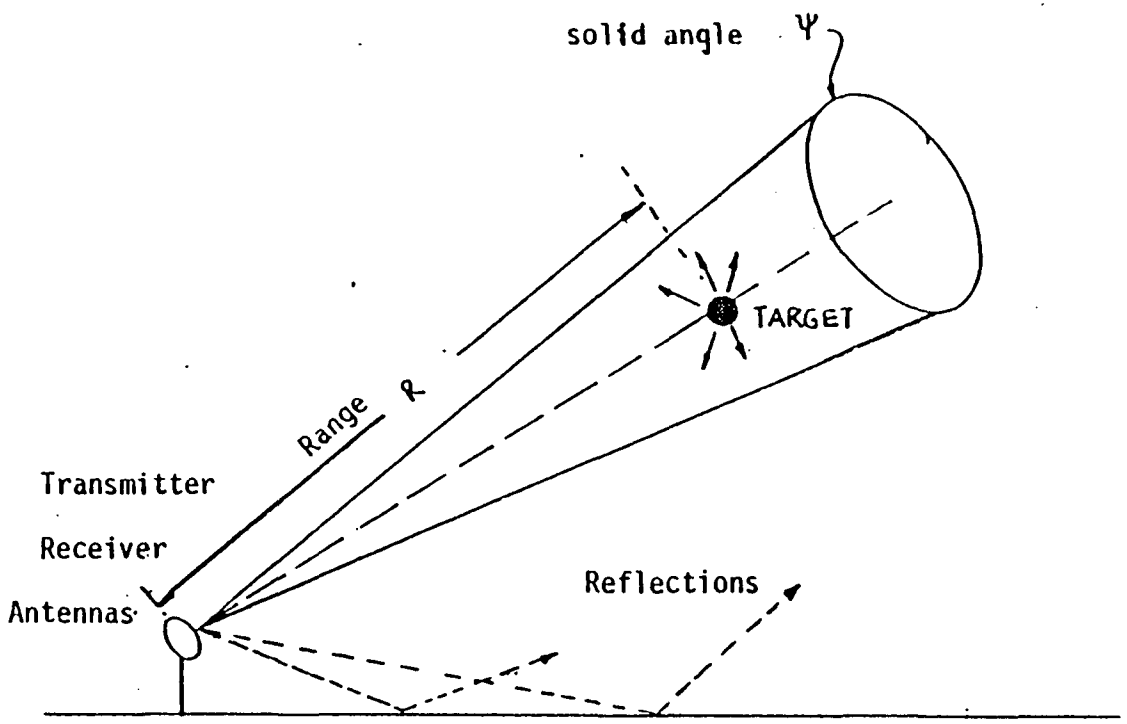

Figure 1- The Typical Radar-to-Target Geometry

Through some signal processing, the received signal is processed such that a human eye could actually see that there is a target present. This is usually presented in terms of a display scheme showing that the there is a target.

The received signal, often referred to as the returned signal, from a point-source target [16] will be an exact reproduction of the transmitted signal shifted in time by an amount which corresponds to the range delay. Range delay in frequency domain is termed as the "Doppler shift" [1]. The method of operation in this manner is classified as a Frequency Modulated Continuous Wave (FMCW) radar system. If the radar system transmits a train of reactangular pulses modulating a sinusoidal carrier, the returned signal will appear as a train of pulses which is delayed. The latter radar system is termed as a pulsed radar system. For a given observation, the total returned energy by all pulses may be used as a measure of detectability and sensitivity of the system.

Frequency Modulated Continuous Wave Radar System

The operational block diagram of a FMCW radar system is presented in Figure 2a. Figure 2b illustrates the operation of an FMCW Radar System. The RF frequency is modulated over a bandwidth Δf at a rate of fm. For a point target, the time domain response of a transreceiver is illustrated in Figure 2b. The IF frequency is constant except at the crossover points of the triangular modulation.

In conjunction with remote sensing experiments, the University of Kansas at Lawrence has built an FMCW radar system which is in operation

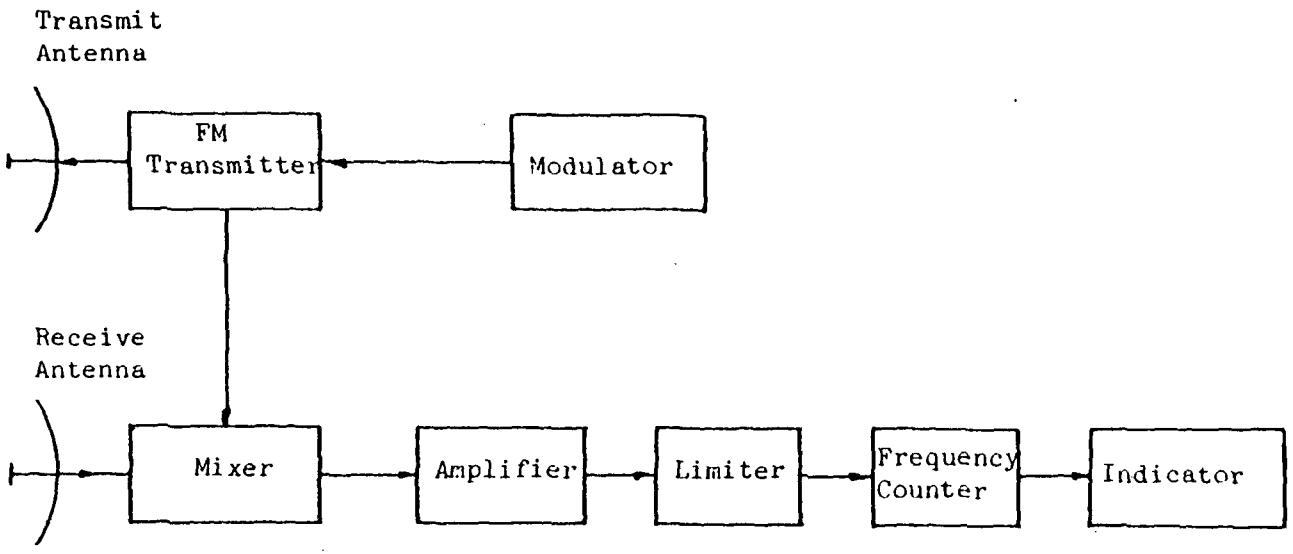

Figure 2a- Block Diagram of Frequency Modulated Continuous Wave Radar System

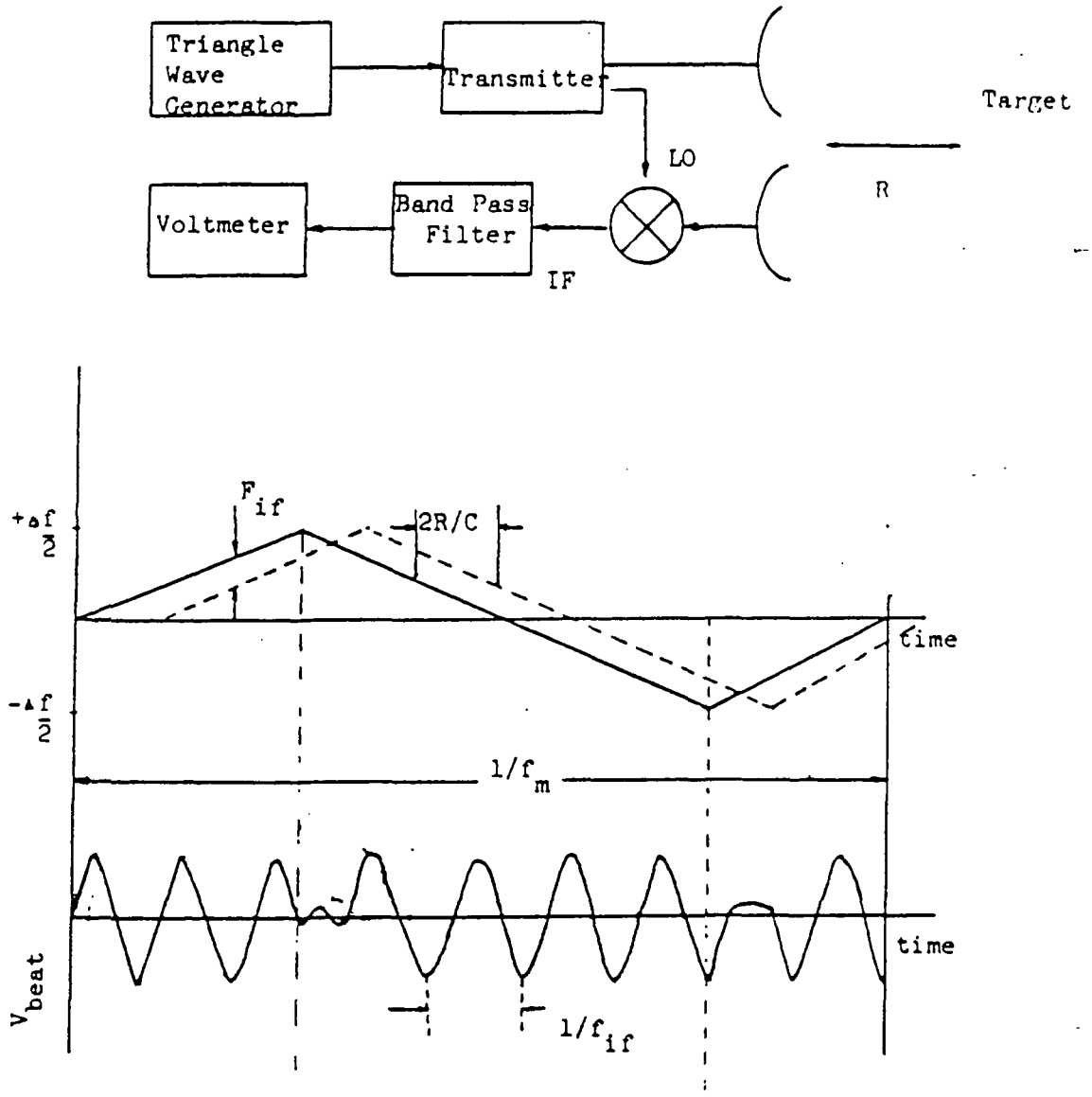

Figure 2b-Simplified Frequency Modulated-Continuous Wave Radar System

at the present time. Refer to [2] for further operational characteristics of an FMCW radar system.

Pulse Radar System

The operation of a typical pulse radar system may be described by the block diagram shown in Figure 3a. Its operation is governed by a timing circuitry that keeps the system in synchronization. Trigger pulses are sent from the synchronization circuitry to the modulator which generates high-power pulses of appropriate shape and width. These pulsed signals are used to modulate a radio frequency (RF) oscillator or amplifier in the transmitter. The duplexer in the Figure 3a serves the purpose of protecting the receiver from the high power of the transmitter. It is also a channel to route the received signal to the receiver section. The mixer takes the returned pulse, and then mixes it with a local oscillator. This process produces signal in the Intermediate Frequency (IF) which is then amplified properly to a level for detection. The detected signal is then amplified further in a video amplifier to a level required to drive a cathode-ray-tube (CRT) display. Signal representation of a typical pulse radar system is presented in Figure 3b. The operation is triggered by the periodic transmitter trigger pulse that comes from the synchronizer. This then causes the modulator to produce a rectangular pulse. The rectangular pulse is converted into a more rounded shape as it is transmitted because of the finite bandwidth of the transmitter circuitry [16]. The returned pulse as shown in Figure 3b is the type that would be observed from a ground target. The first part of the received pulse comes from

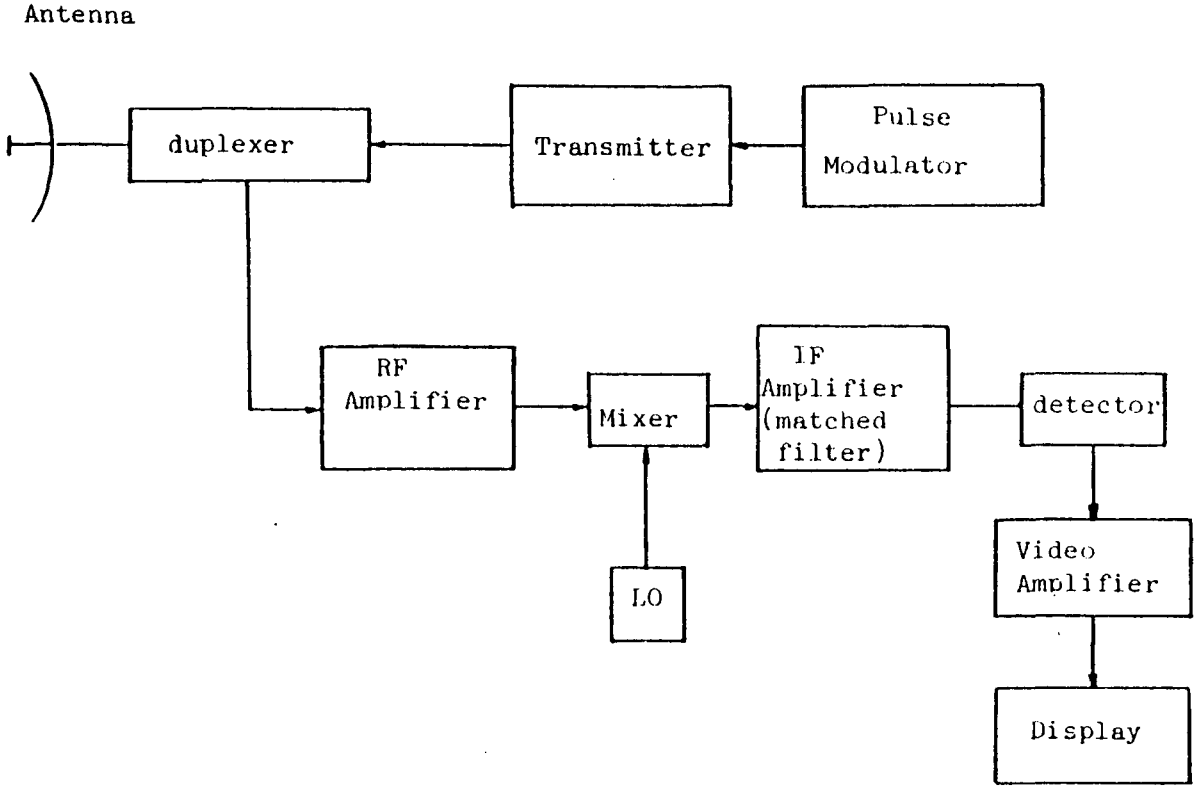

Figure 3a-Block diagram of a pulse radar system

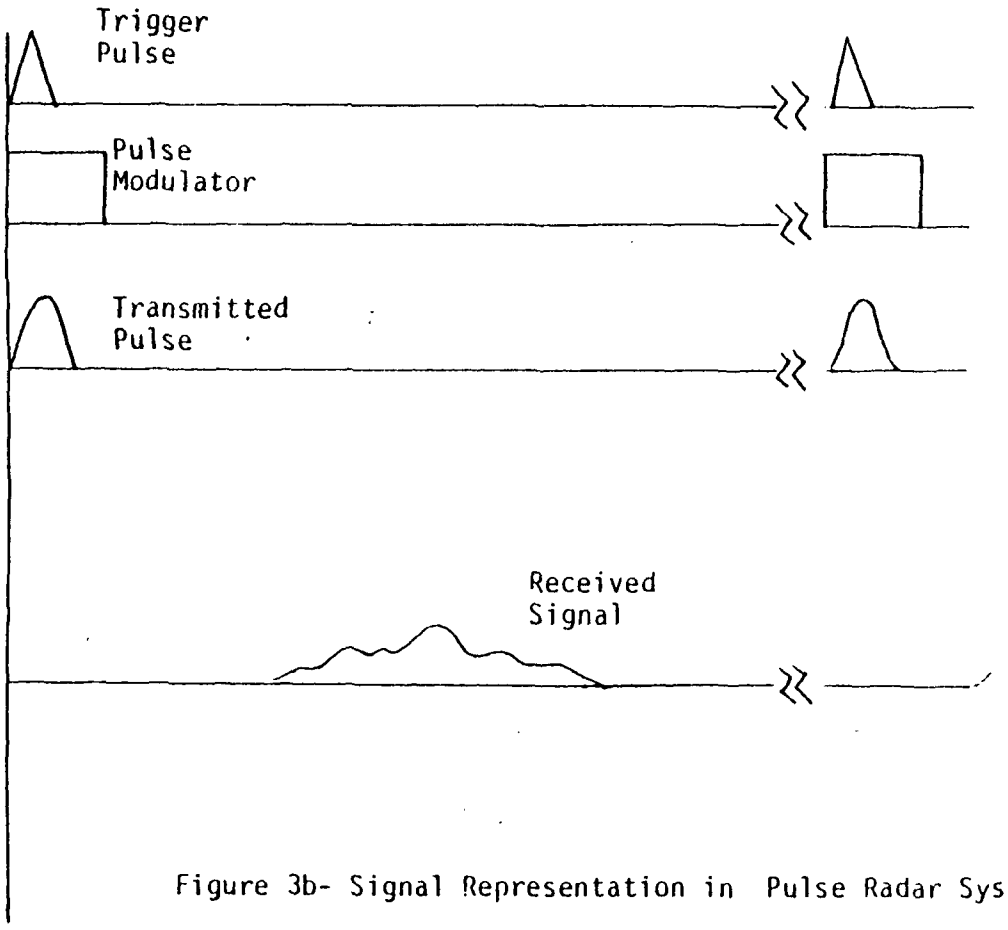

Figure 3b- Signal Representation in Pulse Radar System

the nearest section of the target as it is being illuminated by the transmitter antenna. The remaining part of the received pulses is due to the farthest point that is still being illuminated by the antenna or from a distance such that the signal is no longer strong enough to be detected.

Thus, pulse radar operates by transmitting a waveform consisting of a train of narrow pulses modulating a sinewave carrier. The modulation is 100 percent; that is, the amplitude goes down to zero between pulses, which is accomplished by turning the transmitter off between pulses and on for the pulse. An approach to pulse compression technique was through linear modulation of the frequency during the pulse, described as "chirp" by analogy to the audio transmission of the cricket. Chirp radar systems are used when the length of the pulse required for a pulse radar is so short that the pulse must have a very high peak power for the term Pr in the radar equation (3-1) to exceed the noise by the required amount. It is often an inconvenience to generate a high peak power. Thus, a method has been devised which permits the same energy in the pulse with a lower peak power. This method involves a longer pulse with a modulation interior to the pulse, allowing the fine resolution associated with the wider bandwidths of the modulation. The general principle of the FM pulse radar is described in figure 4. The instantaneous frequency of the pulse received from a point target and the effect of "de-chirping" such a pulse by passing it through a filter whose time delay is a function of frequency is illustrated in Figure 5. The filter should have a time delay such that the frequency transmitted first is delayed long enough that it arrives at the output of the filter at the same time as the

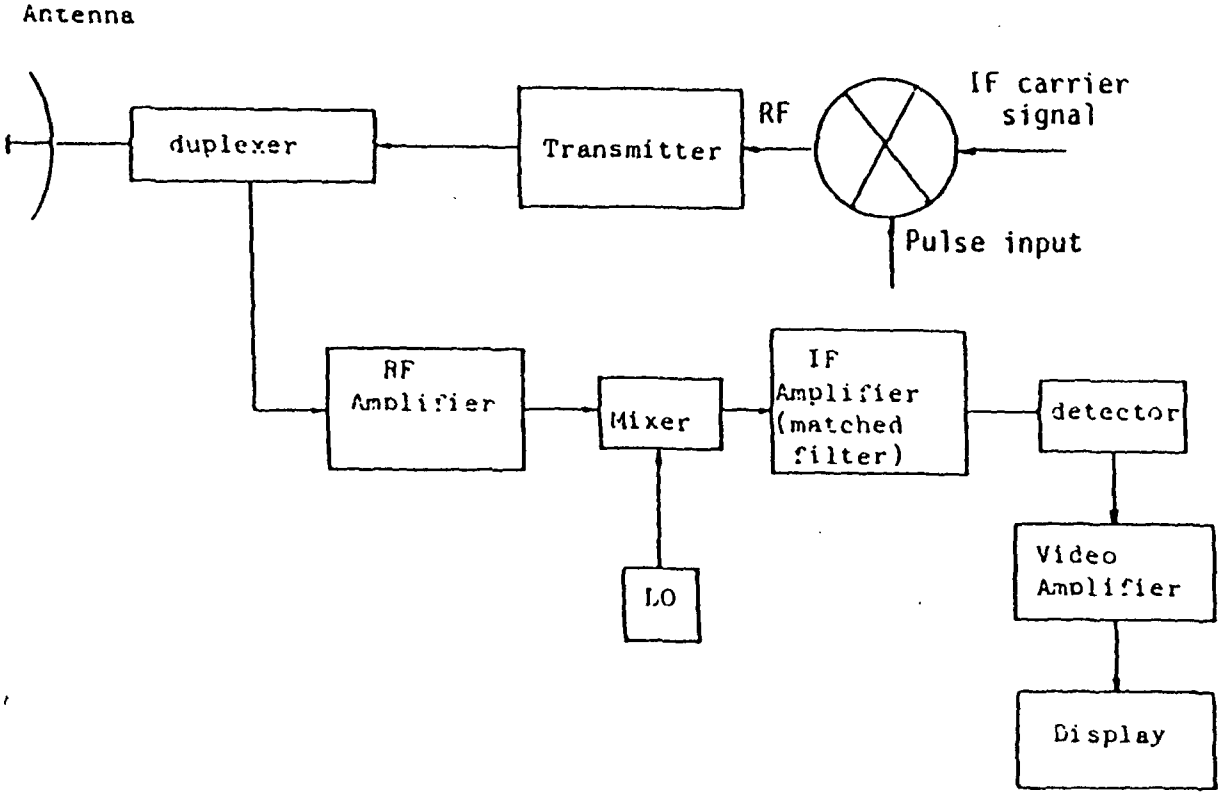

Figure 4- FM Pulse Radar System

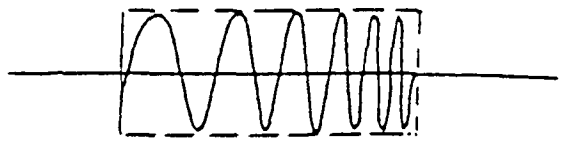

Figure 5a- The Transmitted Waveform in FM Pulse Radar

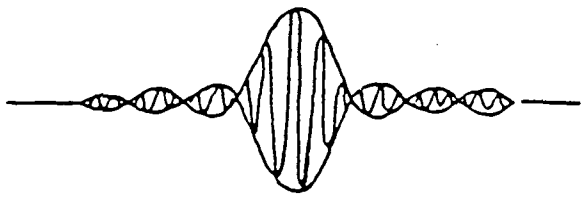

Figure 5b- The Received "de-chirped" Waveform

signal transmitted last. Figure 5 shows the waveforms for the point-target response of the chirp radar. The transmitted waveform shown in part (a) is modulated in frequency from a low frequency to a high frequency. The inverse, the "de-chirped" version, is shown in part (b) where a shape of (sin x)/x appears. A way to implement the chirp radar is to utilize a frequency-modulated pulse for transmitting and a frequency-selective delay line in the receiver. However, a single filter may be used for both generating the chirp pulse and dechirping it, thereby assuring that the filter properly matches the waveform. From an analysis of an FM chirp radar [16], it has been shown that the resolution obtained with the chirp pulse is the same as that obtainable with an FM system of the same bandwidth.

Overview of the Radar Polarimeter System

The Remote Sensing Center (RSC) at Texas A&M University is currently developing and testing a mobile radar system. One of the design criteria is that the radar system might be able to be used in controlled remote sensing experiments to investigate the depolarization phenomena [13] in the physical interaction process related to electromagnetic energy backscattered from natural earth scenes [14]. The radar system being developed and tested by the RSC is termed Radar Polarimeter System (RPS). Since range is of important criteria, the design of the RPS utilizes a short pulse system that will yield a good system resolution. The RPS in general is a short pulse radar system similar to the description of the chirp radar systems discussed previously. Pulse compression technique is implemented in the design

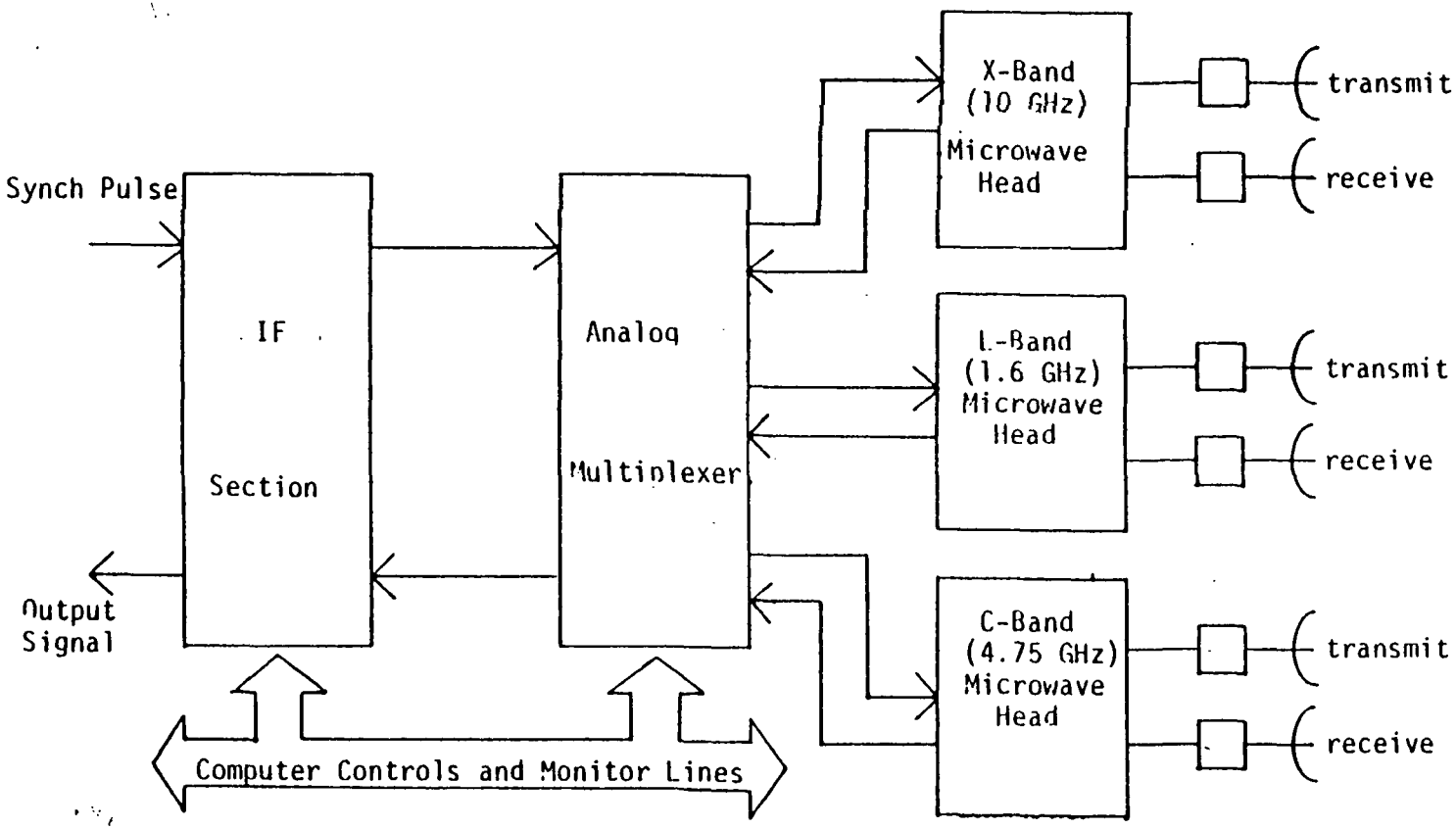

Figure 6- The Block Diagram of the RPS

of matched filtering the waveforms in the system. The block diagram of the RPS is presented in Figure 6. Physically, the RPS is a multi-frequency, multi-polarization scatterometer operating at X-Band (10 GHz), C-Band (4.75 GHz), and L-Band (1.6 GHz). It was designed to match the system parameters (bandwidths, pulse compression techniques) of a conventional airborne and spaceborne imaging radar system. It is a multipolarization system in that it can operate in horizontal, vertical or any combination of the two. Since depolarization is of interest, the RPS is equipped with two antenna for each frequency of operation, one for the transmitter, and another for the receiver. This will allow the RPS to transmit in one polarization while receiving in a different polarization.

In the recent past, different FMCW radar systems have been built to be used in controlled remote sensing experiments [2]. The RPS was designed to have operational parameters similar to FMCW radar systems. However, it is unique in its operation. It is different in that the RPS is a short pulse radar using pulse compression techniques on transmit and receive, and is a digitally controlled attenuator to measure the returned energy. The receiver is designed optimmaly utilizing the concept of matched filtering. The concept of pulse compression technique and match filtering is presented in Appendix A. Pulse compression is implemented in the design of the RPS mainly because it is an inconvenience to generate a very high peak power that is required when the length of the pulse required in the system is very short. The high peak power is required such that it exceeds the noise surrounding the environment. In principle, the pulse may be widened to approach a

modulated continuous-wave (cw) type of transmission. The advantage of pulse-compression technique is that it combines the merits of wide-bandwidth phase or frequency modulation with the isolation of pulsed systems.

Configuration of the RPS

The RPS is a mobile radar system to be used in controlled remote sensing experiments. It is mobile in the sense that the system may be moved about from one location (field) to another. The physical configuration of the RPS can be divided into 4 assemblies. They are :

a. The truck system specification

b. The radar head assemblies

c. The Intermediate-Frequency (IF) section

d. The computer and its peripherals

The Truck System Specification

The RPS contains sub-systems such as the radar head assembly, IF section, and a computer. These subsystems are housed in individual weather sealed aluminum boxes which are placed on a truss assembly along with the antennas. The picture in Figure 7 shows the components being placed on the truss. The truss is then mounted on top of a boom truck which is hydraulically operated. The boom truck also generates its own Alternating Current (AC) supply such that the RPS may be operated in remote areas. It is capable of an elevation height up to 55 feet, and azimuth rotation of 360 degrees. Refer to the diagram shown in Figures 8 and 9. The elevation mechanism is also capable of

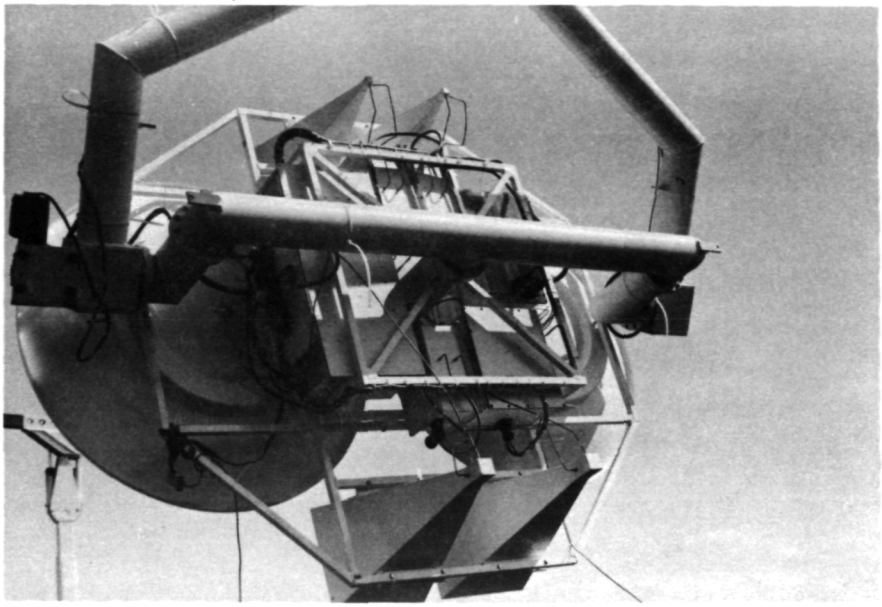

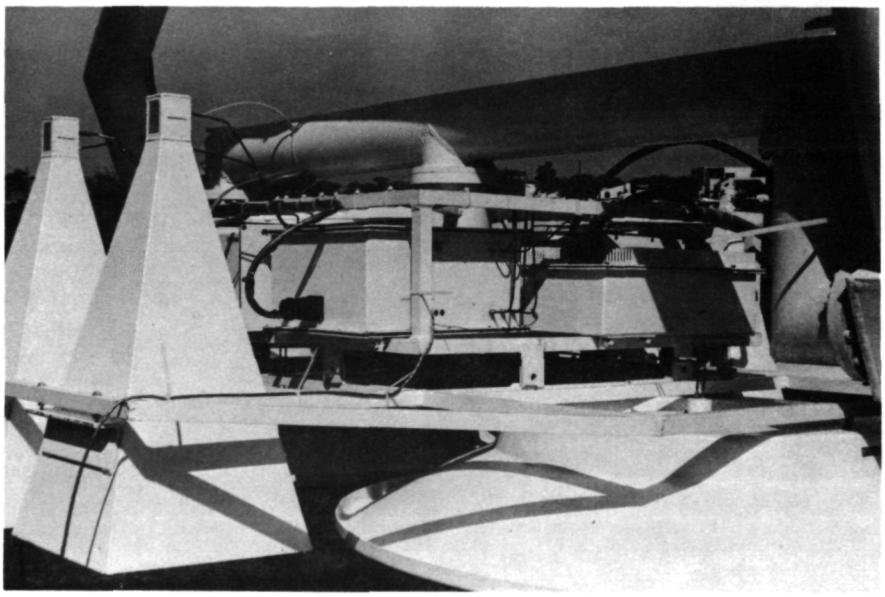

Figure 7 - The Truss Showing the Components of the RPS

rotation from nadir to 270 degrees. As mentioned earlier, the radar transmitter is connected to an antenna which illuminates the solid angle often is defined in terms of azimuth and elevation angle. The RPS is equipped with the proper mechanism to provide the different azimuth and elevation angles required to acquire data pertaining to the cross section of the target. The computer that is attached on top of the boom truck serves the purpose of initializing the RPS prior to acquiring data. A separate truck data van, houses another computer along with its peripherals for display and storage purposes. This computer is utilized to send the operation parameters such as polarization choice, choice of frequency of operation, sweep rate, and others to the computer on the truss. The computer in the data van is operator oriented as far as the function of the RPS is concerned. Both computers are connected together via an RS-232 communication link.

The Radar Head Assembly

The RF head sub-assembly of the RPS consists of components shown in the block diagram of Figure 10. The microwave source that is used in each radar head corresponds to the frequency operation of the particular radar head. The RF head sub-assembly serves the purpose of generating signals that have been properly processed such that the input and output of the sub-assembly is readily interfaced to the IF section. Besides the IF input and output lines, the RF head has two other sets of input and output lines which are the transmit and receive port at their respective polarization. The IF input and output signal definition may be described in the following fashion. An input to the

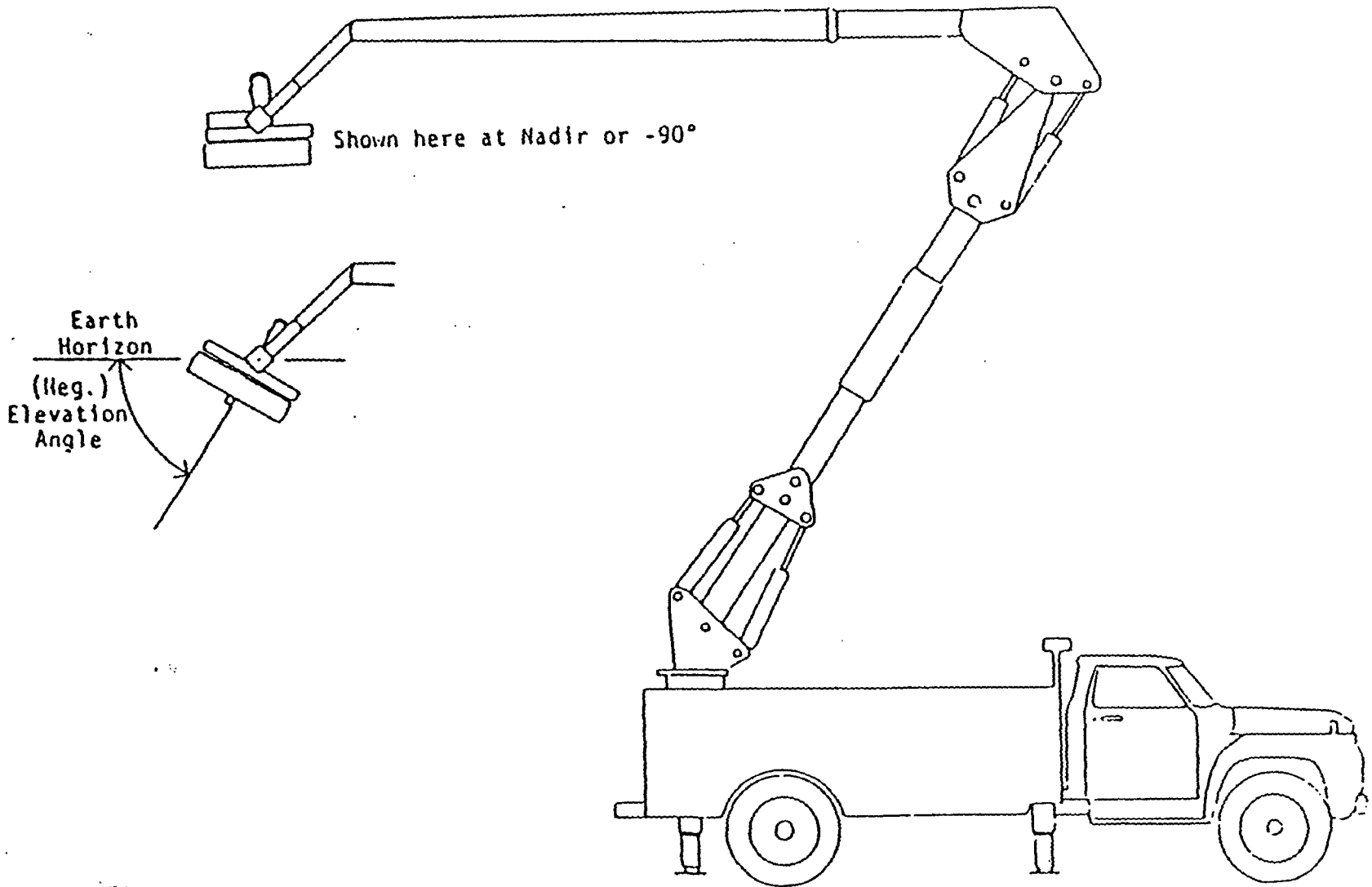

Figure 8- Side View of the Radar Boom Truck Showing the Elevation Angle of the Polarimeter Head

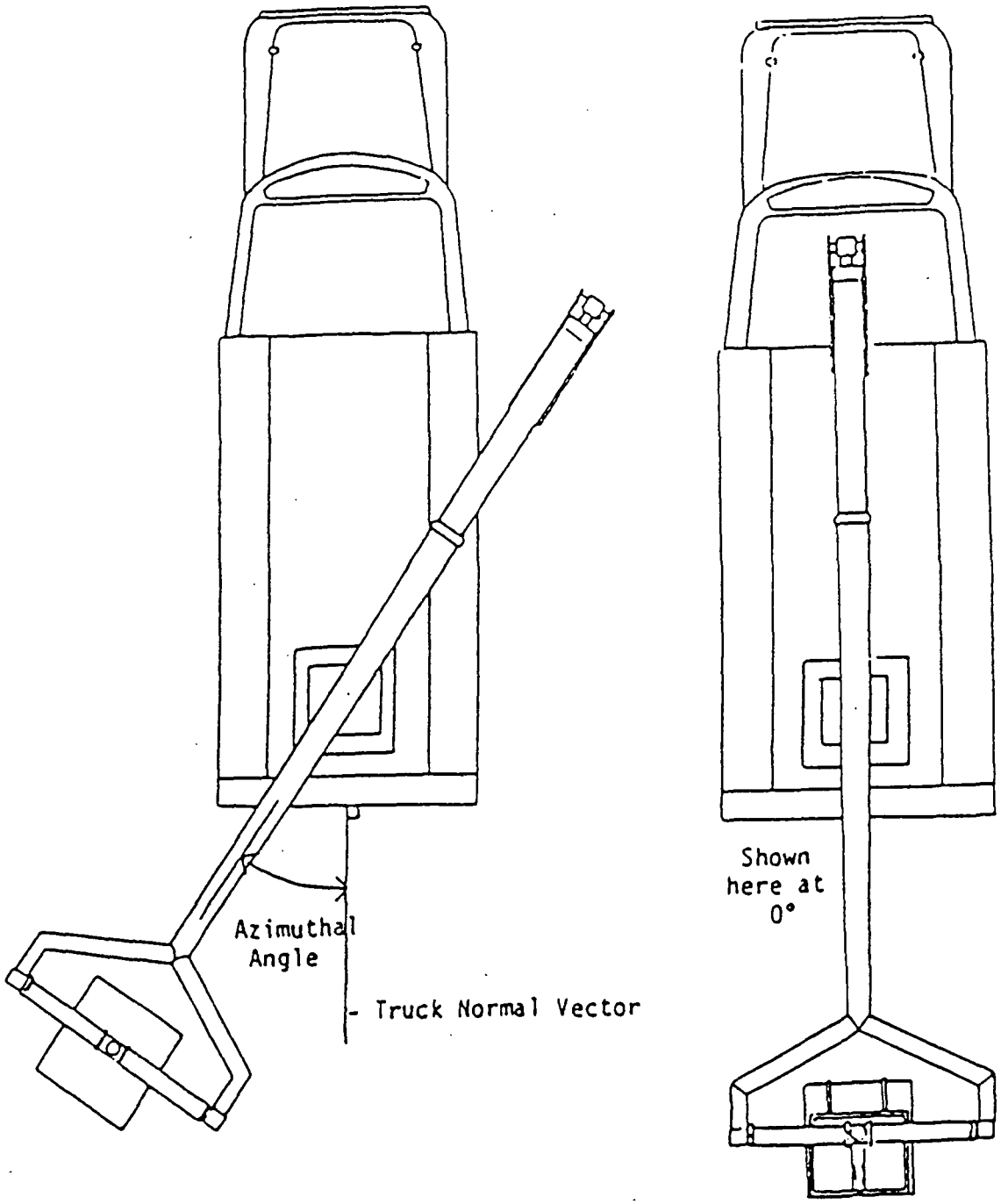

Figure 9- Top View of the Radar Boom Truck Showing the Azimuthal Angle of the Boom

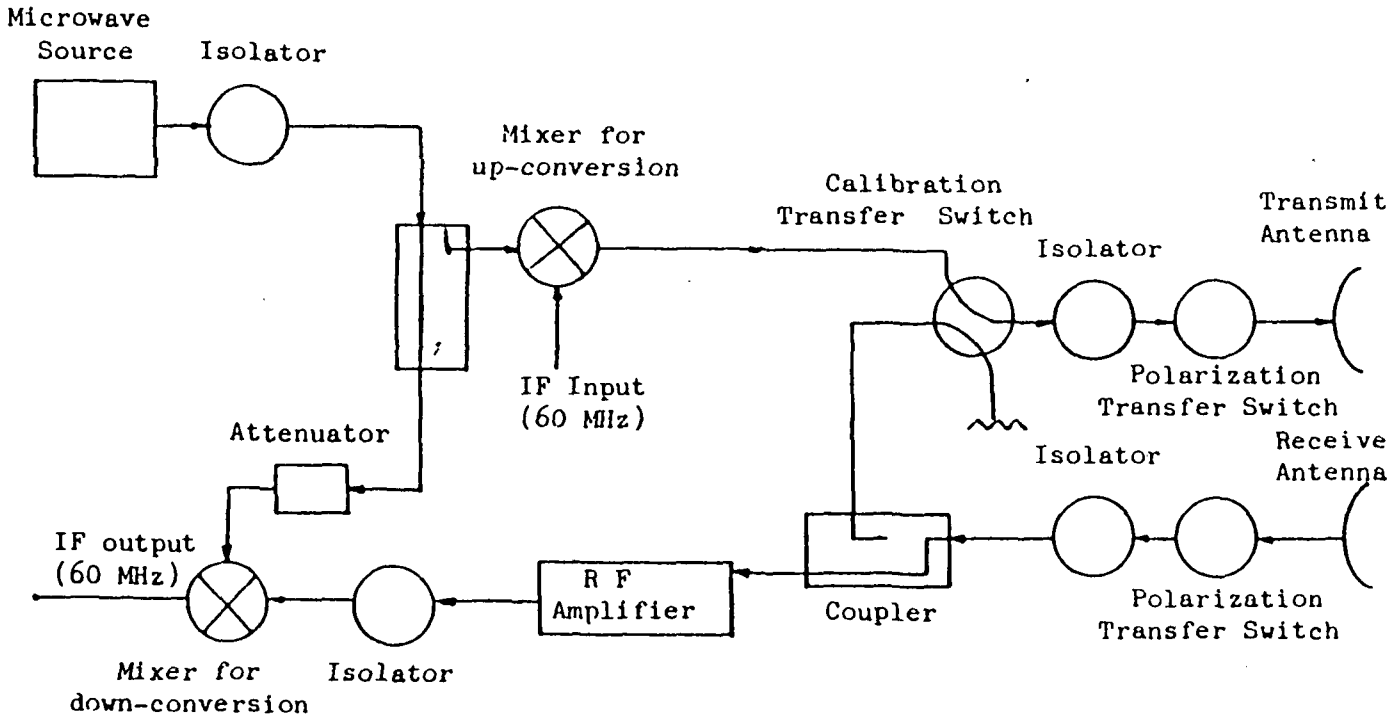

Figure 10. The Block Diagram of the RF Head Assembly.

radar head is an IF signal from the IF section. This signal is the pulses on the order of 50 nano-seconds mixed with a sine wave carrier at 60 MHz. The characteristics of the input signal are presented in Figure 11. When transmitting, this IF signal will be up-converted to the frequency of operation by the use of a mixer as depicted in Figure 12. After passing through the mixer, this signal is then ready for transmission. An output from the radar head is also an IF signal. The received signal reflected from a target is amplified and isolated properly. It is then mixed with a portion of the source at a lower power level. The output of the mixer is IF signal. The procedure of down-converting the received signal is the reverse procedure as the up-conversion described above. This signal is then sent to the IF section for further processing.

The energy reflected from a target which is captured by the receiver is referenced to the power output of the microwave source. A calibration procedure is performed at a fixed interval such that point of reference may be known at all times. The block diagram of Figure 13 presents the components in the RF head that will pass all the signals when set to the calibration mode. A portion of the signal from the microwave source is sent back to the IF section through a coupler. More detail on the calibration procedure as well as its induced error will be discussed in the next section.

The IF Section

One of the sub-systems in the Radar Polarimeter System is the Intermediate Frequency (IF) section. The IF range is more popular for

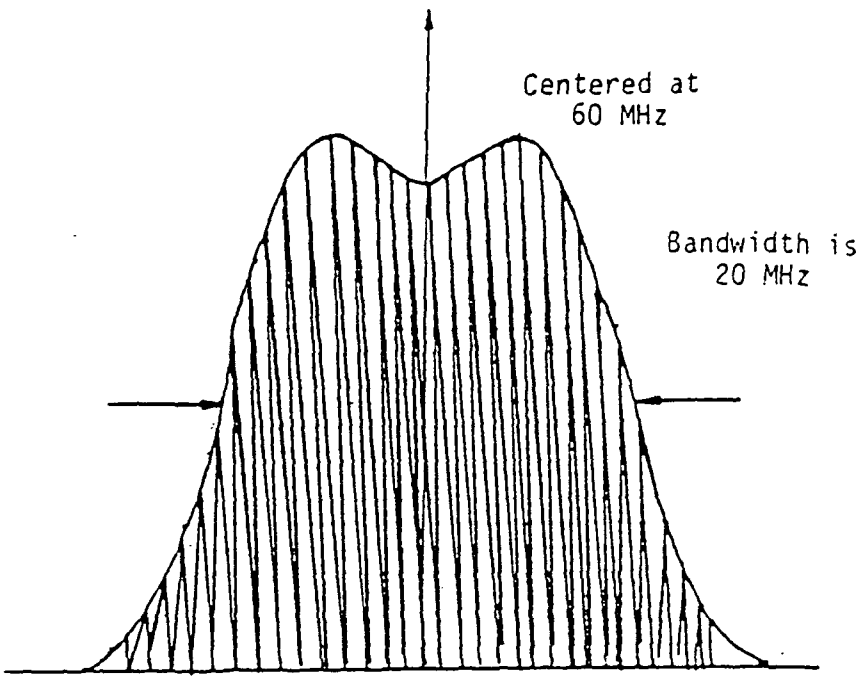

Figure 11- The Characteristics of the Input Signal to the RF Head

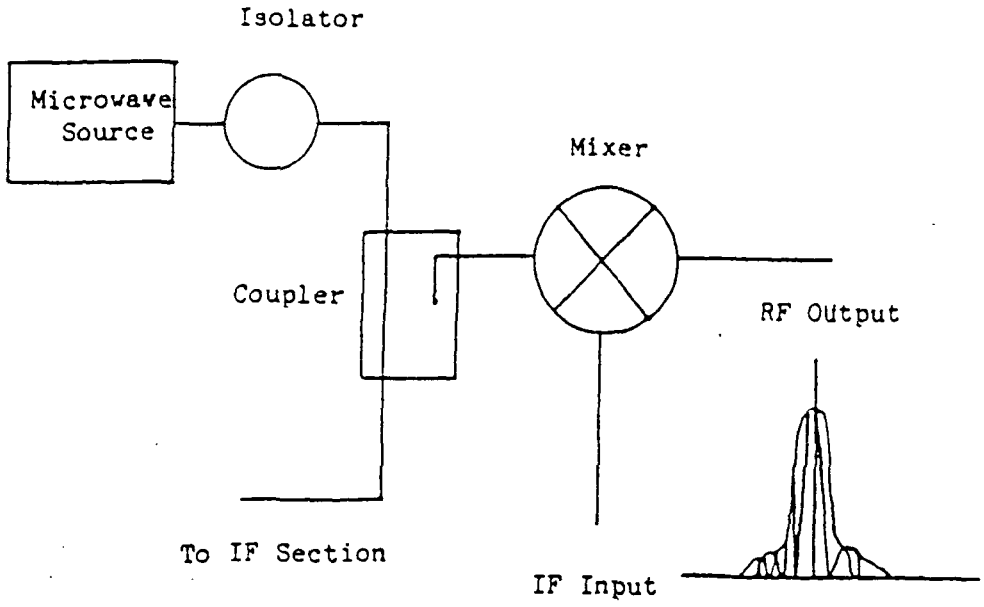

Figure 12- Up-conversion Circuitry and its Signal Representation

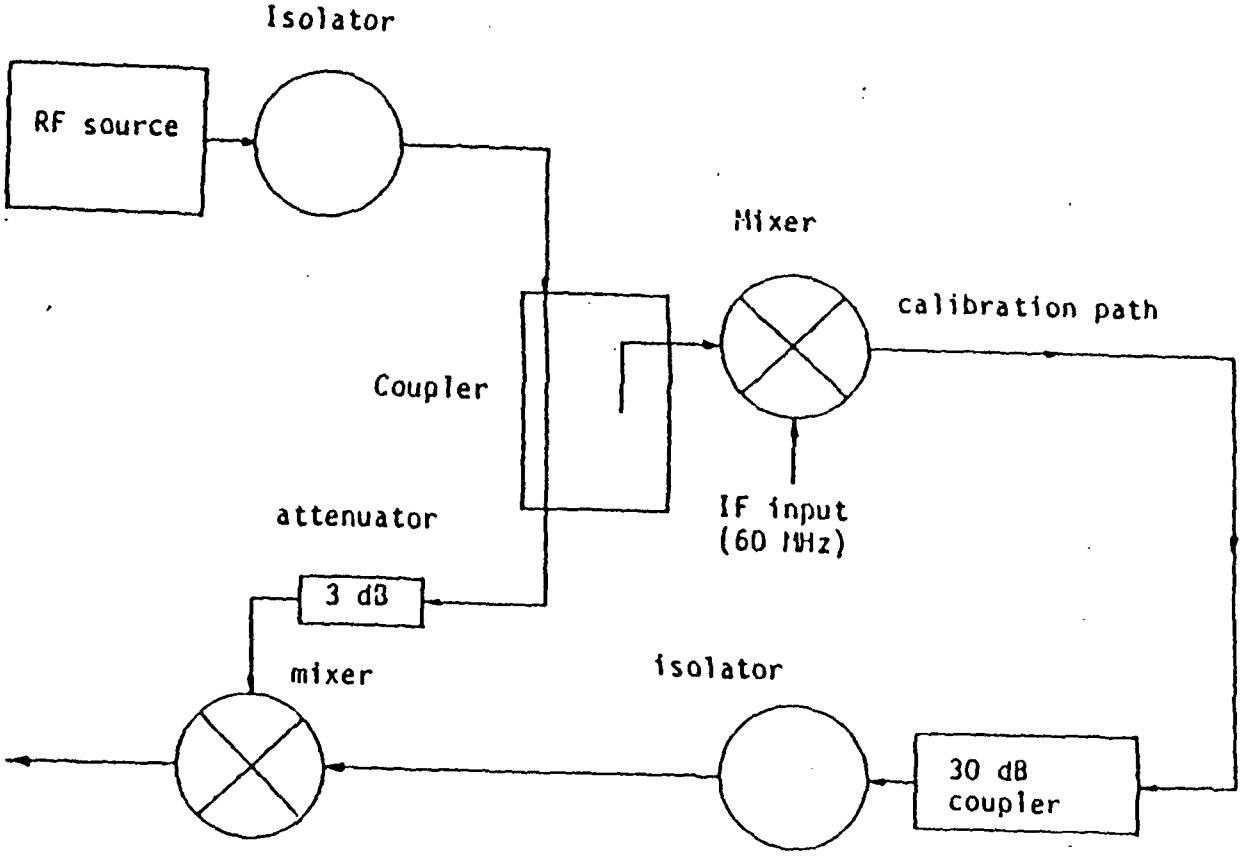

Figure 13 - The components in the RF sub-assembly that the calibration path is going through.

signal processing rather than manipulating radar signals in radar frequencies (RF). This section will explain the steps that are done to incoming signals to the IF Section as well as signals that are sent out by the IF Section. The block diagram of the IF section is presented in Figure 14.

The IF Section itself may be divided into three distinct parts. They are the pulse shaper section, the receiver section, and the Digital Controller Circuitry.

Pulse Shaper (Pulse Expander) Section - As mentioned previously, the RPS utilizes pulse compression technique to generate high resolution short duration pulses. Due to the availability of surface acoustic wave (SAW) technology [19] and system bandwith restrictions, compressed pulses on the order of 50 nanoseconds are used. This implies that the system bandwidth is 20 MHz. Refer to Figure 15 for the pulse generation circuitry diagram. The pulse expansion is accomplished using a Surface Acoustic Wave delay line with a bandwidth of 20 MHz centered at 60 MHz. The drive signal required by this device is a pulse of 60 MHz carrier frequency with a duration of 50 nanoseconds. Refer to Figure 16 for the representation of the signals being generated. To obtain a 60 MHz carrier frequency with a duration of 50 nanoseconds, a double balanced mixer [22] is used as a switch so that those two signals are multiplied in essence producing the required drive signal for the SAW filter. The 50 nanosecond pulses are generated utilizing TTL counters on the digital board which is clocked by the same 60 MHz oscillator. This assures synchronization in the IF Section as well as guaranteeing that the mixer is turned on and off at

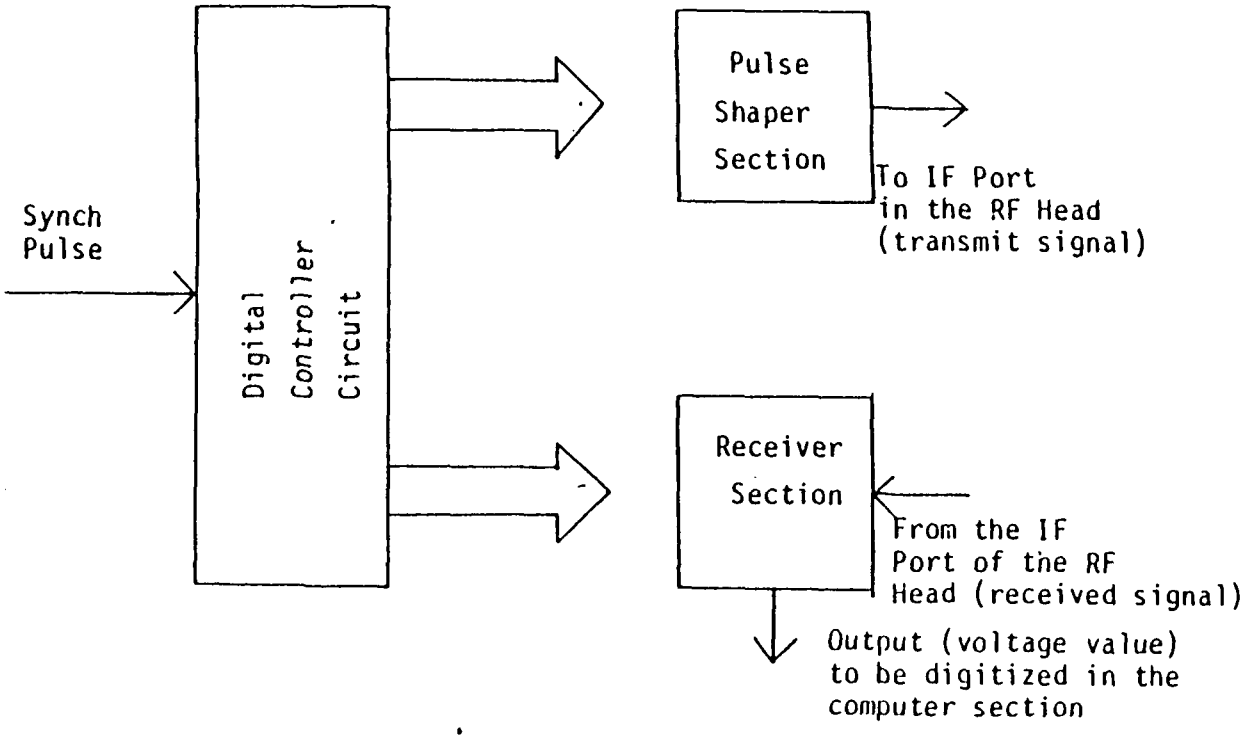

Figure 14- The Block Diagram of the IF Section in the RPS

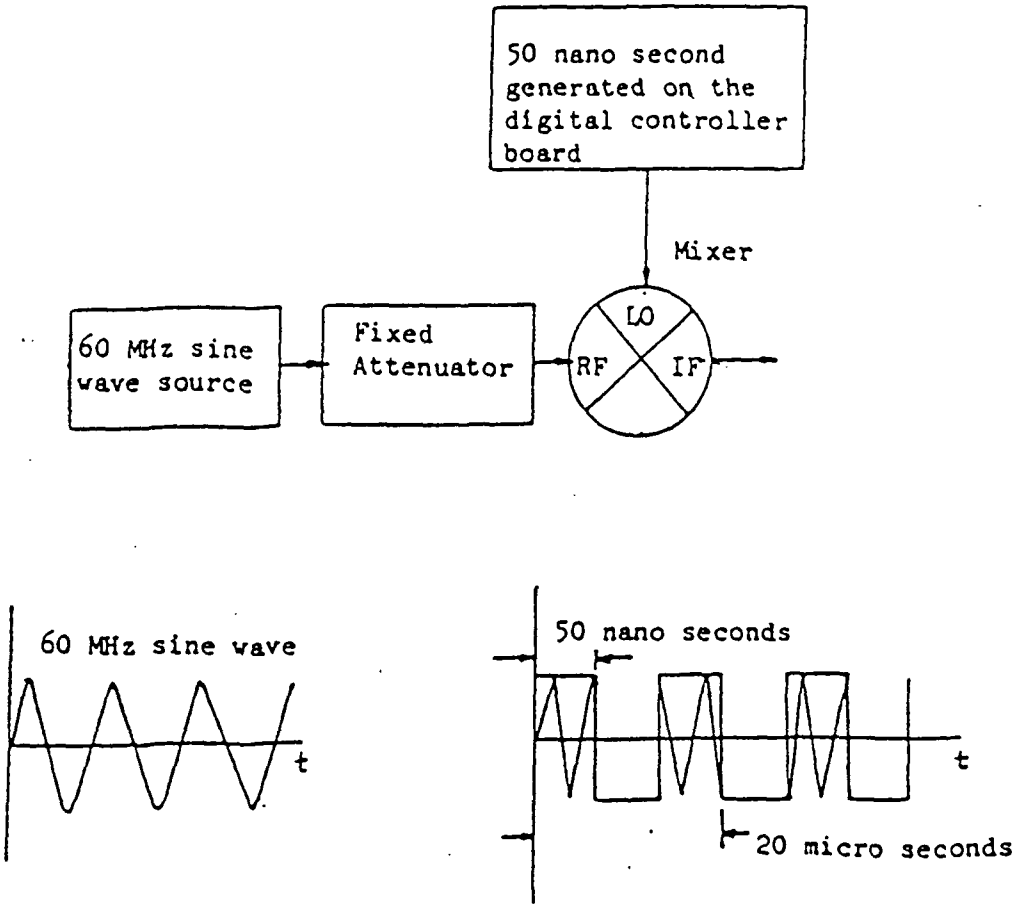

Figure 15- The Block Diagram of the 50 nano-second Pulse Generation Circuit and Its Signal Representation

the zero crossing of the 60 MHz signal. Because of the SAW characteristics, an input of 50 nanosecond pulse will become expanded to a 5 microsecond pulse. See Figure 16 for the signal representation. This expanded signal is then amplified and multiplexed into the proper radar head to be transmitted. The idea is that signals will be expanded when they are being transmitted, and vise versa they will be compressed back when received. The expansion of the transmitted signal is governed by the fact that the signal has to travel through a medium (air) before reaching the target (soil or vegetation) [11],[18]. The lists of components in the IF Section along with their specifications, are given in Tables 1 and 2. The individual components in the IF Section were housed in separate modular boxes because :

1. It minimizes cross talk within the system.
2. It decreases the chance of circuit resonance by induction.
3. It provides an easier way to test individual components.
4. It provides RF shielding [9]

The IF signal that has been generated would then be upconverted in the RF head assembly to be transmitted.

The IF Receiver Section - The IF Receiver Section de-multiplexes the down-converted return radar pulse and prepares the the return pulse for compression. From a particular radar head assembly, the RF signal that is received will be down-converted into IF as explained in the RF head assembly section. Thus the returned signals are in the range of IF. The receiver section then processes the returned signal and manipulates the obtained value for storage. The obtained value is in terms of a voltage level which is the representation of the return

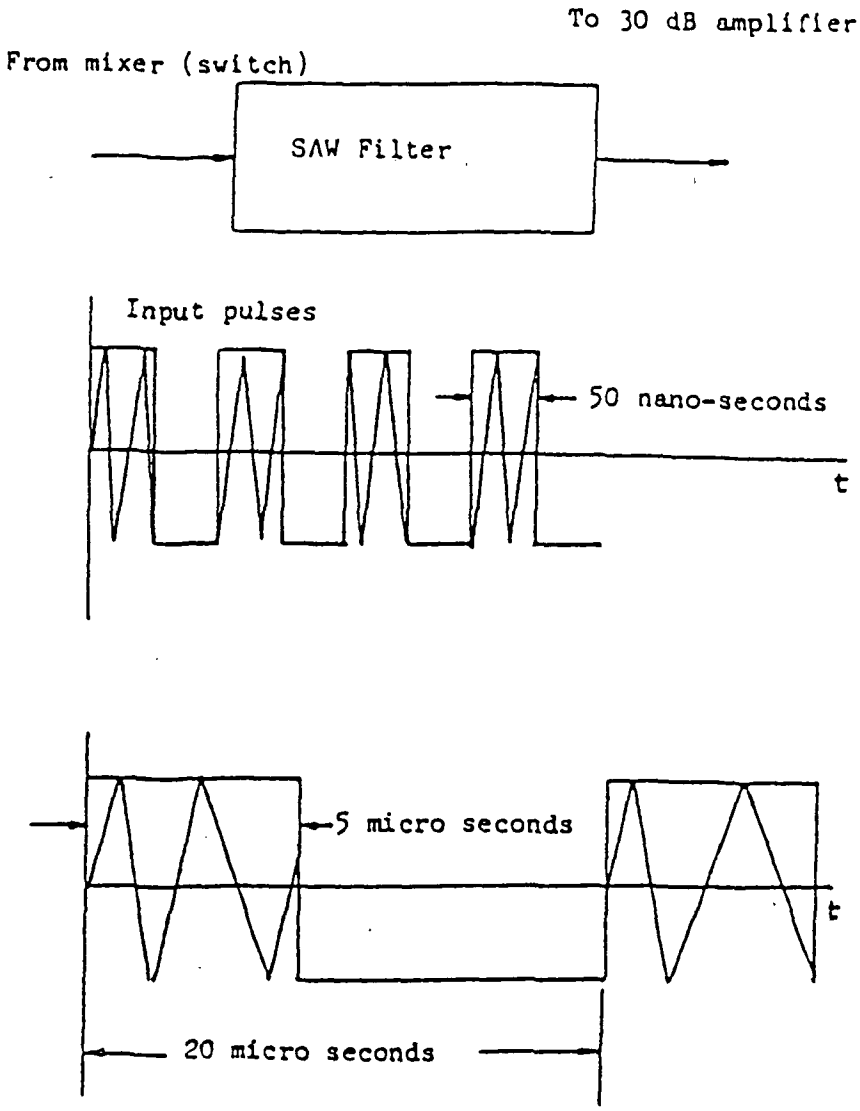

Figure 16- The Pulse Expansion Procedure

Table 1. Component List in the IF Section

Components	Manufacturer
80 dB IF amplifier	RHG EVT60G11DM
SAW Filters	SAWTECH-8010
Oscillator (120 MHz)	Green Ray Y-906
Mixer	Mini-Circuit 2LW-1-3
Transfer Switch	Micronetics L-TTL-1
Digital Attenuator	Daico 0285
35 dB IF amplifier	RHG ICFT6040C
Oscillator (60MHz)	Green Ray Y967XKG6
30 dB IF amplifier	Avantek AMG-502M
35 dB IF amplifier	RHG ICFT6040C
Integrator Circuitry	A0507 Operational Amplifier
Switch Circuitry	Teledyne CDA-18 switch

Table 2. Specifications of the Component in the IF Section

I.	For each transfer switch, the Micronetics 2D-I-L-TTL, the insertion loss is 0.2 dB maximum.	
II.	Digital Attenuator	: DAICO DA0185-1
	RF power	: +10 dBm continous wave maximum +20 dBm non-destruct
	Insertion loss	: 4 dB at 60 MHz (typical) 6 dB maximum
	Attenuation range	: 0 to 63.3 dB
III.	30 dB amplifier	: RHG ICFT6040
	Maximum power gain	: 31 dB
	Power output	: 0 dBm at 1 dB compression
IV.	Mixer	: Mini Circuits ZLW-1-3
	Conversion loss	: 6.5 dB typical 8.5 dB maximum
	Input signal	: +1 dBm at 1 dB compression
	Input power	: 50 mW absolute
V.	35 dB amplifier	: Amplica AVD714201
	Power gain	: 35 dB
	Power output	: +5 dBm at 1 dB compression
VI.	SAW filters	: Rockwell 524-3003-010
	Insertion loss	: 45 dB
VII.	80 dB amplifier	: RHG EVT60-G11DM
	Power gain	: 80 dB maximum
	Power output	: +15 dBm at 1 dB compression
VIII.	Integrator switch	: Teledyne Crystalonics CDA-18
	Input voltage	: -10 V to +5 V
	On resistance	: 20 Ohms minimum, 35 Ohms typical and 50 Ohms maximum
XI.	Integrator circuitry	: Analog Device AD507
	Input voltage	: + or - 11 Volts range
X.	Each coaxial line	:
	Insertion loss	: 0.10 dB minimum 0.20 dB typical 0.40 dB maximum

radar energy. After receiving the proper RF head assembly IF output, the signal is then passed through a 7 bit digital attenuator. This attenuator has a total of 63.5 dB of attenuation in 0.5 dB steps. This attenuator is the controllable element in a digital automatic gain control (DAGC) loop [23]. As a result, the system has a capability of 63.5 dB dynamic range. By controlling the attenuator, the output of the system is forced to a predetermined value. The system output is then the digital number used to set the digital attenuator to the value that will provide this predetermined value.

As the task of the receiver section is to compress the incoming signals, the IF section uses two identical SAW filters to perform both the pulse expansion and the pulse compression. To achieve the proper pulse compression, the incoming signal must go through a process which is called side band swapping. Refer to Figure 17a and Figure 17b for the circuit representation and signal representation respectively. The signal is mixed with a 120 MHz crystal oscillator output. The effect of this operation is to take a pulse which has up-chirp (frequency increase with respsect to time) characteristics and transform it to a pulse which has down-chirp (frequency decrease with respect to time) characteristics. In this manner, identical SAW filters can be used to both expand and compress the pulse. The output of the SAW filter is the compressed pulse of approximately 50 nanosecond width (see Figure 18). The pulse is then amplified by a low noise 80 dB gain video amplifier. This output is passed through a programmable range gate [23]. This circuit is controlled by the microprocessor and has a 5 nanosecond rise time with pulse resolution of 16.67 nanoseconds. The

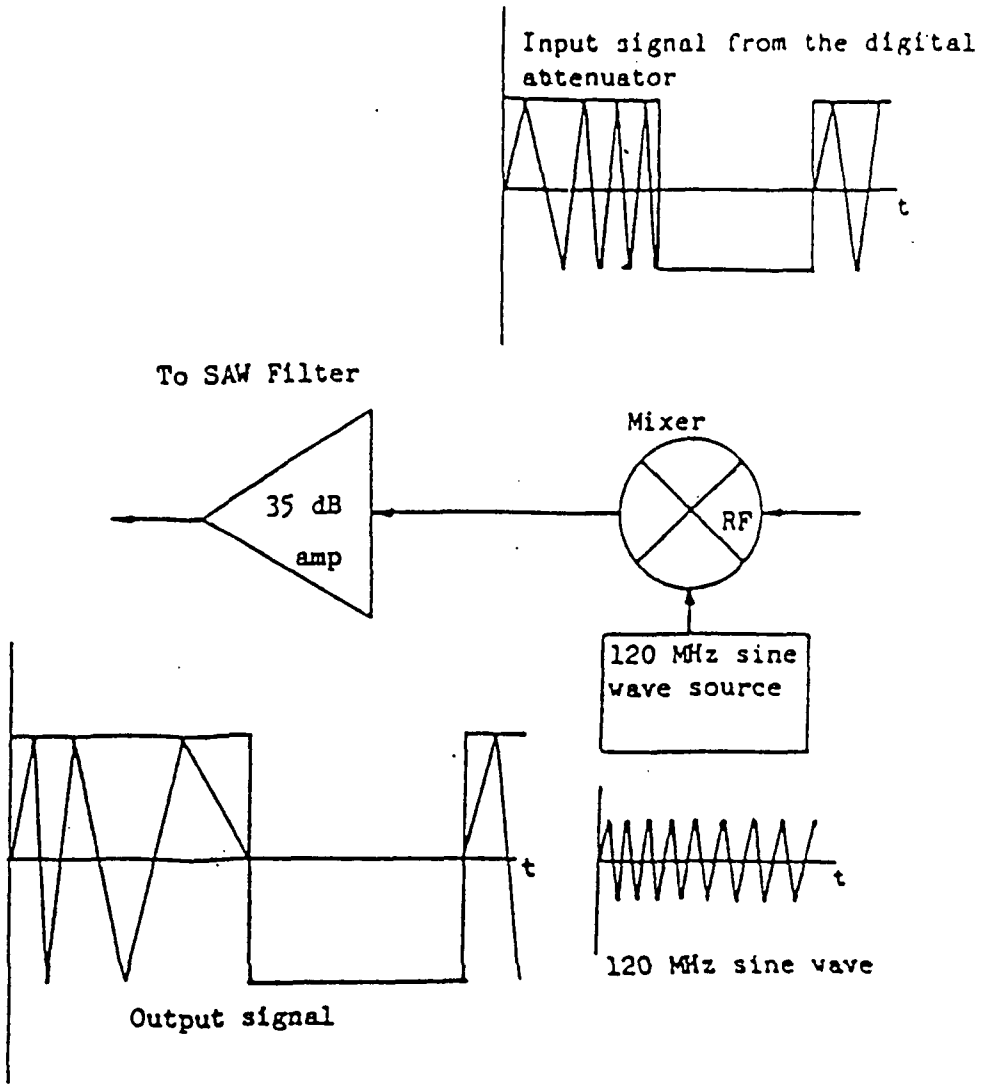

Figure 17a- The "Side-Band Swapping" Circuitry

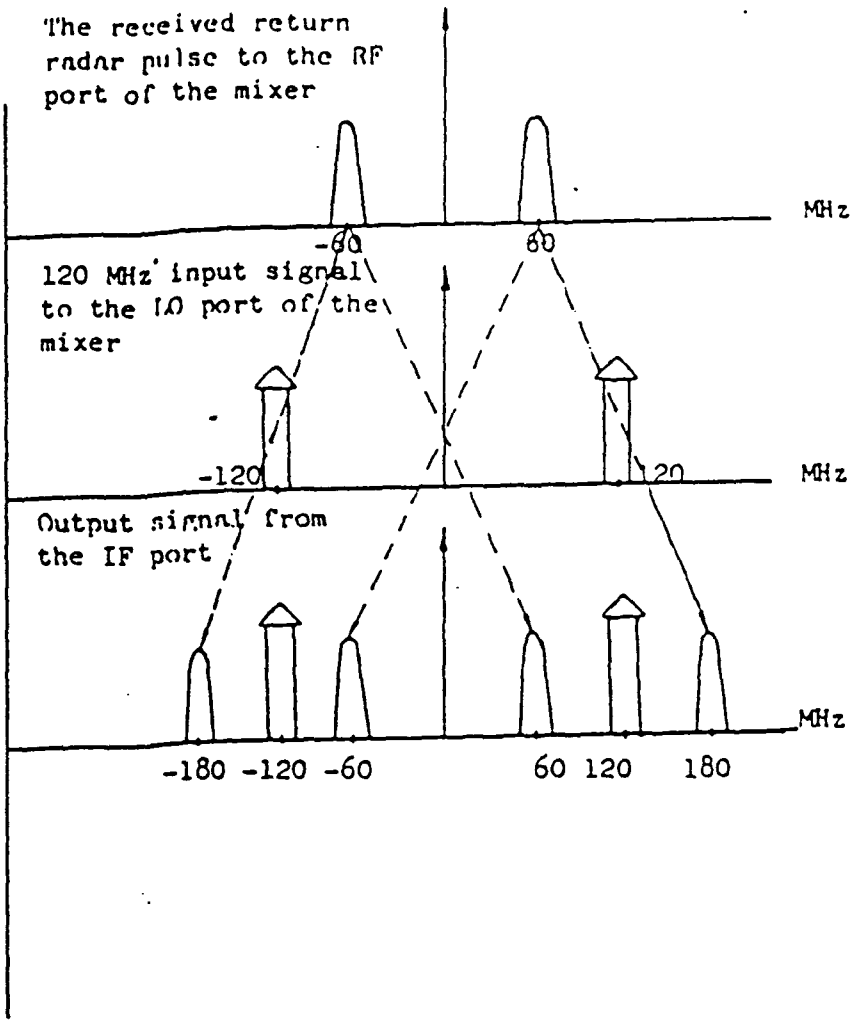

Figure 17b- The Signal Representation of the "Side-Band Swapping" Procedure

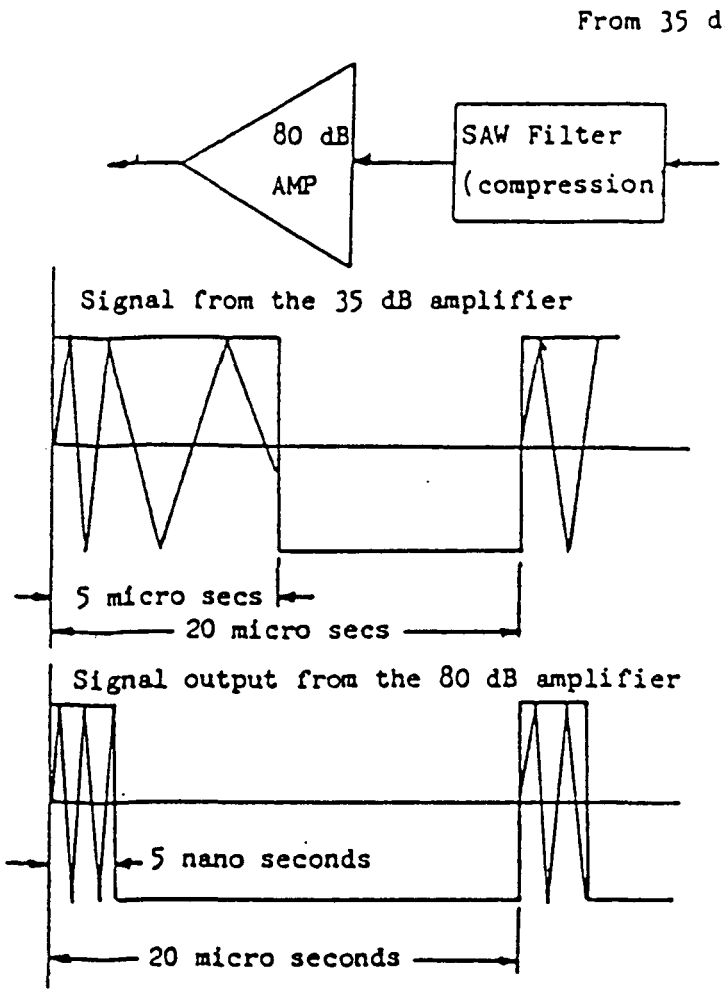

Figure 18 Pulse Compression Procedure

range gate circuitry is to eliminate unwanted direct feed-through from the antennas and extraneous noise inputs from outside the gate window. Because the energy level in each of the 50 nanosecond return pulses is very low, a very fast high gain integrator is used to bring the voltage to a level that can be handled by the analog to digital converter. The integrator circuitry is presented in Figure 19. The representation of signals being put through the integrator is presented in Figure 20. The output of the integrator is a negatively increasing 'stair-case' of voltages. The circuit integrates ten pulses and the integrated value is then put through a sample and hold circuit. After integrating ten pulses, the integrator is set back to zero to keep the system from going into saturation. From the sample and hold circuit, this value is then digitized and stored by the microprocessor. It is this voltage that the DAGC will force to a predetermined value.

The Digital Controller Circuit - The Digital Controller Circuit accepts data from the microprocessor, distributes power, provides timing, monitors the IF section, and controls both the pulse shaper and the receiving section. It also serves the purpose of sending the digitized data onto the microprocessor for storage and further data manipulation. The entire digital controller circuit was implemented on a double-sided 8.5" x 10 " printed circuit board. Refer to Figure 21 for the configuration of the digital controller circuitry. To summarize, the digital controller circuit performs the following:

1. Controls the multiplexer switches -- digital signals are generated such that a selection of the three radar head assemblies can be made. Similar signals are also generated

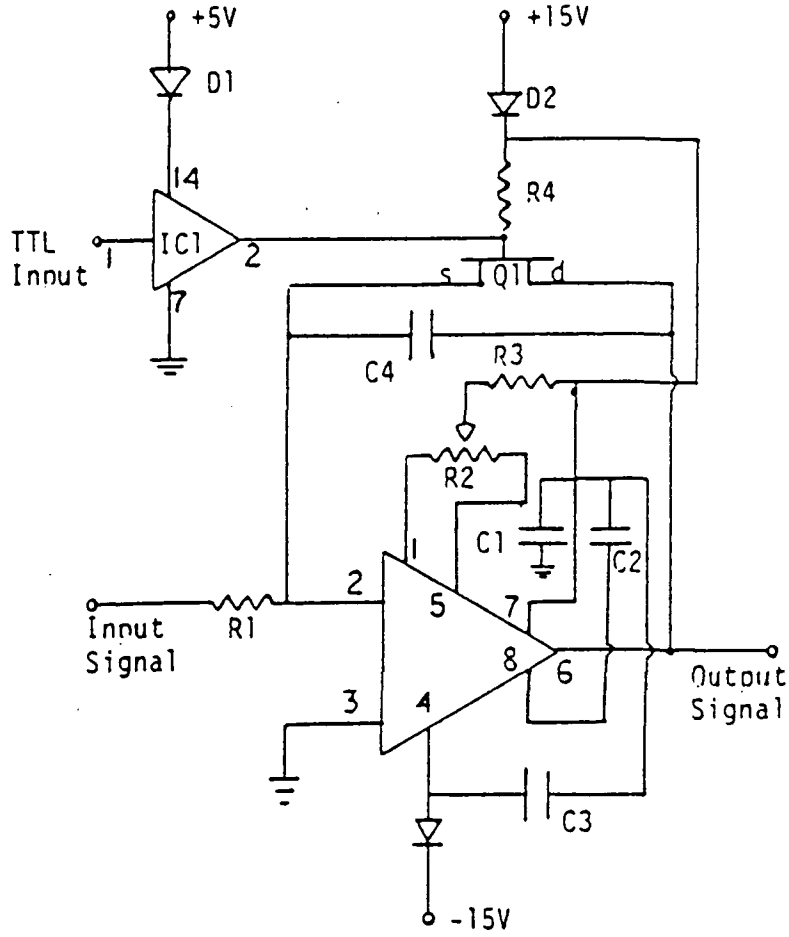

Figure 19- The Schematic Diagram of the Integrator Circuit

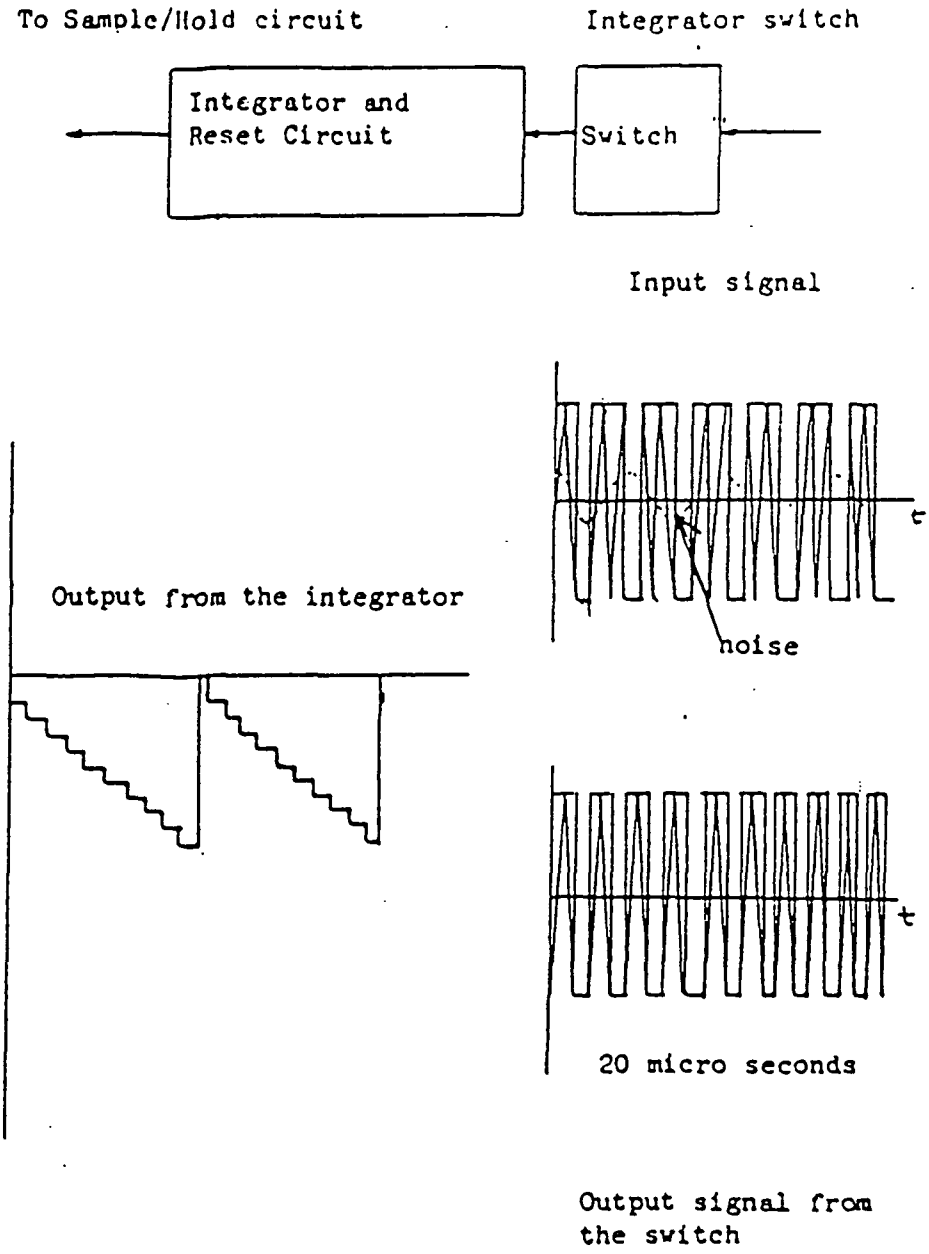

Figure 20- The Signal Representation of the Integration Procedure

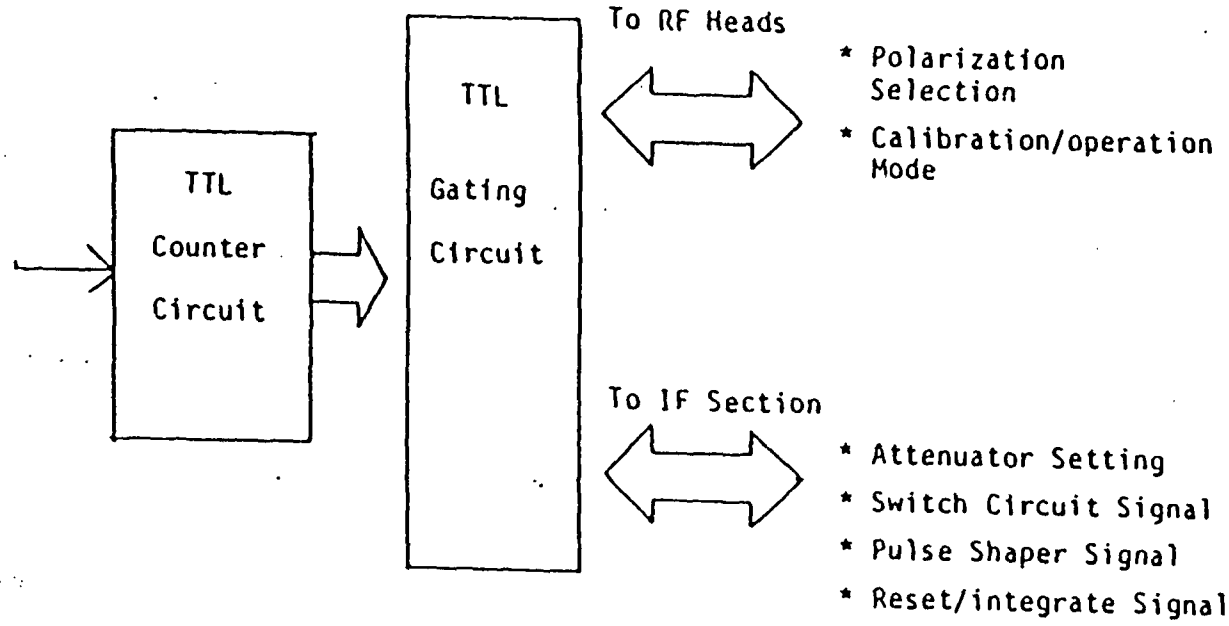

Figure 21- The Block Diagram of the Digital Controller Circuitry

to select the mode of the radar heads in terms of their transmit or receive, and their polarizations.

2. Controls the digital attenuator -- controls how much attenuation should be put onto the return signal in order to maximize the signal to noise ratio but not saturating any of the amplifiers in the IF Section. This level of attenuation is predetermined but programmable.
3. Controls the operation of the integrator, receiver gate, and transmit pulse.

DEVELOPMENT OF COMPUTER ALGORITHM FOR DATA REDUCTION

Background

Finding the radar reflectivity characteristics of a target may be accomplished by theoretical calculations and experimental measurements. Neither functions perfectly without the other. However, either one can yield a good description of a target signature when properly augmented [21].

Both methods are complicated by numerous parameters on which the radar cross section (RCS) of a scatterer depends. They are such things as the shape, size, geometry of the scatterer, the material constituency in relation to the frequency, polarization, and angle of illumination and observation. An exact solution to the scattering problem exists for only a few simple shapes. However, acceptable values of RCS may be obtained experimentally. In the past, theoretical works have guided and interpreted many measurements methods [10].

The RPS is a gain modulated, digitally controlled receiver system. Upon receiving a signal, the RPS will produce hexadecimal numbers as the output. These numbers correspond to the relative measurement of the target in reference to the transmitted power. When reduced properly, these numbers will define the target signature in terms of its RCS. In reducing the data into RCS, the method used is to implement the radar equation. The following will present the development of the radar equation for the general case, and continue to the development of the radar equation when used in conjunction with the RPS.

Development of the Radar Equation for General Case

The radar equation relates the range of a radar system to the characteristics of the transmitter, receiver, antenna, target, and the surrounding environment [1]. If a point radiator which is an ideal isotropic radiator is considered, the power being transmitted by the source can be viewed as having a spherical power density. In radar remote sensing applications, an electromagnetic source that has a pencil beam characteristic is usually used. So, concentrating on an area on the imaginary sphere as with the case of the point radiator, the power transmitted that is associated with the beam is directly proportional to the quantity:

$$P(t) = \frac{\text{Area of sphere}}{\text{Area of the beam}}$$

Consider a pencil beam source that radiates an amount of energy quantified as Pt. The amount of energy that is intercepted by some particular target is given by

$$P(r) = \frac{Pt}{4\pi R^2 G_t} \qquad (1)$$

where

Pt = power being transmitted

Gt = gain of transmitter

Ac = effective area of antenna = the physical area

s = radar cross section

R = distance from the source to target

The amount of the energy that is intercepted by the target will be

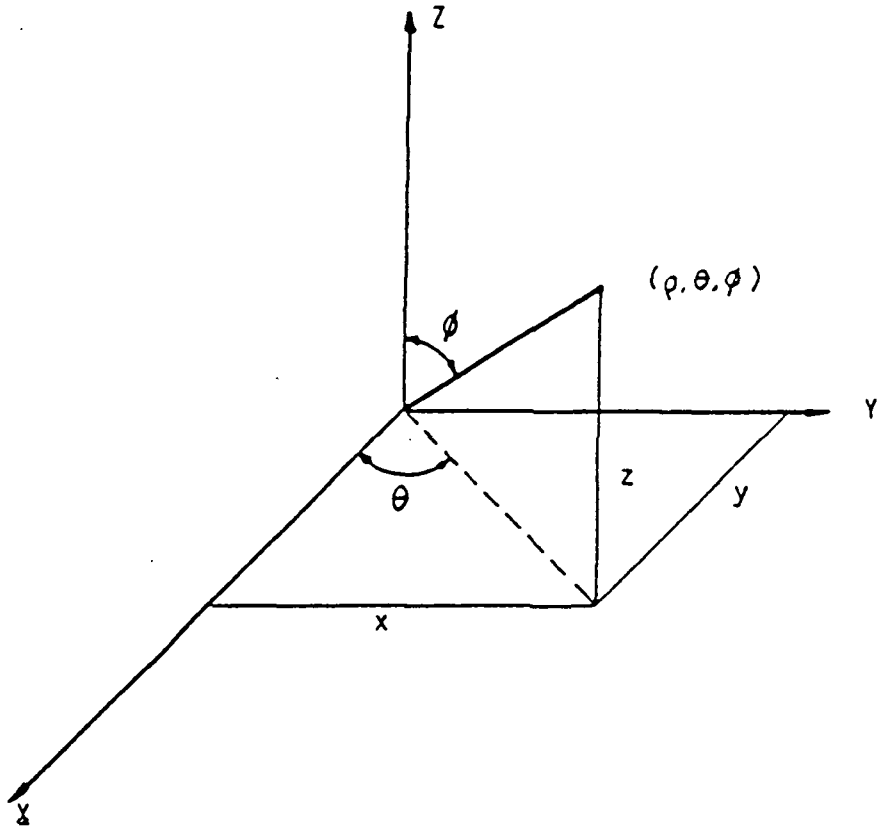

Figure 22- The Spherical Coordinate System

reradiated or scattered in all directions. One of the scattering directions will be in the direction of the receiver. The scattered energy will have traveled a distance of R. Now, the gain of the receiver is related to the effective antenna area as

$$G(\text{receiver}) = \frac{4\pi A_c}{\lambda^2} \qquad (2)$$

where λ is the radar wavelength. Rewriting the received power, the power which will be partially intercepted by the receiver, it is given as

$$P(r) = \frac{P_t G_t(\theta,\phi) \cdot G_r(\pi,\phi)\sigma(\theta,\phi)\lambda^2}{(4\pi)^3 R^4} \qquad (3)$$

where the variables bear the same meaning as equation (1). The radar cross section, the gain of the transmitter as well as the receiver are defined in the spherical coordinate system in terms of the angle θ and ϕ. The spherical coordinate system is shown in Figure 22.

When electromagnetic energy is being impressed onto a target, some of this energy will be absorbed by the target, while a fraction of it will be reflected or scattered. The scattered energy is reradiated in various directions. The relationship between the energy incident upon a target and the scattered energy in the direction of the receiver is defined to be the radar cross section of that particular target [20]. In other words, the radar cross section of a target is the fictional area intercepting the amount of power which, when scattered equally in all directions, produces an echo at the radar source equal to that from the target. The radar cross section of a target has units of

area. This amount is a characteristic of the particular target and is a measure of size as seen by the radar system. Briefly, the radar cross section of a target is described by:

$$S = \frac{\text{Power reflected toward source/unit solid angle}}{\text{Incident power density/4 pi}}$$

which has a limiting value of

$$\sigma = \lim_{R \to \infty} \frac{|E_r|^2}{|E_i|^2} \qquad (4a)$$

where R = distance from radar source to target

Er= reflected field strength at the source

Ei= strength of incident field at the target

In terms of the previous equations, the radar cross section is given by

$$\sigma = \frac{(4\pi)^3 R^4 P_r}{G_t G_r \lambda^2 P_t} \qquad (4b)$$

Equation (3) which is a simplified form of the radar equation does not adequately describe the performance of practical radar system. There might be discrepancies occurring in the actual measurements and calculated values. Part of these discrepancies are due to the failure of equation (3) to include the various losses that exist throughout the system.

From equation (3), a minimum detectable signal can be calculated. The minimum detectable signal and the radar cross section of a target are statistical in nature. There is no statistical expression in equation (4b) to describe the statistical nature of the minimum

detectable signal or the radar cross section. A more detailed or more involved radar equation might be represented by

$$Pr = \frac{P_t G_t G_r \lambda^2 \sigma}{L_t 4\pi \cdot r^2_t 4\pi \cdot r^2_r \cdot Lm_r 4\pi \cdot L_r \cdot Lp \cdot Lm_t} \qquad (5)$$

where the parameters in the equation are defined as :

P_t = transmitted power

G_t = gain of the transmitting antennas in the direction of target

L_t = losses in the transmitter

L_r = losses in the receiver

R_t = distance between the transmitter and target

s = radar cross section

Lm_t = losses associated with the propagating medium with respect to transmitter

Lm_r = losses associated with the propagating medium with respect to receiver

G_r = gain of the receiver

R_r = distance between target and receiver

L = radar wavelength

L_p = polarization losses

Since the RPS employs two identical antennas for its transmitter and its receiver, equation (5) might be slightly reduced to:

$$Pr = \frac{P_t G^2 \lambda^2}{(4\pi)^3 R^4 L_p} \qquad (6)$$

In summary, the traditional approach of measuring the radar cross section of distributed target using a ground-based scatterometer is to use a relatively narrow pencil-beam source, in which case the radar equation is

$$Pr = Pt \cdot \frac{\lambda^2}{(4\pi)^3} \int_{\substack{\text{illuminated} \\ \text{area}}} \frac{G_t(\theta,\phi)G_r(\theta,\phi)}{R^4} \sigma dA \qquad (7a)$$

which can be approximated to

$$Pr = \frac{P\ G\ G\ \lambda^2 \sigma A}{(4\pi)^3 R^4} \qquad (7b)$$

Modified Radar Equation To Be Used in the Operation of the RPS

The RPS employs an automatic gain controlled IF section the its operation will be discussed in more detail in a later section. From the automatic gain controller scheme, there is a digitally controlled attenuator which will fix the received signal to a forced level. So, data acquired will be in term of the attenuator settings.

Now, from equation (3) for a point target, the cross section may be written as

$$\sigma = \frac{P_r}{P_t} \cdot \frac{(4\pi)^3 R^4}{G_r G_t \lambda^2} \qquad (8a)$$

For the RPS, an initial calibration measurement was made which is dependent on the transmitted power P_t. The calibration power is given by:

$$P_{ca} = K_1 \cdot P_r \tag{8b}$$

where the attenuator setting for the internal calibration is P_{ca}. Then, the cross section for point target can be expressed as

$$\sigma = \frac{K_1 P_{ap}}{P_{ca} G_r} \cdot \frac{R^4}{\lambda^2} \cdot \frac{(4\pi)^3}{G_t} \tag{8c}$$

where P_{ap} = attenuator setting for the measurement

K_0= system gain constant

and the other terms bear the same meaning as in equation (5). The expression is simplified further by introducing new constants such that

$$\sigma = \frac{P_{ap}}{P_{ca}} \cdot \frac{R^4}{\lambda^2} \cdot K \tag{9a}$$

$$\text{where } K = \frac{K_0 K_1 (4\pi)^3}{G_t G_r} \tag{9b}$$

is the system constant.

The system constant K can be calculated for individual targets for each frequency of operation in the RPS. It is obtained in the following manner. The system constant is composed of terms in equation (9) that are independent of the target response or location. From a target of known cross section, the system constant can be calculated. By combining this system calibration constant and field measurement, radar cross section of various targets may be acquired.

Development of the Computer Algorithm

From equation (9a), the radar cross section may be approximated in terms of system constants. This equation is in the terms of constants and variables in the RPS. The radar cross section of a particular target is a linear averaged quantity of numbers obtained in a scan of data acquisition. The number of data points obtained per scan is controllable by an operator. Numbers that are generated or obtained by the RPS are in Hexadecimal values signaturing the radar cross section of a particular target. These hexadecimal (hex) numbers are the numbers set by the digital attenuator in the IF section as discussed in Chapter II. A computer algorithm has been developed and shown in Appendix D. The algorithm will have its inputs from a file assumed to be the data filed transferred from the RPS computer system onto the VAX system. If implemented in FORTRAN, the algorithm will consist of several nested DO loops. From appendix D, it could be seen that values of the radar cross section may be interpreted by utilizing the linear averaging of the data points, or the logarithmic averaging of the data points.

OPERATIONAL ANALYSIS OF THE RPS

The RPS is a multi-frequency radar system which operates at X,C, and L bands. A block diagram of the system is presented in Figure 23. It divided into three distinct sub-sections. They are the RF head assembly, the IF section, and the computer.

Assembling the RPS

While there is a radar system that is built by the RSC currently under field experiment, the RSC is also developing a similar RPS. The development of the duplicate system is under contract by the NASA Goddard Space Flight Center. The duplicate system will be operated in the laboratory to obtain some particular operational parameters of the RPS. These include parameters such as the power output of the system, losses in the system, and receiver saturation levels.

The first step in developing the duplicate RPS is to assemble the RF heads. The components in the RF heads are listed in Table 3, 4 and 5. These components are interconnected with each other by flexible coaxial cable with SMA type of connectors attaching to the components. The components are mounted on the sides of an aluminum sheet which is placed inside an aluminum housing. The mounting on the aluminum sheet is divided into placing the transmitter components on one side, while placing the receiver components on the other. The RF head housings have output as well as input lines through SMA of connectors. The output lines include the transmitter ports and the IF output while the

Table 3. List of Components in the L-Band RF Head

Components	Manufacturer
1.6 GHz source	Techtrol-406
Isolator	P&H Laboratory
Mixer	Mini-Circuit-ZAM42
Directional Coupler	EMCO C1-1020-10
Transfer Switch	Micronetics D-L-I-TTL
RF Amplifier	MITEQ AM4A10256018

Table 4. List of Components in the C-Band RF Head

Components	Manufacturer
4.75 GHz source	Techtrol M410
Mixers	Western Microwave M3005
Isolators	Western Microwave 2JC2049
Couplers	ARRA 5164-10
Transfer Switches	Micronetics D-L-I-TTL
Amplifier	Amplica 824 CSL

Table 5. List of Components in the X-Band RF Head

Components	Manufacturer
10 GHz source	Techtrol M415
Isolators	P&H Laboratories C1-X13357
Mixers	Lorch Laboratories FC-325H
Directional Couplers	ARRA 5164
Transfer Switches	Micronetics D-L-I-TTL
Amplifier	Amplica XM243301

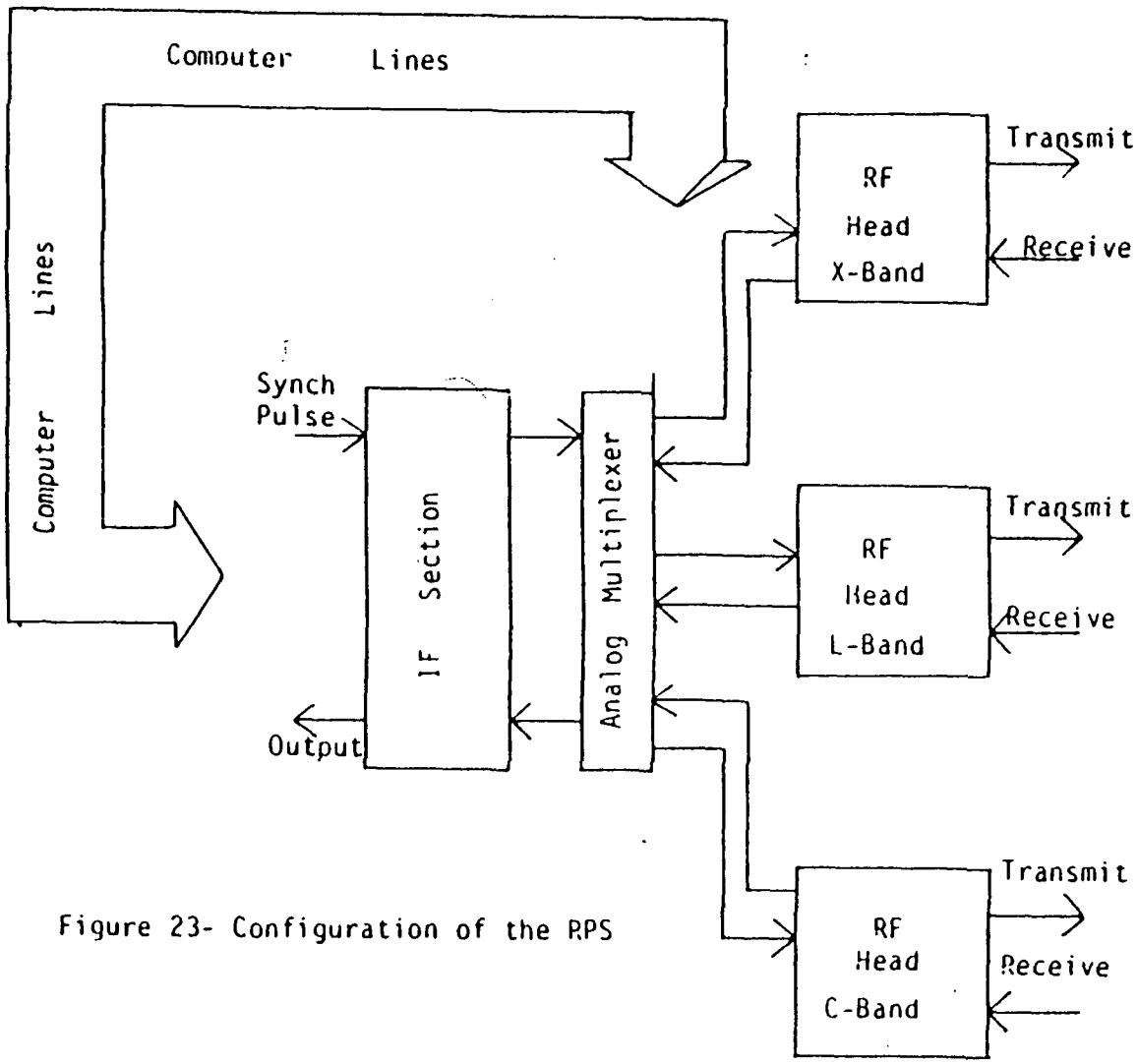

Figure 23- Configuration of the RPS

input lines include the receiver ports and the IF input. These input and output lines are related as discussed earlier.

The block diagram of the IF section is presented in Figure 24. The assembly of the IF section is performed similarly to the procedure taken for the RF heads. The components are mounted on the sides of an aluminum sheet placed inside an aluminum housing. In addition to the discrete components such as the oscillator, the mixer, and the IF amplifier, there are two custom made circuits which are housed in two separate RF-shielded enclosures. These circuits are the switch circuit and the integrator circuit. The operation of these circuits in terms of the IF section is described earlier. The schematic diagram of the switch and the integrator circuits are presented in Figures 25 and 26 respectively. The synchronization circuitry that controls the timing of the IF section is implemented with TTL parts that are arranged on a p.c. board housed inside the aluminum box as well.

The radar heads, the IF section, and the computer are interfaced directely via an interface board. In testing the RPS in laboratory, the RF and IF sections are interfacted directly to a computer via an interface board. The purpose of the board is to route signals from the computer to the IF section and the RF head and vise versa. It also distributes Direct Current (DC) power to the radar head and the IF section assembly.

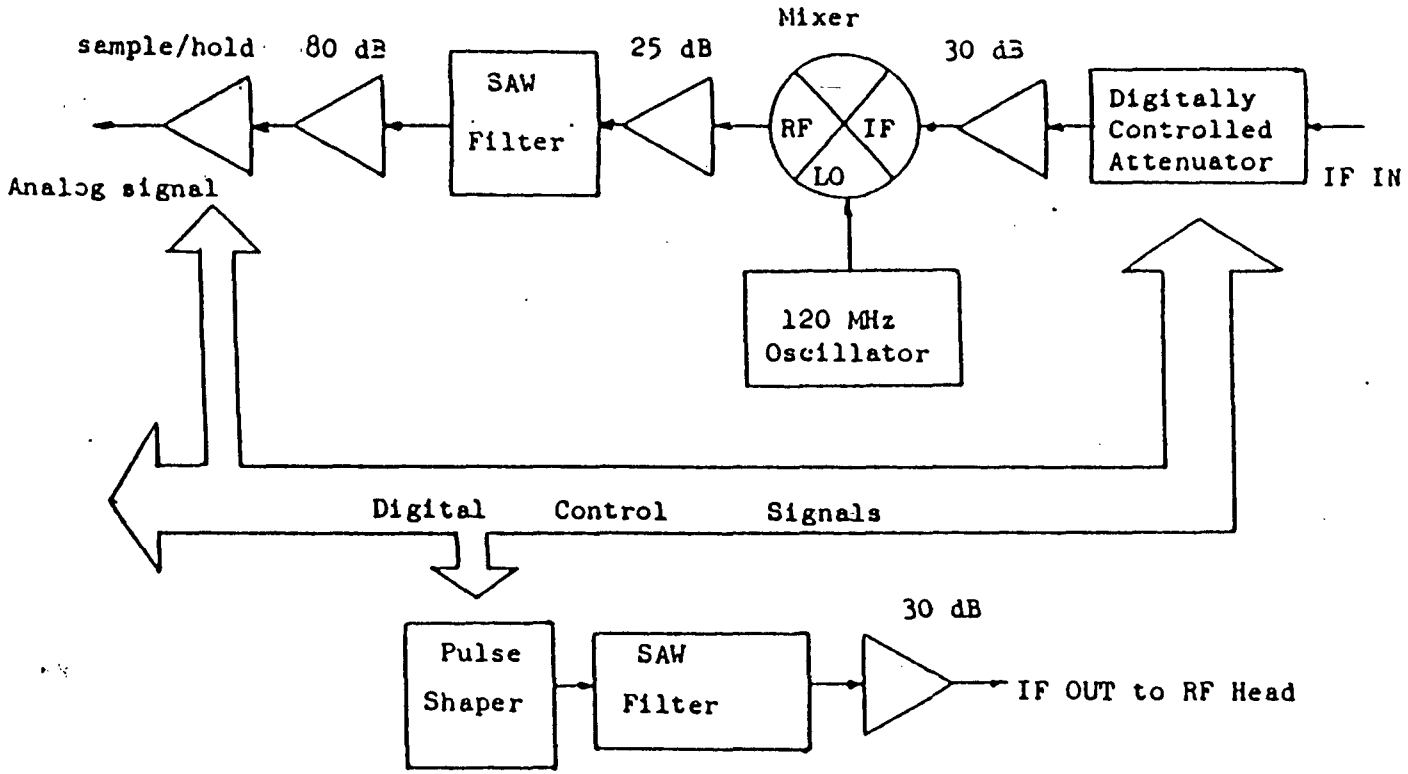

Figure 24- The Block Diagram of the IF Section in the RPS

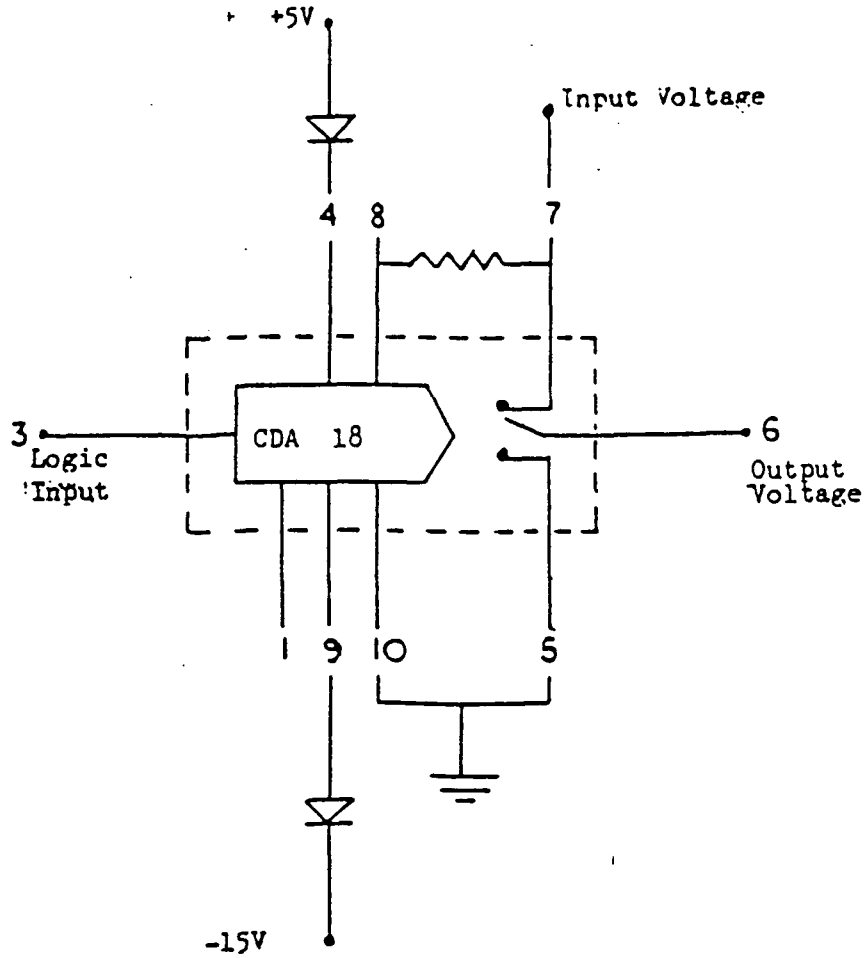

Figure 25 The Schematic Diagram of the Switch Circuit

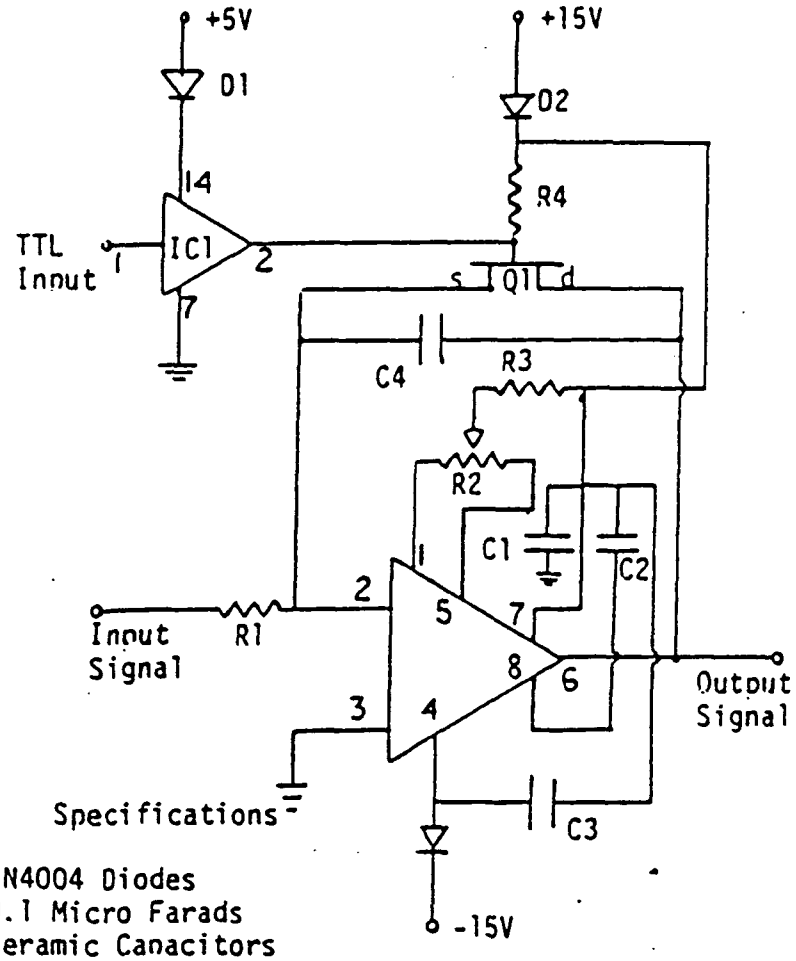

Parts	Specifications
D1,D2,D3	1N4004 Diodes
C1,C3	0.1 Micro Farads Ceramic Capacitors
C2	10 Pico Farads Capacitor
C4	2000 Pico Farads Polystyrene Capacitor
IC1	TTL 7417
IC2	AD507 Op Amp
Q1	P-Channel JFET 2N3820
R1	51 Ohms Metal Film Resistor
R2	100 K Ohms Potentiometer
R3	2 K Ohms Resistor
R4	5.6 K Ohms Resistor

Figure 26. The Schematic Diagram of the Integrator Circuit

Theoretical Calculations

Losses in the RF Heads

Losses in the RF heads are mainly due to the losses in the semi-rigid coaxial cable that is used as the interconnection means in the system. The loss calculations will be based on the manufacturers specifications for each component. The loss calculation will be presented by dividing the RF heads into their transmitting and receiving section such that the transmit power and the calibration power may be determined. The operation of these RF heads is controlled by a digital circuitry as represented in Figure 27. The following is the presentation of the loss calculation for each of the radar head assemblies.

1. The L-Band Radar Head (1.6 GHz):

The components in the L-Band radar head and their specifications are listed in Tables 6a and 6b. They are shown in the form of the block diagram in Figure 28. The microwave source has a specified output power of 21 dB. The total component loss as obtained from their specifications listed earlier is calculated to be about 8.15 dB in the transmitting section. The semi-rigid coaxial cable is specified to have a loss of 0.4 dB per foot. The total loss in the interconnection means which include the losses in the individual SMA type connectors, is calculated to be about 20 dB. Subtracting all losses from the source power, the transmit power is calculated to be -7.15 dB. In the receiving section, the total component loss is calculated to be 11.4 dB. An attenuating pad of 10 dB is also placed in the receiving section along with a 30 dB coupler. The total attenuating factors in

Table 6a. The L-Band Transmitter Component Characteristics

Manufacturer #	Serial #	VSWR		Isolation	Insertion Loss	Comments
406	2080					1.6 GHz source
C1-L46312	105	1.17*	1.20**	18 dB	0.30 dB	*input **output
C1-L46312	108	1.12*	1.13**	18.5 dB	0.25 dB	*input **output
ZAM-42	M814317			17 dB LO/RF	7.00 dB	conversion loss
CL-1020-10	208-8227	1.1*	1.1**	0.20 dB		*primary **secondary
RSM2D-I-L-TTL	7416-8222	1.25		70 dB *	0.20 dB	* between ports
D-L-I-TTL	75778217	1.25		60 dB *	0.20 dB	* between ports

Table 6b. The L-Band Receiver Component Characteristics

Manufacturer #	Serial #	VSWR	Isolation	Insertion Loss	Comments
AM-4A-1025-6018	40699	1.92, 1.29		30.2 dB gain	in, out VSWR
C1-L46312	106	1.12, 1.13	18 dB	0.25 dB	
C1-46312	107	1.17, 1.15	19 dB	0.25 dB	
ZAM-42	M814317		17 dB LO/RF	7.0 dB	conversion loss
CL-1020-30	2128232	1.1, 1.1		0.20 dB	
RSM2D-I-L-TTL	74188222	1.25	60 dB *	0.20 dB	* between ports

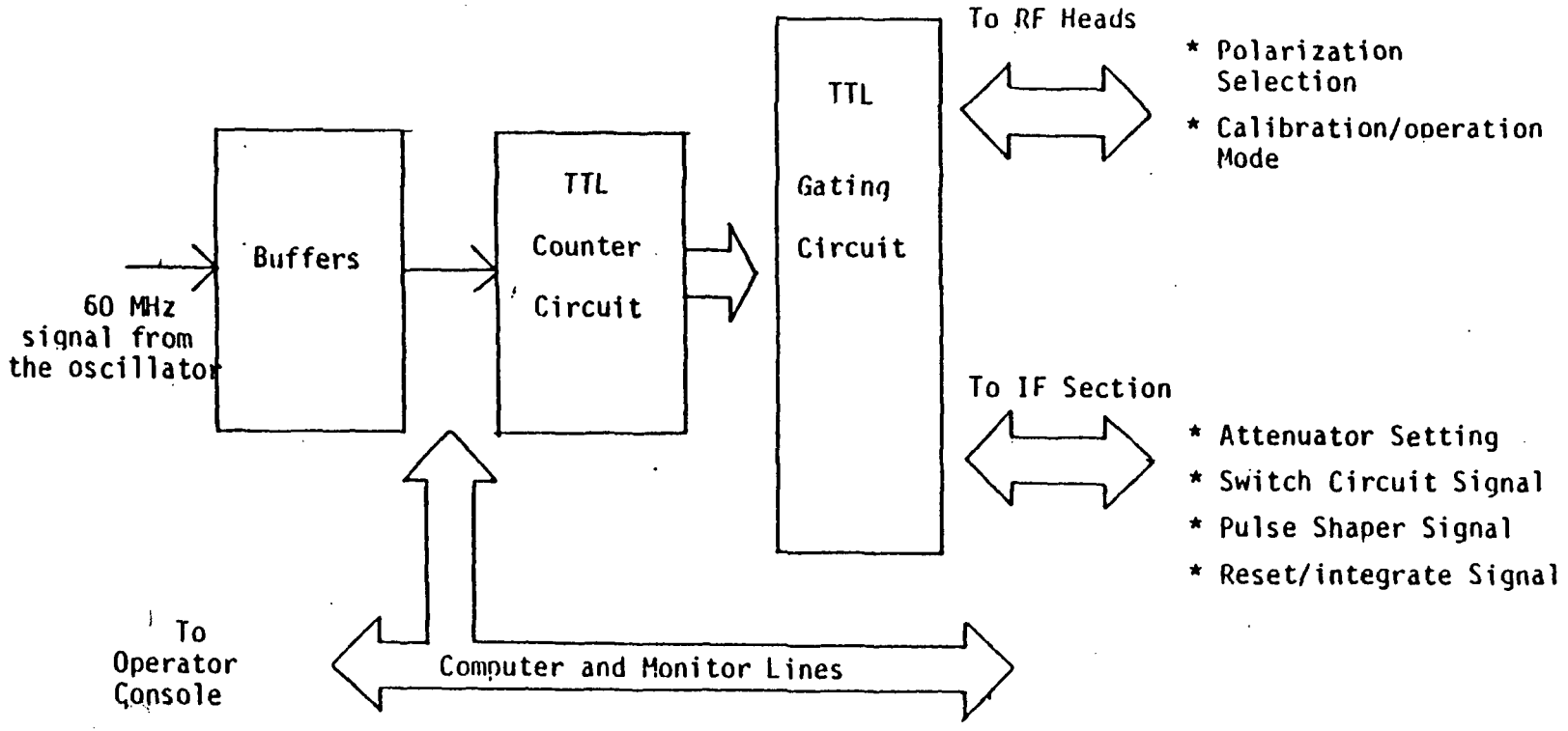

Figure 21- The Block Diagram of the Digital Controller Circuit

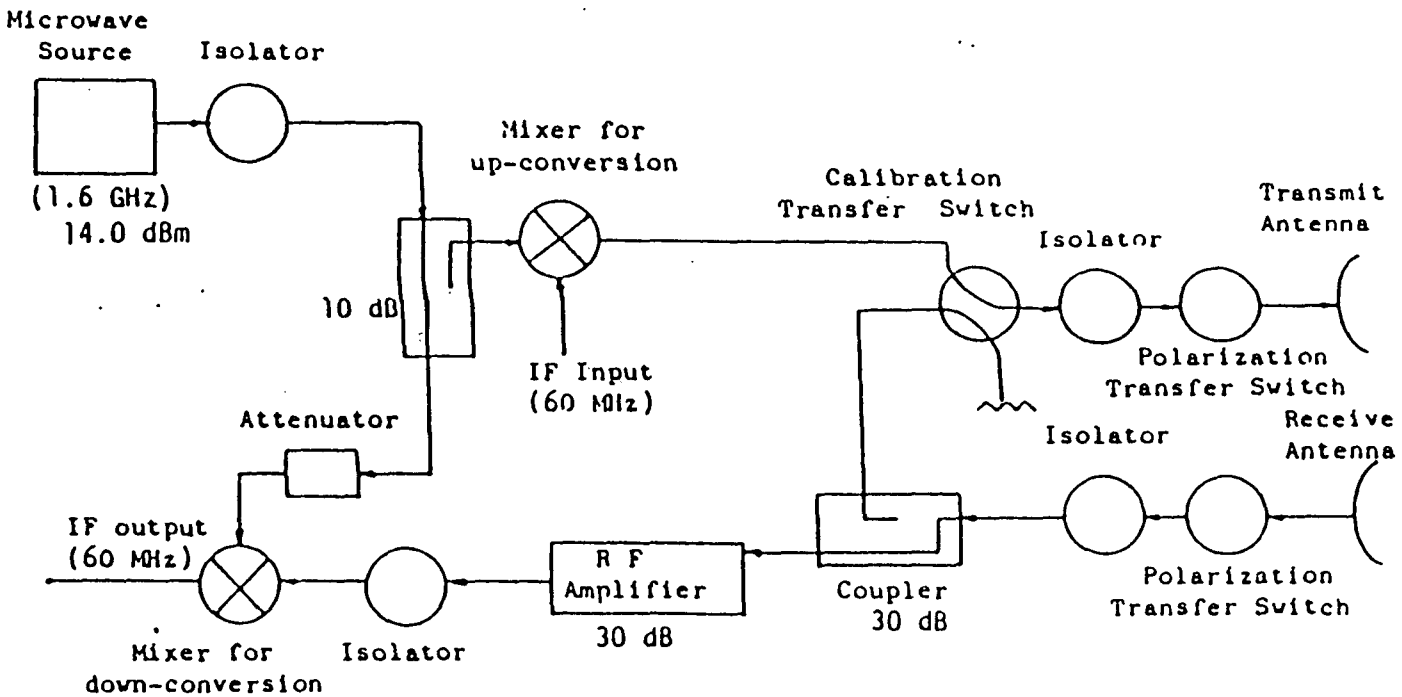

Figure 28. The Block Diagram of the L-Band RF Head.

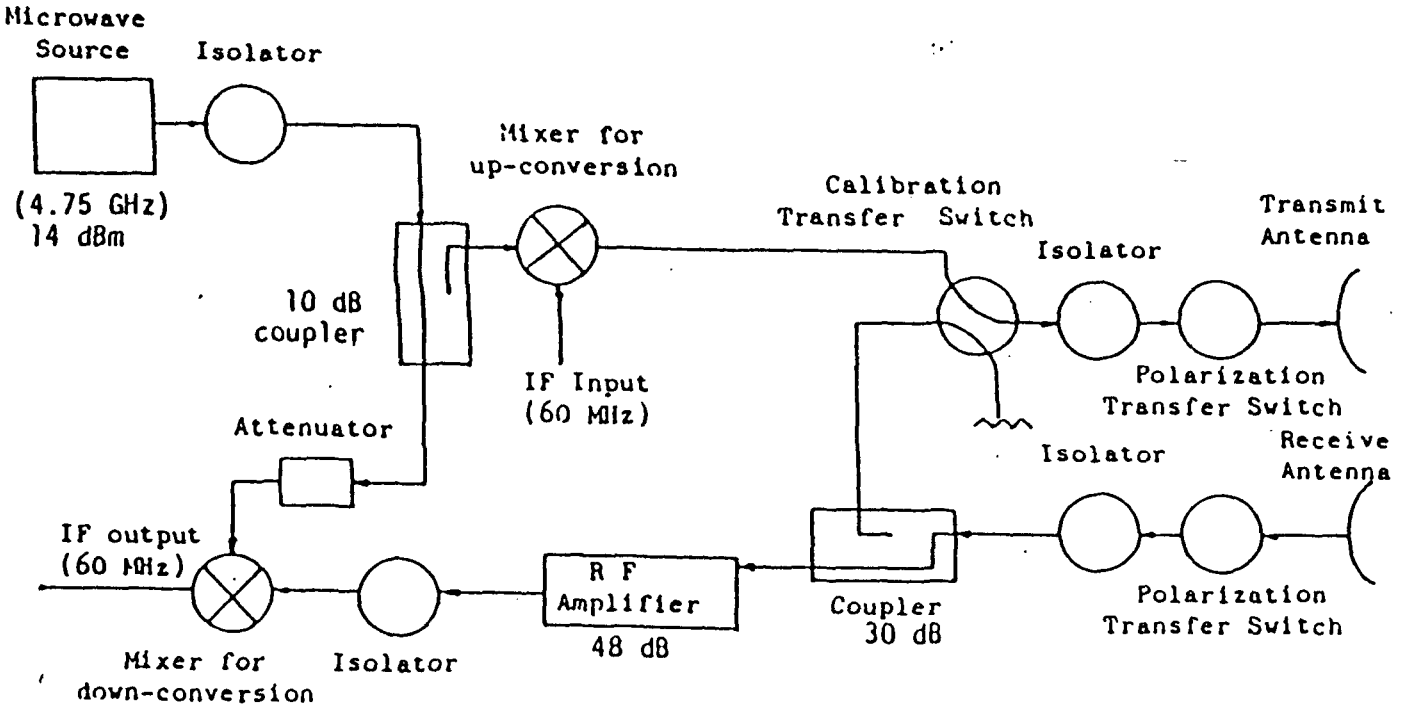

Figure 29. The Block Diagram of the C-Band RF Head.

the receiving section is calculated to be 41.4 dB. An amplifier of 30 dB gain is placed to compensate for the large losses in the RF head assembly. From this, a calibration power is calculated to be -21.4 dB.

2. C-Band Radar Head (4.75 GHz):

The microwave source in the C-Band radar head has a specified output power of 14 dB. Components and their specifications are listed in Table 7a and 7b. The block diagram is presented in Figure 29. The total loss in the transmitting section including cable losses is calculated to be -26.9 dB. From this, the transmit power is calculated to be -12.9 dB. In the receiving section the total attenuating factors are calculated to be 44 dB. This loss is compensated by an amplifier of 28.4 dB gain. The calibration power is then -21.7 dB.

3. X-Band Radar Head (10.003 GHz):

The specified output power of the microwave source in the X-band radar head is 12 dB. Components and their specifications are listed in Tables 8a and 8b. The schematic diagram is presented in Figure 30. In the transmitting section, the total component and interconnection losses are calculated to be 26.7 dB. The transmit power is then calculated to be -14.7 dB. In the receiving section, the total of the attenuating factors is 39.65 dB, the Figure of which a 30 dB gain amplifier. The calibration power is determined to be -27.65 dB. The loss parameter of the RF heads is summarized in Table 9.

RF Head Stability as Measured in the Laboratory

The RF heads are measured for their transmit power and the calibration power by the procedure described in Figure 31a. Data were

Table 7a. The C-Band (4.75 GHz) Transmitter Component Characteristics

Description, serial #	VSWR	Isolation	Insertion loss
4.75 GHz RF source, 1028			
Mixer,57		25 dB LO/RF	5.8 conversion loss
Isolator,194	1.06 in, 1.07 out	30 dB	0.20 dB
Isolator,193	1.06 in, 1.07 out	30 dB	0.20 dB
Coupler,424	1.25 primary 1.30 secondary		0.30 dB
Switch, 7412-8222	1.25	60 dB	0.20 dB
Switch, 7578-8217	1.25	70 dB	0.20 dB

Table 7b. The C-Band (4.75 GHz) Receiver Component Characteristics

Description, serial #	VSWR	Isolation	Insertion loss
Isolator, 191	1.06 both ports	30 dB	0.2 dB
Isolator, 192	1.06 for port 1 1.07 for port 2	30 dB	0.2 dB
Mixer, 56		25 dB LO/RF	5.7 conversion loss
Amplifier, 103	1.49 in, 1.18 out		48.3 dB gain
Coupler, 425	1.25 primary 1.3 secondary		0.4 dB
Switch, 6973-8148	1.25	60 dB	0.20 dB

Table 8a. The X-band (10.0 GHz) Transmitter
Component Characteristics

Description, serial #	VSWR	Isolation	Insertion loss
10 GHz RF source, 2468			
Isolator, 104	1.09 in, 1.07 out	28.0 dB	
Isolator, 105	1.08 in, 1.07 out	30.0 dB	
Mixer, F3		28 dB LO/RF	5.5 dB conversion loss
Switch, 7419-8222	1.25 maximum	60 dB	0.20 dB
Switch, 7576-8217	1.25 maximum	60 dB	0.20 dB
Coupler, 81	1.25 primary 1.25 secondary		0.30 dB

Table 8b. The X-band (10.0 GHz) Receiver Component Characteristics

Description, serial #	VSWR	Isolation	Insertion loss
Isolator, 103	1.09 in, 1.07 out	28 dB	0.25 dB
Isolator, 106	1.16 in, 1.10 out	25 dB	0.25 dB
Amplifier, 102	1.65 in, 1.49 out		30.0 dB gain
Mixer, F2		28 dB LO/RF	5.5 dB conversion loss
Coupler, 7414-8222	1.25 max	60 dB	0.2 dB

Table 9. The Loss Parameter in each of the Radar Heads

Band	Total Loss Transmitting section	receiving section	Transmit power	Calibration power
L	28.15 dB	41.4 dB	-7.15 dB	-21.4 dB
C	26.9 dB	35.7 dB	-12.9 dB	-21.7 dB
X	26.7 dB	39.65 dB	-14.7 dB	-27.65 dB

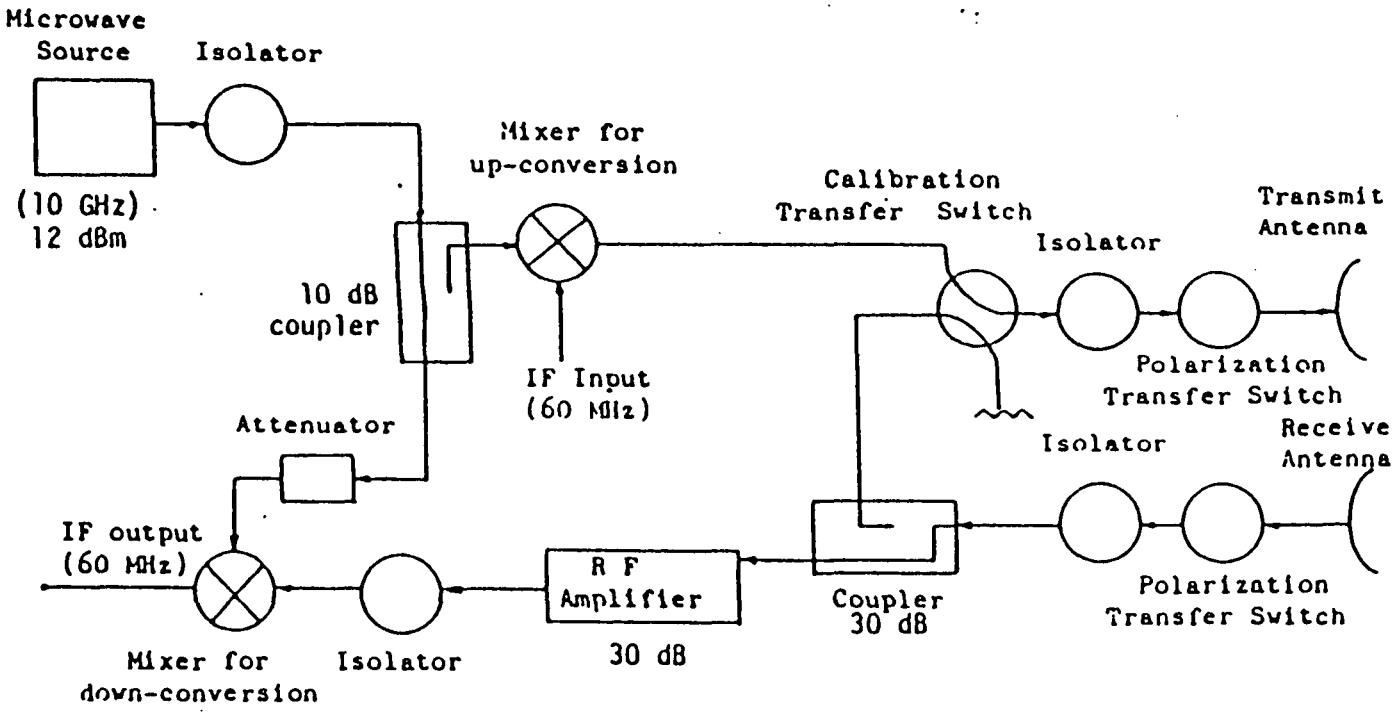

Figure 30. The Block Diagram of the X-Band RF Head.

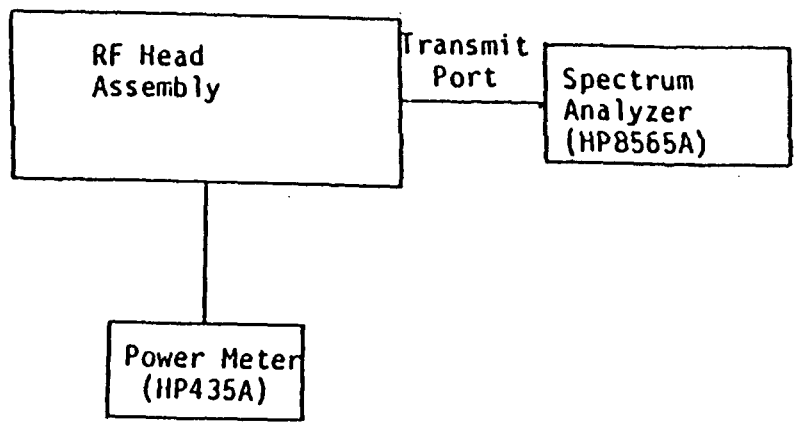

Figure 31a- Test Configuration to Measure the RF Power Level

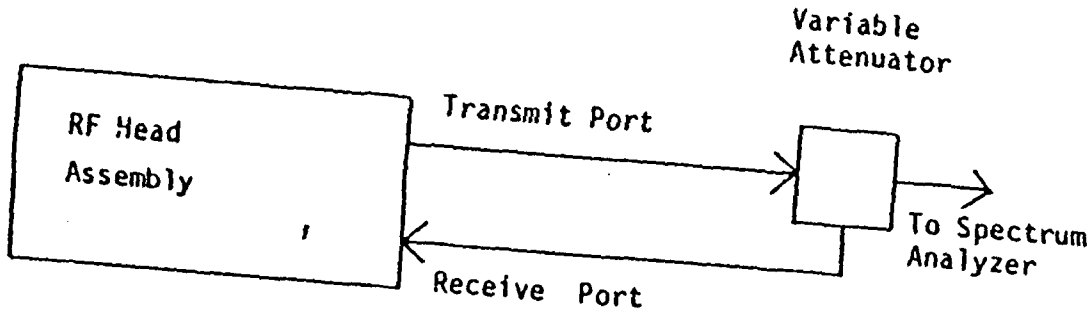

Figure 31b- Test Configuration to Measure the Minimum Detectable Signal

collected to determine the RF head stability over a period of 5 hours. The transmit power was measured by a power meter (HP-435A), while a spectrum analyzer (HP-8565A) was used to measure the calibration power. The measurement results are presented in Tables 10, 11 and 12. The data were taken at an equal time interval in the period of 5 hours. As seen from the tables, the power levels on both the horizontal and vertical ports are invariant with time. This is to say that the RF heads are putting out a stable power characteristic that is invariant with time. Comparing to the calculated values, these measured numbers are lower. This is caused by the reflections from the SMA type connectors in the system. Often, this type of connectors does not provide a 100 % reflection-free. There might be excessive loss of power through the connectors. Another contribution to the loss of power is the bending of the semi-rigid coaxial cable in making the interconnections in the system.

Determining the Minimum Detectable Signal

Background

As mentioned earlier, the strength of the return radar pulse is made to be proportional to the voltage level of the integrator output. The integrated values are interpreted as being saturated when the output of the sample and hold circuit is measured to be -11.0 Volts. Since the RPS is a gain modulated system, this voltage is maintained at a predetermined level by controlling the digital attenuator. The pre-determined value presently utilized is -2.5 Volts which could be changed in the future via the software [23]. This value assures that

Table 10. Power Measurements of the L-Band RF Head

Frequency: L-Band (1.6 GHz)

Transmitting Power

Vertical (dBm)	Horizontal (dBm)	Calibration Power
-8.0	-8.0	-48.0
-8.0	-8.0	-48.0
-8.0	-8.0	-48.0
-8.0	-8.0	-48.0
-8.0	-8.0	-48.0
-8.1	-8.0	-48.0
-8.1	-8.1	-49.0
-8.2	-8.2	-49.0
-8.2	-8.2	-49.0
-8.2	-8.25	-49.0
-8.25	-8.3	-49.0
-8.3	-8.3	-49.0
-8.3	-8.3	-49.0
-8.3	-8.3	-49.0
-8.3	-8.3	-49.0
-8.3	-8.3	-49.0

Table 11. Power Measurements of the C-Band RF Head

Frequency: C-Band (4.75 GHz)

Transmitting Power

Vertical (dBm)	Horizontal (dBm)	Calibration Power
-8.0	-8.0	-38.0
-8.0	-8.0	-38.0
-8.0	-8.0	-38.0
-8.0	-8.0	-38.0
-8.2	-8.2	-38.0
-8.1	-8.2	-38.0
-8.1	-8.1	-39.0
-8.2	-8.2	-39.0
-8.2	-8.2	-39.0
-8.2	-8.25	-39.0
-8.25	-8.4	-39.0
-8.4	-8.4	-39.0
-8.4	-8.4	-39.0
-8.5	-8.5	-39.0
-8.5	-8.5	-39.0
-8.5	-8.5	-39.0

Table 12. Power Measurements of the X-Band RF Head

Frequency: X-Band (10.003 GHz)

Transmitting Power

Vertical (dBm)	Horizontal (dBm)	Calibration Power
-17.0	-17.0	-26.0
-17.0	-17.0	-26.0
-17.0	-17.0	-26.0
-17.0	-17.5	-26.0
-18.0	-18.0	-26.0
-18.1	-18.0	-26.0
-18.1	-18.1	-30.0
-18.2	-18.5	-30.0
-18.5	-18.5	-30.0
-18.5	-18.55	-30.0
-18.55	-18.6	-33.2
-18.6	-18.6	-33.2
-18.6	-18.6	-33.2
-18.6	-18.6	-33.2
-18.65	-18.65	-33.2
-18.65	-18.6	-33.2

no saturation will occur in the operation of the RPS, primarily the IF receiver section.

Calculation of the Minimum Detectable Signal

To determine the minimum detectable signal, the digital attenuator is set to its minimum attenuation. A variable attenuator and a 30 dB coupler are connected to the transmit port of the RF head. The test configuration is shown in Figure 31. After it is being attenuated, the transmit power is measured using a spectrum analyzer (HP-8565A). At the same time, the output from the 30 dB coupler is fed back to the receiver in the radar head. This is done so to simulate the receiver antenna and the losses in the transmission medium. The variable attenuator is adjusted until the output of the sample and hold circuit is -2.5 Volts. When that point is reached, the minimum detectable signal is the power measured at the spectrum analyzer reduced by 30 dB. The measured minimum detectable signal for each of the radar head is listed in Table 13. From these measured values, an approximation of the radar cross section that is measureable by the RPS can be calculated. This is a measure of how sensitive the RPS is in terms of detecting a target. This is done by putting the appropriate system constants into the radar equation and solving for the RCS utilizing the minimum detectable power as the received power. Doing this, it is assumed that the return power is constant. The antenna gains were calculated based upon their operating frequencies, and both the transmit and receive antennas were assumed to have the same gain in each case. Approximate values of the RCS were computed at different

Table 13. Laboratory Measurement of the Minimum Detectable Signals and the Typical Power Output

	X-Band	C-Band	L-Band
Power transmitted	-24 dB	- 9 dB	- 8 dB
Minimum Detectable signal	-84 dB	-94 dB	-97 dB

ranges as they are shown in Table 14. The tables show how small a target can be detected by the RPS.

Saturation Analysis of the RPS

Background

The power analysis will be formulated with respect to the IF section of the system since the received signal is processed through the IF section. The objective of the analysis is to assure that there is no saturation occurring in the receiver section of the system while the RPS is acquiring data. The analysis will be conducted based on the specifications of the individual components in the IF section.

Power Analysis of the Receiver Section

To aid the calculations in the power analysis, a block diagram representation of the IF section is presented in Figure 32. The function of the receiver can be accurately described as the analog signal processing section. The accuracy of this analog signal processor depends on the fact that components are operating in their linear region. If saturation occurs in any component, some errors will be introduced, and the resulting processed signal is of little use. The approach to the power analysis is listed as follows:

1. Determine the maximum and the minimum signal magnitude at the input of the receiver section
2. Determine the input power or voltage limitations of all the components
3. Determine the power gain or loss of each component.

Table 14. Radar Cross Section Calculation for the Three Different Radar Frequencies Based upon a Constant Return Power. The Feet Measurements are the Ranges.

	S at 55 ft	S at 75 ft	S at 110 ft
L-Band	-45.13 dB	-41.09 dB	-35.65 dB
C-Band	-50.63 dB	-49.63 dB	-44.30 dB
X-Band	-33.81 dB	-29.77 dB	-25.27 dB

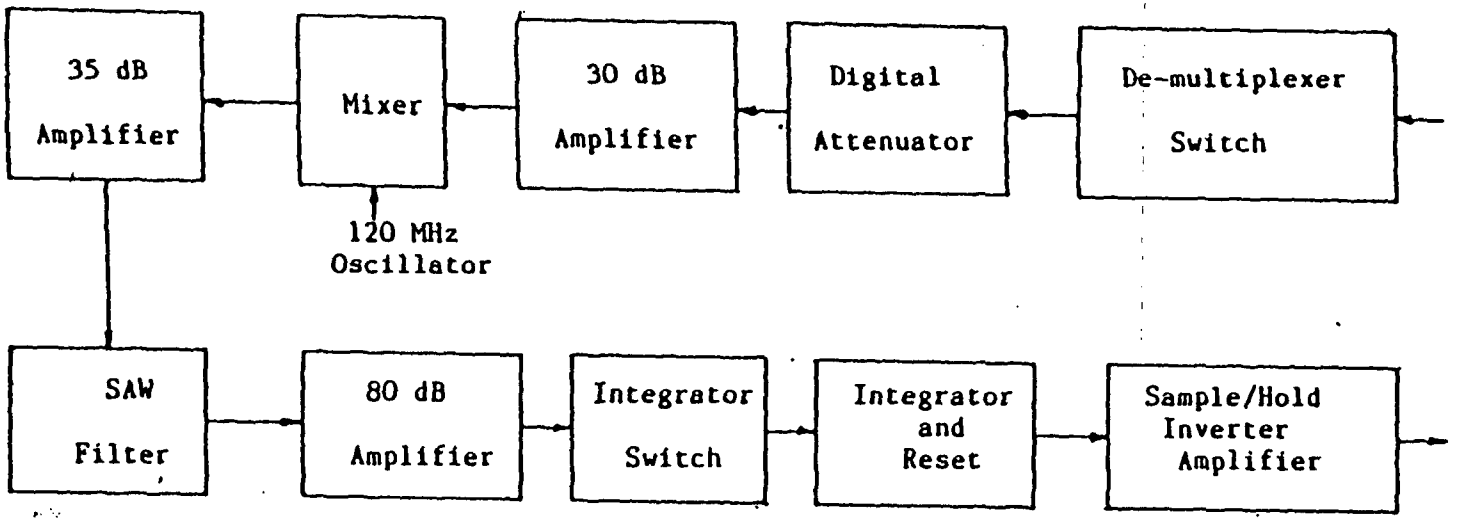

Figure 32 - The block diagram of the receiver section

4. Formulate the power and voltage calculation necessary to determine saturation level of each component.

The level of power that will be "seen" by the receiver in the RPS is in the order of -18 dBm maximum magnitude while for the minimum, it is about -80 dBm. The range of the received signal is chosen to take into consideration the types of targets that the RPS will be analyzing [11]. The input power or voltage limitations of each component were obtained from the specifications provided by the manufacturers. The significant parameters of each component that is needed for the power analyzis are summarized in Table 15. For the power analysis, each power parameter will be designated a degree of maximum, typical, and minimum values.

Appendix B lists the steps taken to arrive at the following conclusion. From the analysis that is performed, it is determined that the receiver in the IF section will not saturate if there is an automatic gain controller to govern the incoming signal to the receiver section. Thus, the incoming signals must be attenuated if they are too large, or they it must be amplified if too small. The digital attenuator must then be controlled according to the power level of the incoming signal. The digital attenuator needs to be set to its maximum attenuation level upon receiving the worst case input signal of -18 dBm (measured at the input of the receiver section). A Digital Automatic Gain Controller (DAGC) was implemented to assure that the receiver section does not operate in the saturation region [23].

Table 15. Summary of the Component Parameters for the Power Analysis

I.	For each transfer switch, the Micronetics 2D-1-L-TTL, the insertion loss is 0.2 dB maximum.	
II.	Digital Attenuator	: DAICO DA0185-1
	RF power	: +10 dBm continous wave maximum +20 dBm non-destruct
	Insertion loss	: 4 dB at 60 MHz (typical) 6 dB maximum
	Attenuation range	: 0 to 63.3 dB
III.	30 dB amplifier	: RHG ICFT6040
	Maximum power gain	: 31 dB
	Power output	: 0 dBm at 1 dB compression
IV.	Mixer	: Mini Circuits ZLW-1-3
	Conversion loss	: 6.5 dB typical 8.5 dB maximum
	Input signal	: +1 dBm at 1 dB compression
	Input power	: 50 mW absolute
V.	35 dB amplifier	: Amplica AVD714201
	Power gain	: 35 dB
	Power output	: +5 dBm at 1 dB compression
VI.	SAW filters	: Rockwell 524-3003-010
	Insertion loss	: 45 dB
VII.	80 dB amplifier	: RHG EVT60-G11DM
	Power gain	: 80 dB maximum
	Power output	: +15 dBm at 1 dB compression
VIII.	Integrator switch	: Teledyne Crystalonics CDA-18
	Input voltage	: -10 V to +5 V
	On resistance	: 20 Ohms minimum, 35 Ohms typical and 50 Ohms maximum
XI.	Integrator circuitry	: Analog Device AD507
	Input voltage	: + or - 11 Volts range
X.	Each coaxial line	:
	Insertion loss	: 0.10 dB minimum 0.20 dB typical 0.40 dB maximum

Signal to Noise Ratio Calculations

Background

Since noise is the main factor that limits the receiver sensitivity, it is necessary to obtain some means of describing it quantitatively. Noise is unwanted electromagnetic energy which interferes with the ability of the receiver to detect the return signal. There are many different types of noises. The noise may originate within the receiver itself, or it may be introduced by the receiving antenna along with the return signal.

Thermal Noise - One of the unavoidable types of noise generated by the thermal motion of the conducting electrons in the ohmic parts of the receiver is called thermal noise or Johnson noise [17]. The amount of this noise is directly proportional to the temperature of the ohmic portions of the receiver and the receiver bandwidth [12].
The introduced thermal noise is given by:

$$= k \times T \times B \qquad (10)$$

where : k = Boltzmann's constant

T = operational temperature in degrees Kelvin

B = the receiver bandwidth in Hertz

For radar receiver of the superheterodyne type as in the case of the RPS, the receiver bandwidth is approximately that of the IF stages.

Noise Figure - The noise figure is often time used as a figure of merit for the performance of an amplifier. The noise figure itself could be written as a quantity of

Table 16. Specifications of the Parts in the Receiver Section Considered in the Noise Analysis

PARTS	GAIN (dB)	GAIN (W/W)	N.F. (dB)	N.F. (W/W)
30 dB amplifier RHG ICFT 6040	30	1000	2.0	1.585
35 dB amplifier Amplica AVD714201	35	3162.27	1.7	1.479
80 dB amplifier RHG EVT60G11DM	80	1 x 10	2.0	1.585
Mixer Mini Circuit ZLW13			9.0	7.943

The mixer has a conversion loss that is being cosidered which is more dominant that that of the Noise Figure (NF). The quantity of gains that are presented are of power gain.

$$NF = \frac{\text{noise from a practical receiver}}{\text{noise from an ideal receiver at a standard temperature}}$$

Signal-to-Noise Ratio Calculation

The approach of obtaining the SNR of the receiver section is taken as follows:

1. Determine the input power constraint for all the components
2. Obtain the gain and noise figure of each component
3. Perform necessary calculations to determine the SNR

Knowing the noise figure and other pertinent specification for each of the components as listed in Table 16, an expression of the SNR of the receiver section may be evaluated assuming the worst input signal that is expected. The calculations and the necessary equations needed to arrive at the SNR of the receiver is presented in Appendix D. As shown, with the worst case input signal, the SNR is calculated to be 11.8 dB while for the best case input signal, the SNR is 20.04 dB. Radar systems in general have an SNR of 12 dB in average. The calculated value of SNR is seen to be an acceptable value as governed by the specifications imposed on the RPS.

Internal Calibration

Background

Internal calibration of a scatterometer system permits the determination of relative scattering coefficients with the precision appropriate to the calibration and the number of independent samples average [24]. In general, there are two different types of internal

calibration that can be utilized--the method of independent or separate calibration of different parts in the system and the ratio method. The method utilized in the RPS is the ratio method. The ratio method is a better approach simply because there is less probability of error occurring in the calibration process. Recall that equation (3-3) shows the relationship of the radar cross section as being proportional to the quantity of received and transmitted power. If the ratio of the power is known, the radar cross section may be determined without measuring other characteristics of the system except for the gains of the antennas. Furthermore, there is no need for separate measurement of transmitter power and the receiver characteristics if a portion of the transmitted signal is used to calibrate the receiver. Figure 33 shows the components in the RF sub-assembly during the calibration process. As seen, a portion of the transmitted power is being routed through the receiver section via a coupler. This signal is then sent to the IF section to be processed as if it were a return radar signal. Thus, the readings of the return radar signals are always in reference to the transmitted power, and the calibration power. The ratio method of calibration as implemented in the RPS introduces little or no error at all as far as system induced error is concerned. The calibration signal is a part of the transmitted signal which goes through the same path as a return radar signal does. So, components' losses will be the same in all cases,which will introduce no error as far as the signal path is concerned.

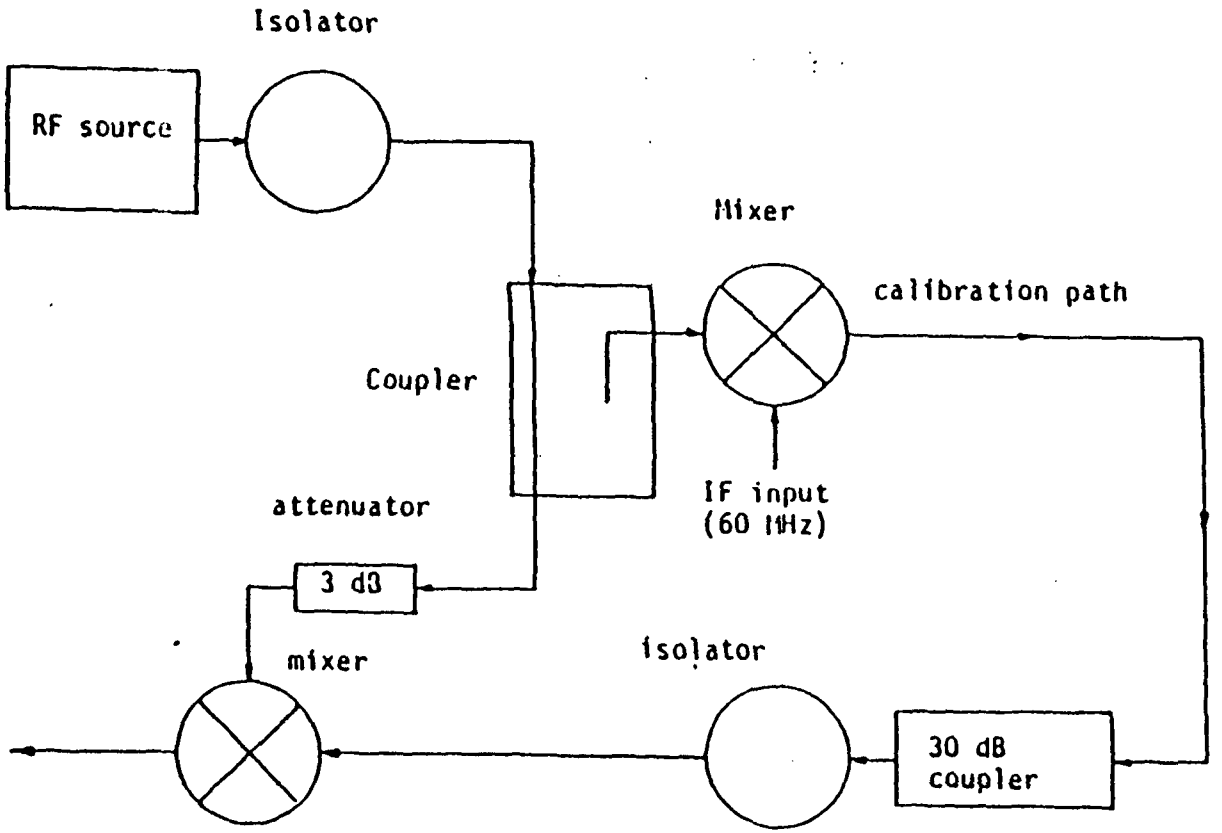

Figure 33. The Components in the RF Head Assembly in Calibration mode.

Calibration Procedures in the RPS

As mentioned earlier, the method of internal calibration implemented in the operation of the RPS is the ratio method. The ratio expression implies that the calibration measurements are referenced to the ratio of the input power to the output power. The components that are involved in the calibration procedure are presented in Figure 33. It shows the elements in the RF section as far as generating the signals with respect to the particular frequency of operation. Basically, signal from the source, after properly isolated, is sent through a coupler as shown. The signal that is being attenuated goes through similar components as if it were the receiving signal. However, losses in this case are made to be constant, that is, the losses that are due internally only, such as the mixer conversion loss, cable loss, and isolator loss. Both of these signals are then multiplied utilizing a mixer, the result of which is sent to the IF section. This resultingsignal is treated by the IF section similarly to a received signal. Thus, this calibration procedure is taking into account a reference point in terms of transmitted power and the system losses. After being processed in the IF section, the calibration signal which is termed as the calibration power used in calculation of cross section measurement, the procedure of which is shown in equation (3-9b). The calibration signal path and the operating signal path are similar in that they go through the same components. The only difference is that the calibration procedure possesses a lower power level from the operating signal. The calibration signal can be thought of as a simulation of a received signal from a known target. Because the RPS

has a very short range in its operation, it is permitted to use the ratio method in the scheme of the internal calibration procedure as outlined above. The simulation of the calibration signal as the received signal is done by utilizing a delay line method where the delay is the losses in the components and in the cable. The delayed signal is then coupled back into the receiver section in the IF sub-assembly. The signal is coupled into the receiver section at an equivalent range that is outside that used for the target, but is close enough that the receiver characteristics are similar. This scheme of internal calibration procedure in the RPS introduces little or no errors in the measurement accuracy. It can be pointed out though, that the placement of the range for the calibration mode must be of that for target to achieve system accuracy.

External Calibration Procedures

Background

The accuracy of the internal calibration procedures described previously depends in part upon the accuracy with which the system functions and antenna gain pattern are known. To obtain a better system accuracy and to determine the constants that are shown in as the system constants, it is often desirable to calibrate a radar system externally by measuring the return power from a target with known cross section. For a truck mounted system such as the RPS, the external calibration procedure is presented in Figure 34. It could be noted that the measurement precision is determined by the magnitude of the radar cross section of the calibration target relative to the cross

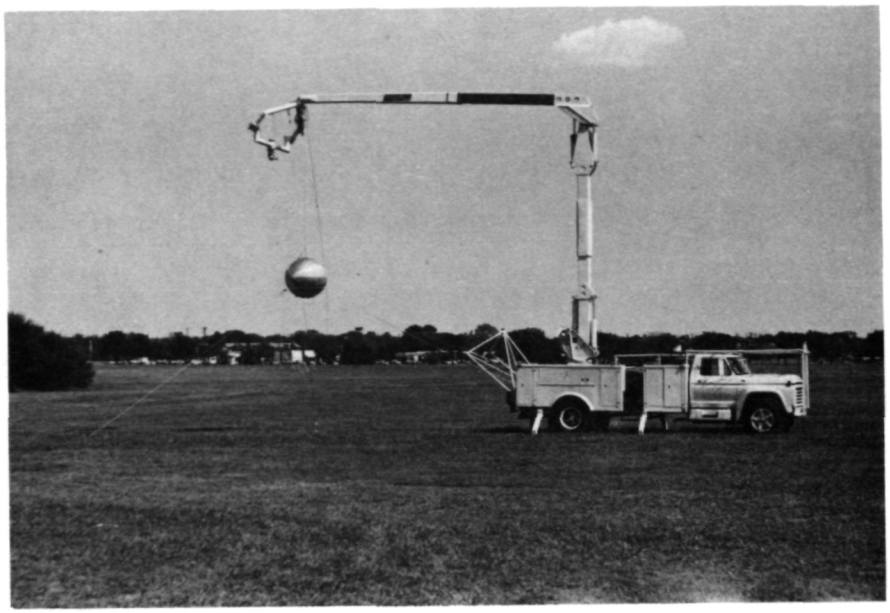

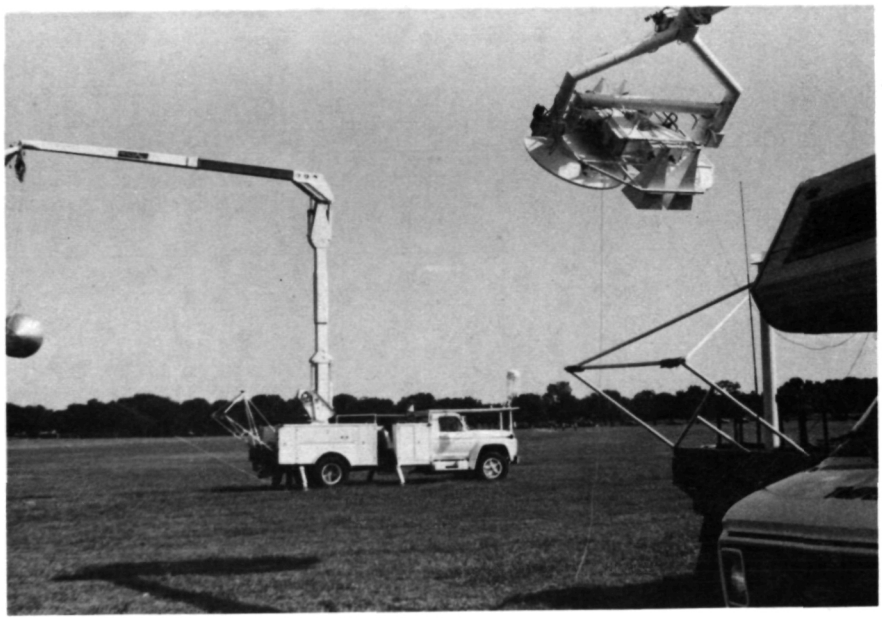

Figure 34 - The External Calibration Test Configuration

section of the background. Thus, to get a better measurement precision, it is desirable for the background of the calibration target to be covered with non-reflecting material.

Calibration Targets

There are many types of calibration targets that could be used in controlled experiments. The RPS is a mobile radar system which is mounted on a truck positioned in a field. For the purpose of calibration, the calibration targets need to have cross sections that are insensitive to the orientation of the radar system. The different types of the calibration targets which are used in the external calibration of the RPS include:

1. Flat Circular Plate (2' diameter)
2. 12" Luneberg-lens
3. 4' diameter aluminum sphere
4. Corner reflector

The characteristics of the calibration targets are summarized in Table 17.

Measurement Results

From the external calibration procedures, system constants are obtained for each frequency and polarization of operation. Ideally, the system constants should be the same for all calibration targets. The resulting system constants are shown in Table 18. A major cause of the inaccuracy or discrepancies in the results is the method of aligning the RPS with the targets. As seen from Figure 34, the target is placed upon a boom truck placed at some height. A slight

misalignment of the target could result in differences in the system constant calculations.

Antenna

Background

An isotropic antenna is a hypothetical antenna that radiates energy equally in all directions. In actuality, such an antenna does not exist because of the nature of electromagnetic fields. The directional function that describes the relative distribution of the energy is often referred to as the antenna radiation pattern. Antennas that are utilized in the RPS possess a reciprocal behavior such that the radiation patterns are the same for transmission and reception [8].

Antenna Patterns

Associated with the electric and magnetic fields encountered in the antenna is a Poynting vector describing the direction of propagation of the electromagnetic wave. In the time domain, the time-average Poynting vector [25] which is frequently called the power density, is given by $S = 0.5 \times Re \{ E \times H^* \}$. Most of the antenna parameters such as the directivity, beamwidth, and effective area are defined by the diretional dependence of the magnitude of S. The energy radiation from an antenna is of spherical nature. The spherical coordinate system is shown in Figure 22 is usually used to present antenna pattern plots. These antenna plots are depending upon variables r, θ and ϕ referred to as the range, elevation angle, and azimuth angle respectively. The directional pattern of an antenna is a

Table 17. Characteristics of the Calibration Targets

Type of Target	Maximum Cross Section
Rectangular Plate	$4\pi A^2/\lambda^2$
Circular Plate	$4\pi A^2/\lambda^2$
Sphere	A
Corner Reflector	$\pi l^4/3\lambda^2$ $16\pi A_c^2/9\lambda^2$
Luneberg-lens	$4\pi A^2/\lambda^2$

where A is the area of the surface
λ is the frequency of operation

Table 18. Measurement Results of the External Calibration Procedures. The numbers obtained are in decibels indicating the System Constants.

	L BAND		C BAND		X BAND	
	HH	VV	HH	VV	HH	VV
4' Sphere	-73.83	------	-63.12	-65.62	-40.5	
12" lens	-64.56	------	-60.54	-52.55	-----	-----
2' dia. plate	-56.72	-62.72	------	------	-27.2	-35.2
corner reflector	-67.40	-69.40	------	------	-30.46	-38.0

plot of the relative power density as a function of direction with the distance from the radiation source held constant. Instead of using the power density $S(r,\theta,\phi)$ to describe the directional properties of an antenna, it is sometimes more convenient to use an r independent function known as the radiation intensity, or radiation pattern $F(0,0)$. The representation of the radiation pattern of an antenna is sometimes given in rectangular coordinate systems, to permit the pattern to be expanded horizontally. A relative power pattern of the antenna sets utilized in the RPS is given in Figures 35 and 37.

Cross Polarization Isolation

When the RPS is transmitting in horizontal polarization while receiving in vertical polarization, it is called cross polarization measurement. The cross polarization isolation of the antenna sets describes how well the cross polarization measurement could be made. From Figure 35 through 37, the cross polarization isolation of each antenna could be calculated. These values, tabulated in Table 19, correspond to how well the antenna is isolated from one polarization to the other. The figure of merit of these antennas in terms of their cross polarization is very important in the process of analyzing the depolarization phenomena in radar remote sensing [15].

Focusing Height

Since the RPS is utilizing a dual antenna system, the antenna sets need to be in focus with each other. From the received power as calculated from equation (3-3), the following procedures are performed

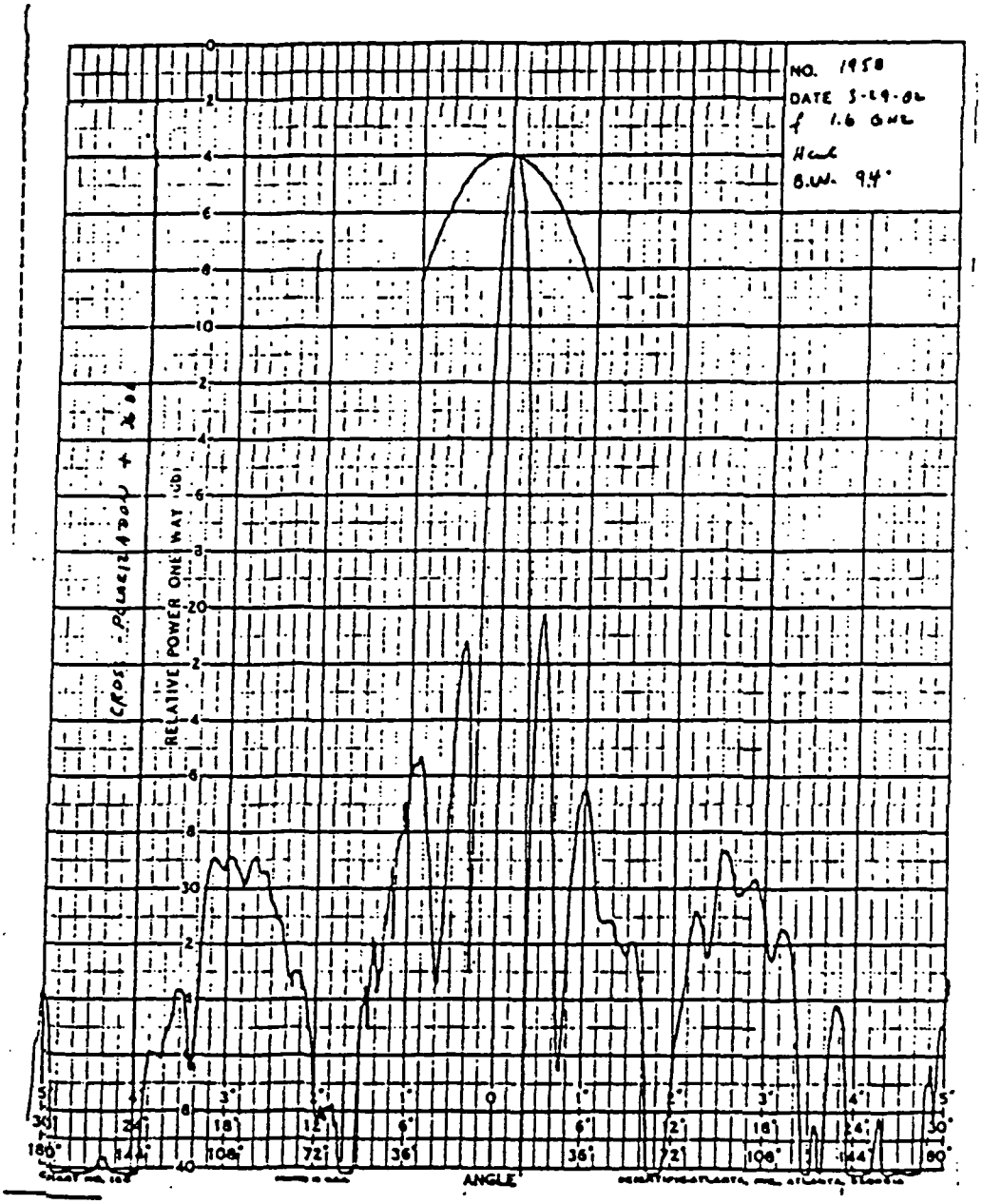

Figure 35a- The Pattern for the L-Band Antenna
(H-cut)

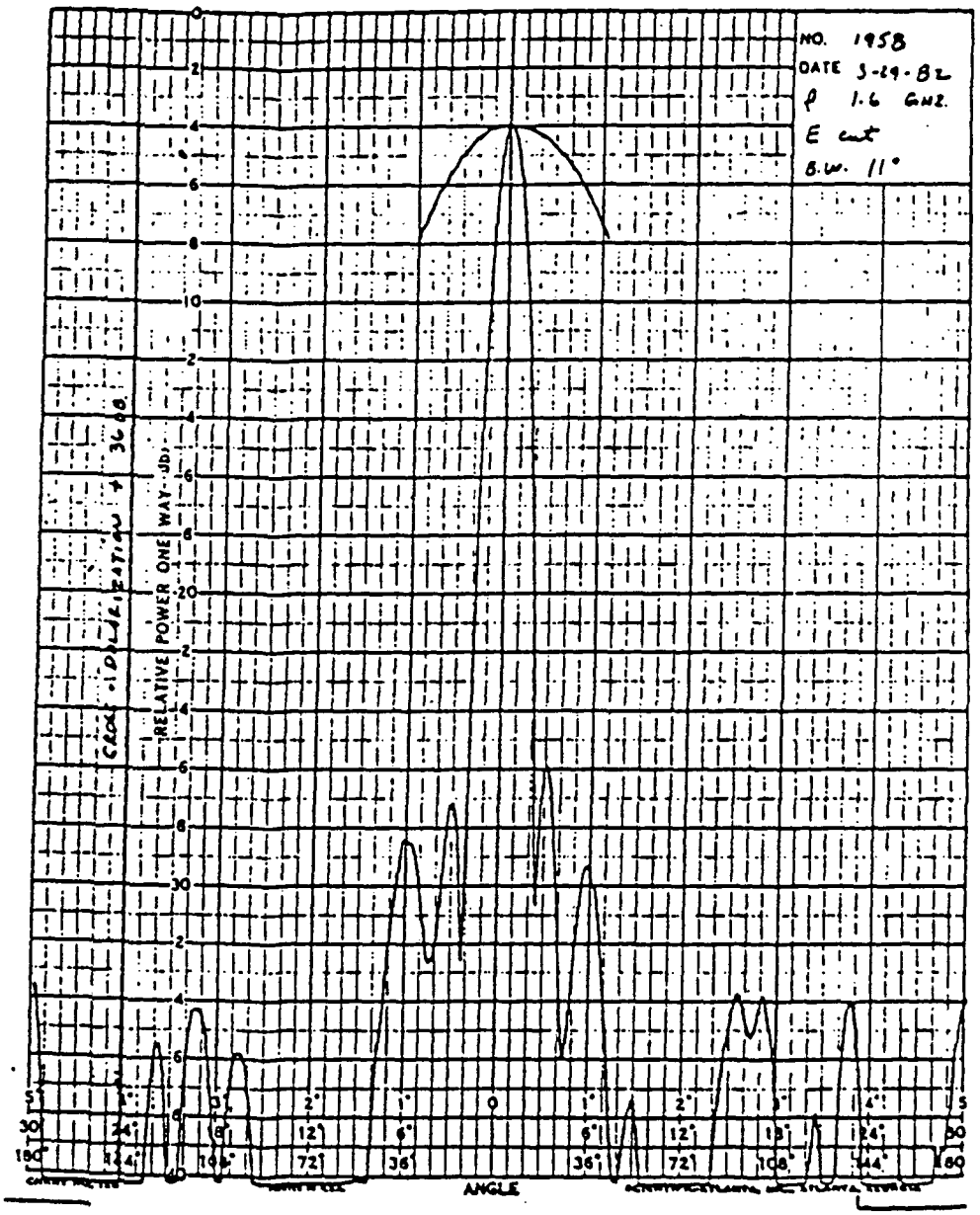

Figure 35b- The Pattern for the L-Band Antenna
(E-cut)

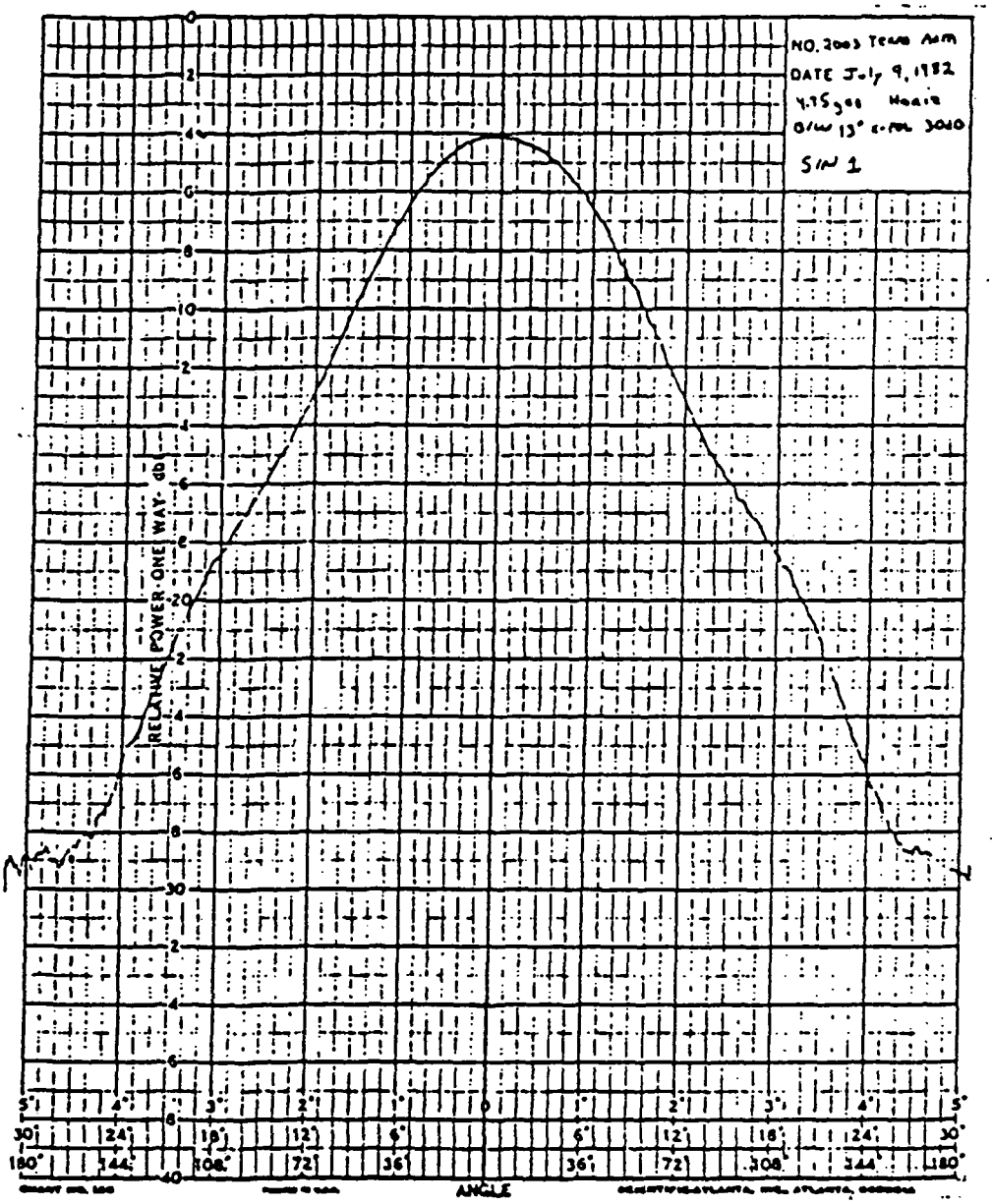

Figure 36a- The Pattern for the C-Band Antenna (Horizontal)

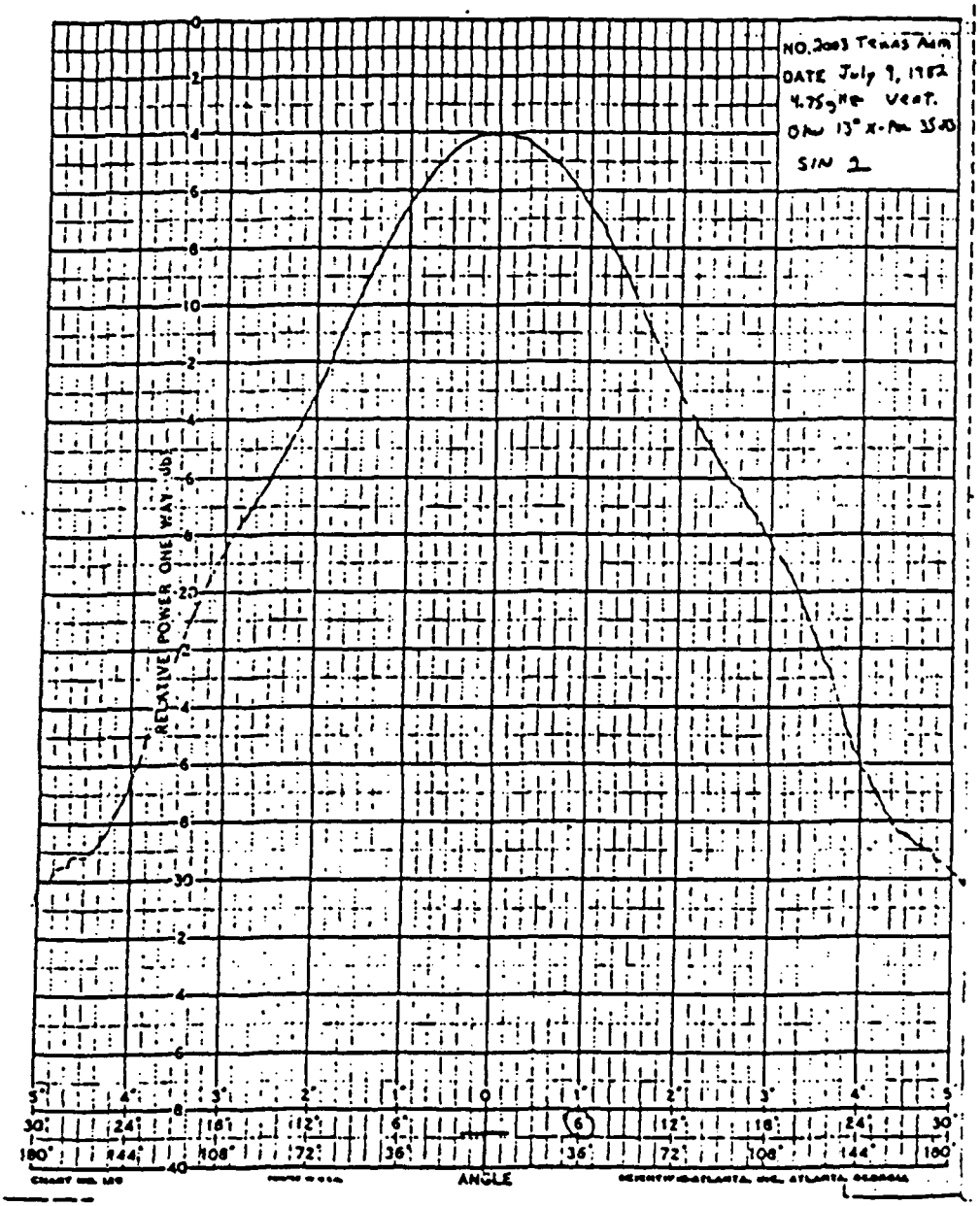

Figure 36b- The Pattern for the C-Band Antenna (Vertical)

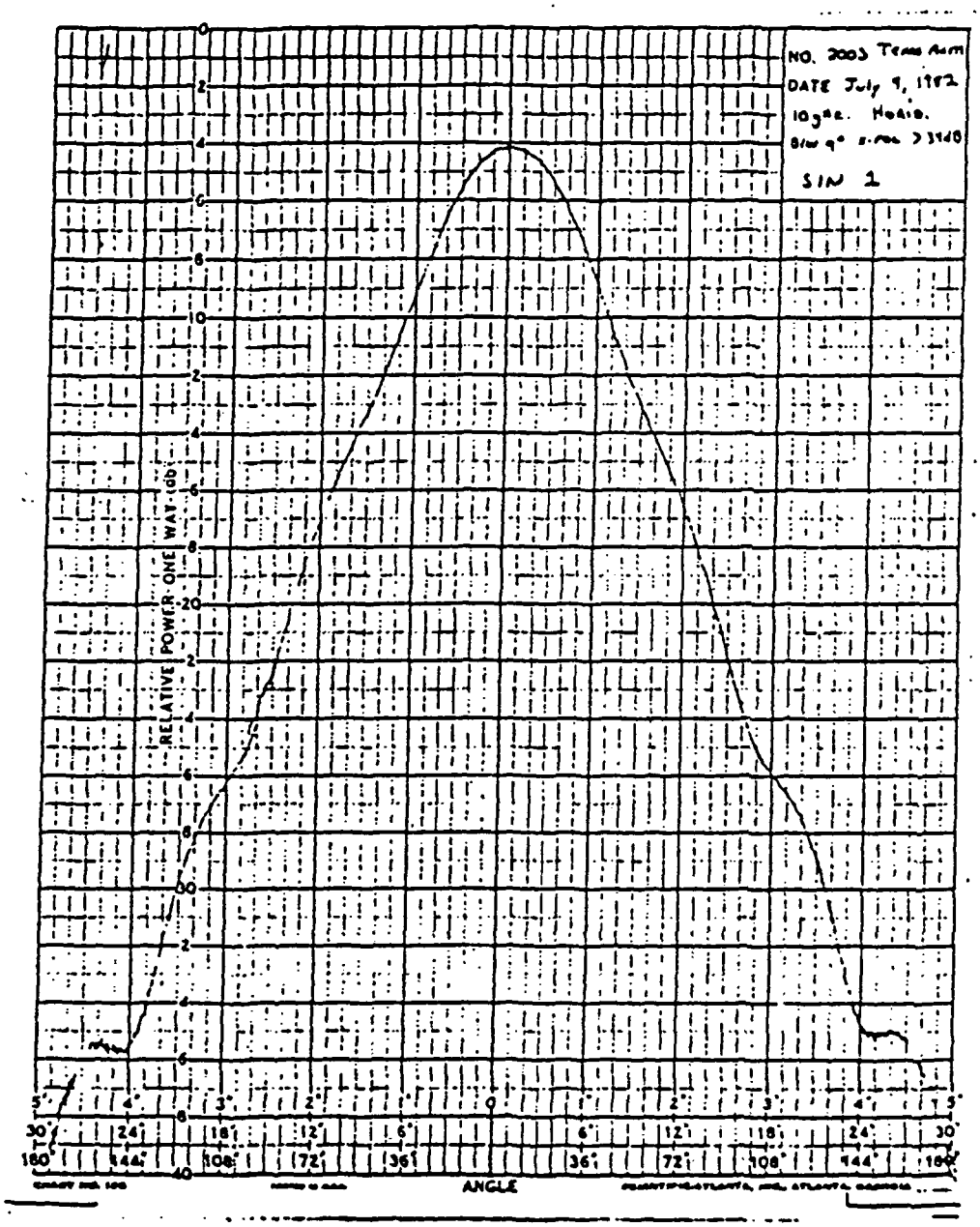

Figure 37a- The Pattern for the X-Band Antenna (Horizontal)

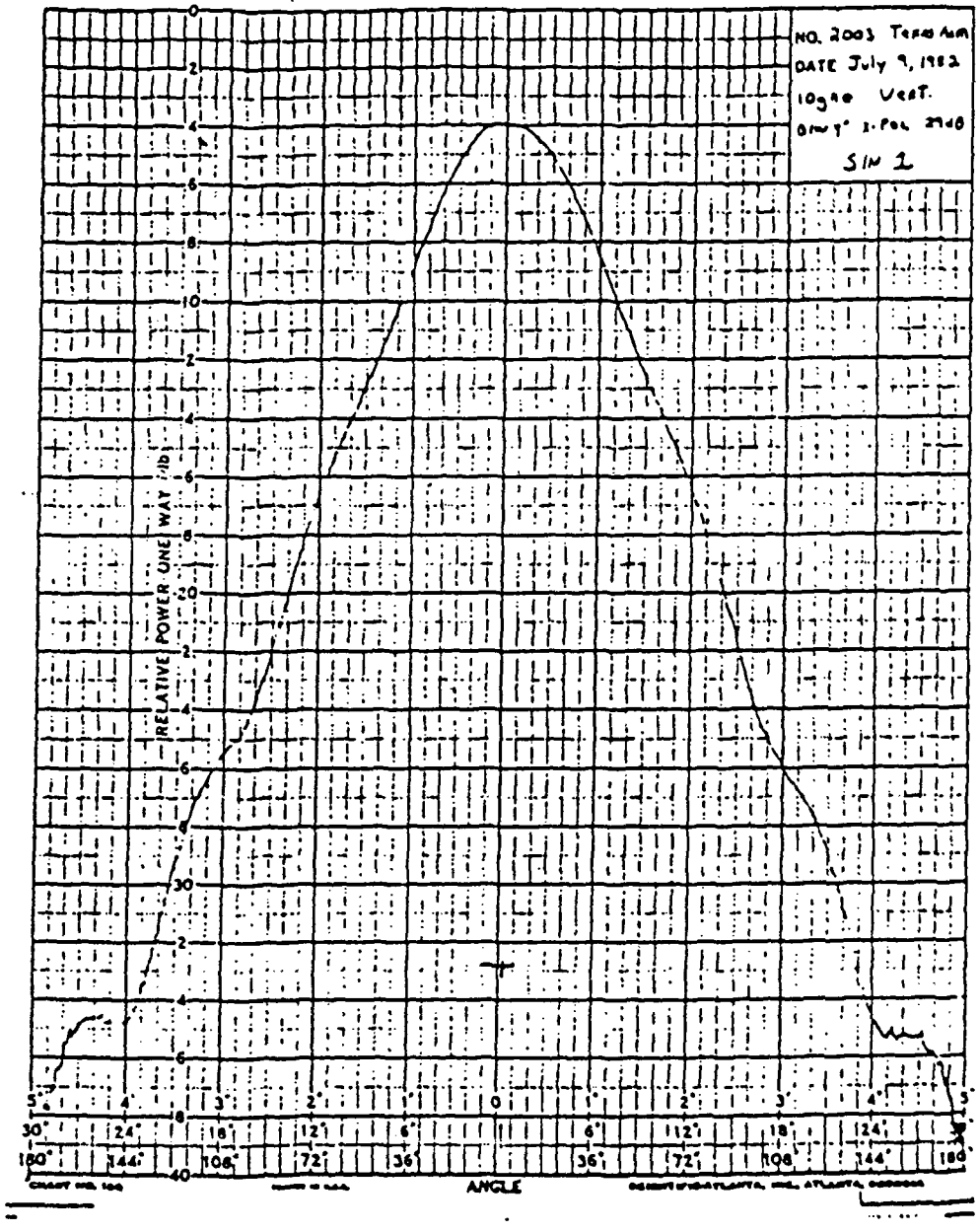

Figure 37b- The Pattern for the X-Band Antenna (Vertical)

Table 19. Cross Polarization Isolation Calculation for the Antenna Pair in the RPS

	Transmitting Vertical	Horizontal	Frequency
Parabolic Dish #1	34 dB	34.5 dB	1.6 GHz
Parabolic Dish #2	35 dB	35 dB	
Horn #1	26 dB	25.5 dB	10.0 GHz
Horn #2	25 dB	25 dB	
Horn #3	23 dB	23 dB	4.74 GHz
Horn #4	23 dB	24 dB	

to arrive at the best suitable focusing height of the antennas.

The field of view of the antenna is approximated to have an area of an ellipse as depicted in Figure 38. Knowing the beamwidths of the antennas and their heights, the area could be calculated. When the antenna pair is in focus with each other, their fields of view will overlap. The method of calculating the focusing height of the antenna pair will approximate the amount of overlap such that transmission and reception will be done efficiently. The method used to arrive at the focusing height is by approximating the field of view of the antenna pair to be an isosceles triangle as shown in Figure 39. Knowing the constants such as the separation distance between the antenna pair and the beamwidth, the focusing height could be calculated. In actuality, what will be calculated is the percentage of area that is covered by the antenna pair. Thus, the higher percentage of area covered by the field of view of the antennas, the better they are in focus. The values of these percentages at different focusing heights are presented in Table 20. As seen from the table, the height of 75 feet proves to be the best focusing height.

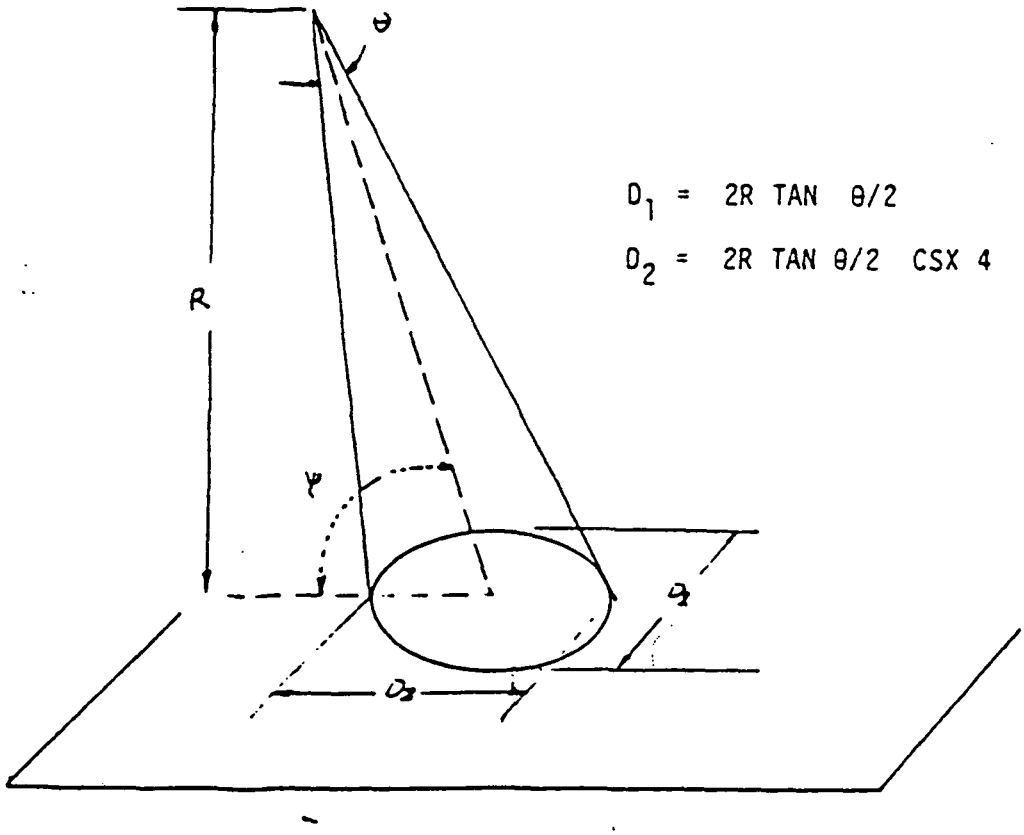

Figure 38. Approximation of the area intercepted by the target.

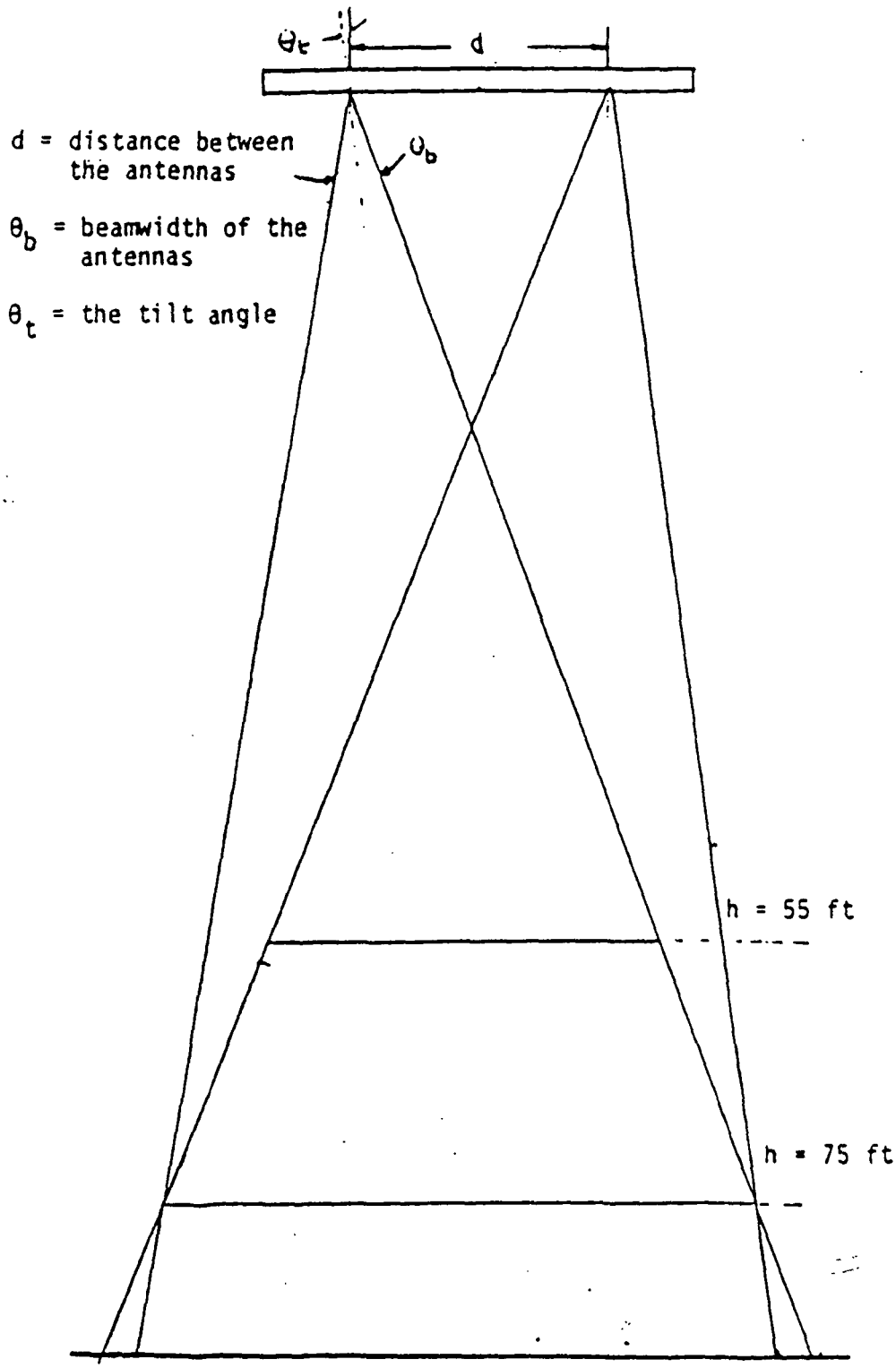

Figure 39. Approximation method for focusing the antenna pair at some height h.

Table 20. Percentage of Area Intercepted by Both of the Antennas in the Set

Viewing Angles:		Percentage of Intercepted Area 0°	60°
Focusing Height:	70 ft (21 m)	90%	88%
	75 ft (23 m)	92%	92%
	80 ft (24 m)	87%	90%

CONCLUSIONS AND RECOMMENDATIONS

The Remote Sensing Center (RSC) at Texas A&M University has developed a mobile radar system for scientific investigations relating to backscatter electromagnetic energy from earth natural scenes. The RSC also developed a similar radar system for NASA Goddard Space Flight Center. This study involved the assembly of the RPS and laboratory measurements to determine performance specifications of the RPS. The RPS is a gain modulated short pulse radar utilizing pulse compression technique on transmit and receive.

This document presents an analysis of a short pulse RPS ground based radar system. The emphasis on this report has been a documentation of the hardware, analysis of system performance, laboratory verification of critical system parameters, and the design of the data reduction algorithm pertinent to this system.

Operational Analysis of the RPS

The analyses performed were concentrated in two major areas:

1. The performance of the IF section was a critical step in the documenting the overall system performance. Measurements were made to identify the minimum detectable signal level. These measurements were in close agreement with the analytical calculations performed prior to this research effort.

2. The polarization performance of the antennas were also assessed through previous analytical calculations which were done aside from

this study. The measured polarization characteristics of the three antenna sets were used to calculate the polarization feedthrough in the orthogonal polarization plane. The results indicate that all antenna sets have at least 29 dB isolation across the first null to first null beamwidth. In the case of the L-band antenna, the isolation approaches 36 dB. Calculations indicate that the 29 dB isolation is sufficient to recover depolarized radar cross section on the order of -30 db [13].

The configuration of the antennas was also analyzed to determine the effect of focusing on scattering coefficient recovery. By focusing the antenna sets at a height of 75 feet, the modulation of the scattering coefficient was 3 dB across the entire incident angle range of 0 to 60 degrees.

The basic data reduction algorithm is also included in this report. The reduction equations include an incorporation of both the internal calibration measurements and the external measurements on known targets. This allows the measurements of unknown targets to be reduced to absolute cross section.

Recommendation for Future Work

Area of future research work would include the investigation of the following:

1. Improvement of the system capability to recover scattering coefficients lower than -30 dB. Calculations of system performance have shown that the RPS is capable of making measurements of target cross section on the order of -30 dB. Depolarized radar cross sections often are less than -30 dB,

therefore a capability to recover scattering coefficients lower than -30 dB is desirable.

2. Development of methods for using external known targets for use in absolute calibration. Both point targets and area extensive targets were utilized in attempting to absolutely calibrate the RPS. There are problems with each. A detailed study should be undertaken to develop a procedure and identify sources of error in absolute calibration of the RPS.
3. Investigate the possibility of recovering phase and amplitude scattering information using a coherent radar. The data acquisition method employed in the RPS is the averaging of data measurement method. The cross section of a particular target can be described by a scattering matrix which include the magnitude and the phase associated with it. With the method employed in the RPS, the phase term in the matrix is being averaged out such that there is no phase expression. In future remote sensing experiments the total scattering information in terms of the amplitude and the phase associated with it will be important. Thus, there is a need to determine how the RPS could be modified in order to recover the phase information.
4. Incorporate the data reduction algorithms on the data acquisition computer. At the present, the RPS has a computer system that gathers data that are being collected. As an improvement to the system, the data reduction algorithms

should be implemented on the computer such that an immediate translation of the data could be obtained while testing the RPS in the field.

REFERENCES

[1] Merril L. Skolnik, Introduction to Radar System, McGraw-Hill Company, New York.

[2] Fawwaz T. Ulaby, "Scatterometer Cross-calibration Experiment," Technical Report #589-1, The University of Kansas Center for Research, Inc., Lawrence, Kansas, 1982.

[3] Buford Randall Jean, "Multibeam Formation Techniques for Synthetic Aperture Radar," Technical Report RSC-99, Remote Sensing Center, Texas A&M University, College Station, Texas, 1978.

[4] Philip N. Slater, Remote Sensing, Optics and Optical Systems, Addison-Wesley Company, Massachusetts 1980.

[5] H. W. Hayward, Introduction to Radio Frequency Design, Prentice Hall Company, Englewood Cliffs, New Jersey, 1982.

[6] George T. Ruck, Radar Cross Section Handbook, Plenum Press, New York, 1970

[7] S.N. Van Voorhis, Microwave Receivers, Dover Publications, New York, 1946.

[8] Gary A.Thiele, Antenna Theory and Design, John Wiley & Sons, New York, 1981

[9] Herbert L. Krauss, Solid State Radio Engineering, John Wiley & Sons, New York, 1980.

[10] Fawwaz T. Ulaby, "Statistical Properties of The Radar Scattering Coefficient of Agricultural Crops," Technical Report #117-76, The University of Kansas Center for Research, Inc., Lawrence, Kansas, 1979.

[11] Fawwaz T. Ulaby, "Radar Return From a Continuous Vegetation Canopy," Technical Reports, The University of Kansas Center for Research, Inc., Lawrence, Kansas, 1975.

[12] Allen W. White, "A Dual Polarized X-Band Pulse Radar for Ground Based Electromagnetic Scattering Experiment," Technical Report RSC-94, Remote Sensing Center, Texas A&M University, College Station, Texas, 1978.

[13] Andrew J. Blanchard, "Volumetric Effects in the Depolarization of Electromagnetic Waves Scattered from Rough Surfaces," Technical Report RSC-83, Remote Sensing Center, Texas A&M University, College Station, Texas, 1977.

REFERENCES (Continued)

[14] Andrew J. Blanchard, "Earth/Land Radar Models," Technical Report RSC-104, Remote Sensing Center, Texas A&M University, College Station, Texas 1979.

[15] Andrew J. Blanchard, "Antenna Effects in Depolarization Measurements," Technical Report RSC-119, Remote Sensing Center, Texas A&M University, College Station, Texas, 1979.

[16] David K. Barton, Radar System Analysis, Prentice Hall, Inc., Englewood Cliffs, New Jersey, 1965.

[17] J. J. Freeman, Principles of Noise, John Wiley & Son, Inc., New York, 1958.

[18] H.E.G. Jeske, Atmospheric Effects on Radar Target Identification and Imaging, D. Reidel Publishing Company, Boston, 1975.

[19] S. A. Hovanessian, Radar Detection and Tracking Systems, Artech House, Dedham, Massachusetts, 1973.

[20] Christian G. Backman, Radar Targets, Lexington Books, Lexington, Massachusetts, 1982.

[21] J. W. Crispin and K. M. Siegel, Methods of Radar Cross Section Analysis, Academic Press, New York, 1968.

APPENDICES

APPENDIX A

PULSE COMPRESSION AND MATCH-FILTERING

Pulse Compression Background

Pulse compression is a technique that allows a radar system to utilize a long pulse to achieve large radiated energy, but at the same time obtaining the range resolution of a short pulse [1]. This is accomplished by employing frequency modulation to widen the bandwidth of the signal. While amplitude modulation is possible, it is seldomly used. The received signal is processed in a matched filter [26] that compresses the long pulse. This method is of interest when the peak power required by a short-pulse radar system cannot be achieved with a practical transmitter.

The pulse compression technique is attractive because of the following advantages:

1. Range resolution: It is easier to separate multiple targets in the range coordinate rather than in angle.
2. Range accuracy: If a radar system is capable of good range-resolution, it is also capable of good range accuracy.
3. Clutter reduction : A short pulse increases the target to clutter ratio by reducing the clutter contained within the resolution cell with which the target competes.
4. Multipath resolution: Sufficient range-resolution permits the separation of the desired target returned energy from those echoes that arrive from scattering of a longer path.

Pulse compression is a method of achieving most of the benefits of a short pulse while keeping within the practical constraints of the peak power limitation.

The pulse compression ratio is a measure of the degree to which the pulse is compressed. It is defined as the ratio of the uncompressed pulse width to the compressed pulse width. It is also sometimes defined as the product of the pulse spectral bandwidth and the uncompressed pulse width. The pulse compression ratio is greater than 1 in magnitude with typical values ranging from 100 to 300. There are many types of modulations used for pulse compression, but specifically the one used in the RPS is the linear frequency modulation.

Linear FM Pulse Compression

The basic concept of the linear Frequency Modulated (FM) pulse compression radar was described by R.H. Dicke, in a patent filed in 1945 [26]. The basic system employing the linear FM pulse compression is presented in figure A1. This basic radar system contains a transmitter that is frequency modulated and the receiver contains a pulse-compression filter. The transmitted waveform is of a rectangular pulse of constant amplitude A with T as its duration. Figure A2 represents the signal characteristics in this radar system. The frequency increases linearly from f1 to f2 over the duration of the pulse. Upon reception, the frequency-modulated return signal is passed through a pulse-compression filter, which is designed so that the velocity of propagation through the filter is proportional to frequency. When this filter is a dispersive delay line, its operation is as speeding up the

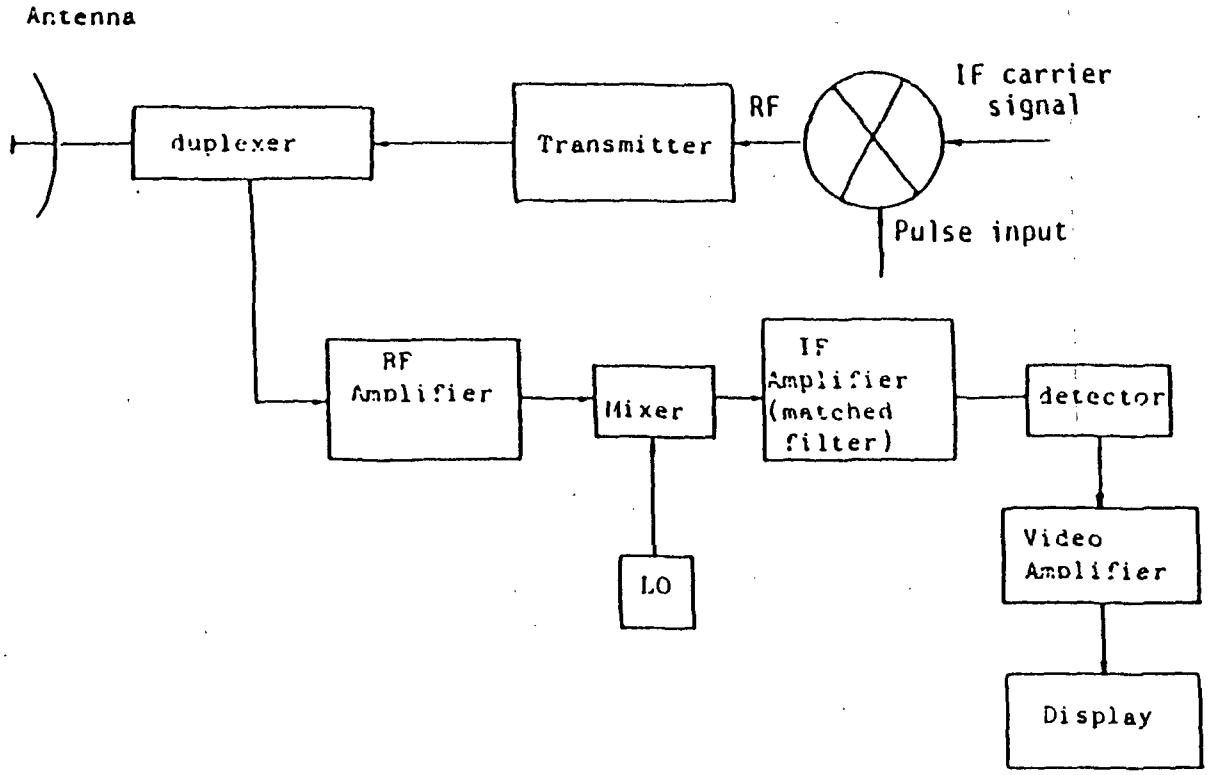

Figure A-1. Linear FM Pulse Compression.

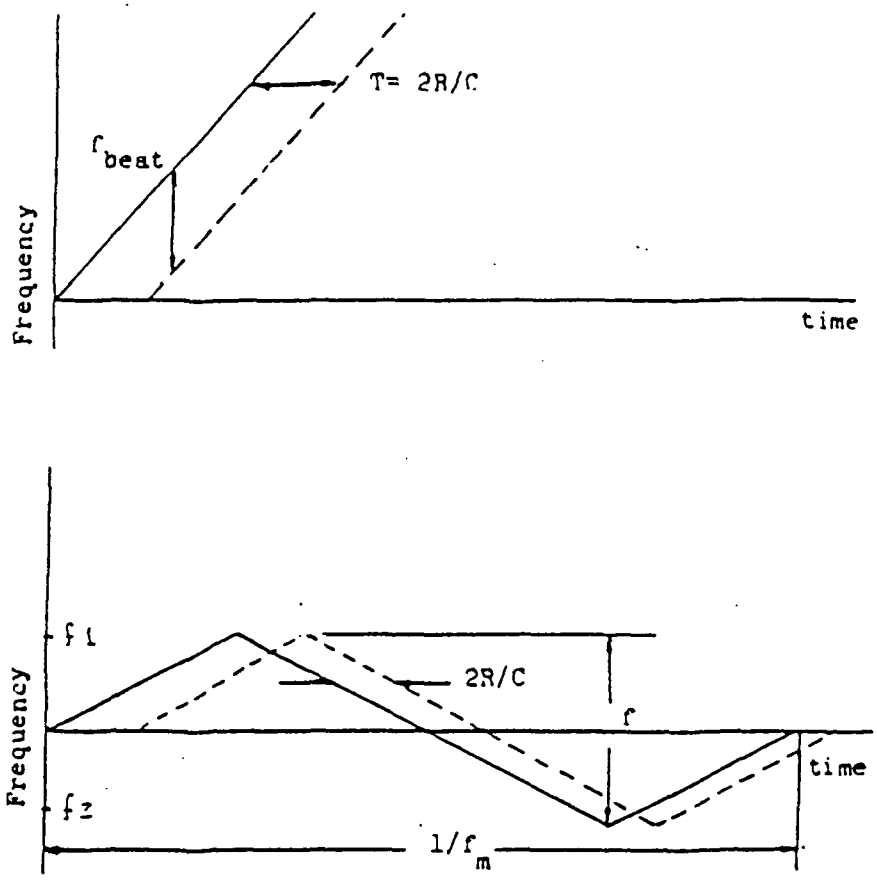

Figure A-2. Signal Characteristics of FM Pulse Radar System.

higher frequencies at the trailing edge of the pulse relative to the lower frequencies at the leading edge so as to compress the pulse to a width 1/B, where b = f2-f1. The peak power of the pulse is increased by the pulse compression ratio BT after passing through the filter.

The method of pulse compression is not limited to frequency and amplitude pulse compression. Other methods applied in various different radar systems are phase coded, non-linear FM, discrete frequency-shift, polyphase codes, compound Barker codes, and numerous others [1]. The technique employed in the design implementation of the RPS is the linear FM pulse compression. This is chosen because a long pulse can be utilized to achieve large radiated energy, but also simultaneously obtaining the range resolution of a short pulse. It is also intended that the RPS is designed differently such that data collected by the system could be compared against data obtained by other FMCW radar systems. Thus, the relevant issue is whether there will be variations in the data obtained by radar systems employing different design implementations.

The Matched Filter Concept

The basic idea of matched filtering evolved from the effort to obtain a better theoretical understanding of the factors leading to optimum performance of radar systems. The technique of matched filtering in essence constitutes the optimum linear processing of radar signals. This type of signal processing transforms the raw radar data that are received into a form that is suitable for performing optimum detection decisions or for estimating target parameters with minimum root mean square (rms) errors.

The characteristics of matched filter can be identified by either its representation in the frequency domain or in time domain, each of which are related by a Fourier transform operation [27]. In its frequency domain representation, the transfer function of the matched filter, H(w), is the complex conjugate function of the spectrum of the signal to be processed optimally. In general, the transfer function is

$$H(w) = aF^{\cdot}(w)\exp(-jwt_0) \qquad (A\text{-}1)$$

where F(w) is the spectrum of the input signal f(t), and t is an arbitrary delay constant of the filter. The normalizing factor a and the delay constant are generally ignored, thus the expression becomes

$$H(w) = F^{*}(w) \qquad (A\text{-}2)$$

The time domain representation is found from the inverse Fourier transform of H(w). This leads to the result that the impulse response of the filter is the copy of the time inverse of the known signal function. Thus, if h(t) represents the filter impulse response, the general relationship equivalent to the representatin of H(w) is

$$h(t) = af(t_0 - t) \qquad (A\text{-}3)$$

As mentioned earlier, the arbitrary delay term, t_0, can be ignored such that the relationship becomes

$$h(t) = af(-t) \qquad (A\text{-}4)$$

The relationship of the representation of the filter response in frequency and time domain is shown in Figure A3 .

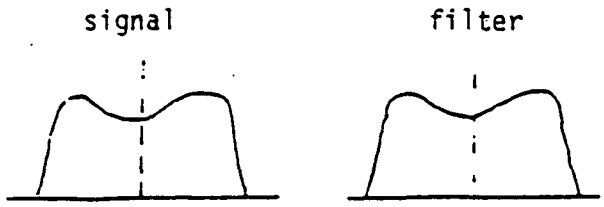

Signal Spectrum in Frequency Domain

Time Domain

Figure A-3. Frequency and Time Representation of the filter Response

Thus, the frequency response function denoted by H(w), expresses the relative amplitude and phase of the output of a network with respect to the input when the input is a pure sinusoid. The magnitude of H(w) denotes the receiver amplitude passband characteristic. If the bandwidth of the receiver passand is wide compared to that occupied by the signal energy, extraneous noise is introduced by the excess bandwidth, which lowers the output signal-to-noise ratio. However, if the receiver bandwidth is narrower that the bandwidth occupied by the signal, the noise energy is reduced, along with a considerable part of the signal energy. The result of this is also a lowered signal-to-noise ratio. Thus there is an optimum bandwidth at which the signal-to-noise ratio is maximum. In pulse radar systems, as in the case for the RPS, the receiver bandwidth should be approximately equal to the reciprocal of the pulse width.

The receiver frequency response function is the output of the IF section in the RPS. The video portion of the detection will have negligible effect on the output signal-to-noise-ratio if the receiver is designed as a matched filter. The matched filter concept is implemented in the RPS, specifically in the receiver of the IF section, to obtain a frequency-response function that maximizes the output peak-signal-to-noise ratio.

APPENDIX B

THE SATURATION ANALYSIS OF THE RECEIVER SECTION OF THE IF SUB-ASSEMBLY OF THE RPS

The purpose of the power or saturation analysis in the If section is to deterine if any of the components or the amplifiers in particular will operate in their saturation region when different levels of signals are imposed at the input.

The approach is to define a set of input signal which has the characteristics of being maximum, minimum, or typical values. The analysis is done upon reviewing the specifications on the individual components. With the aid of block diagrams, the analysis will proceed from one component to the other.

The illustrations in figure B1 to B2, including the illustrations in between them will describe the saturation analysis of the receiver section.

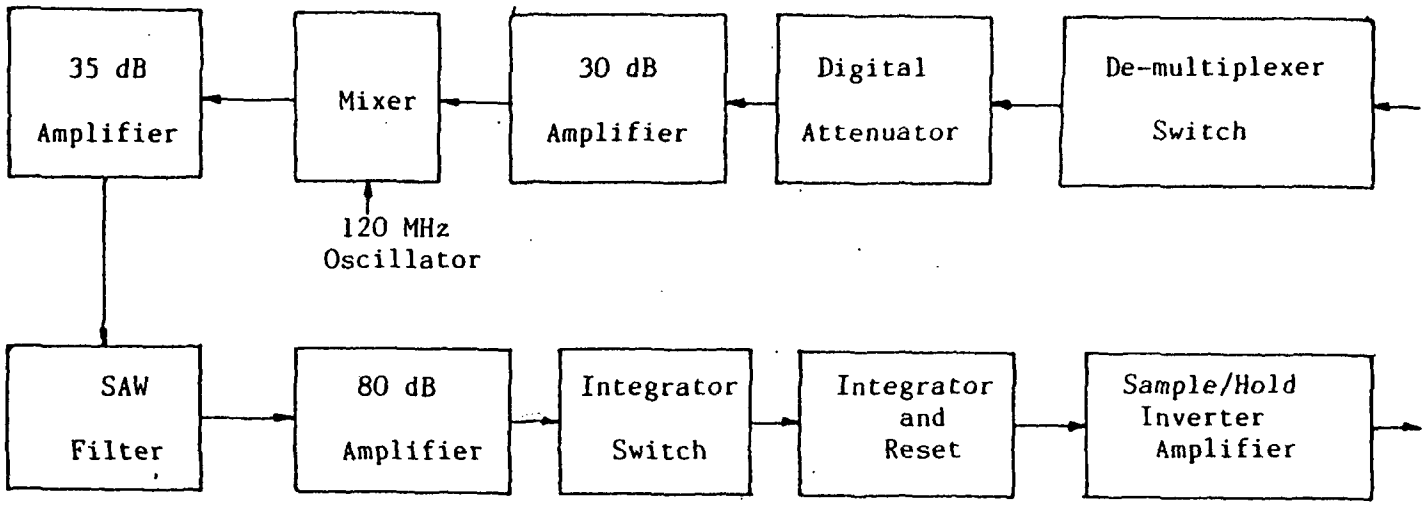

Figure B1 - The block diagram of the receiver section

The power calculation is performed with the aid of figures ofcomponents that are of interest.

80 dB IF amplifier:

It is desirable to operate the 80 dB amplifier just under saturation to get the maximum output level possible. This will increase the S/N ratio which in turn will increase accuracy. The input to the amplifier is specified to be -66 dBm according to its specifications.

Signals are written in units of dBm, and losses in the cable are assumed to be about 0.4 dBm per foot length.

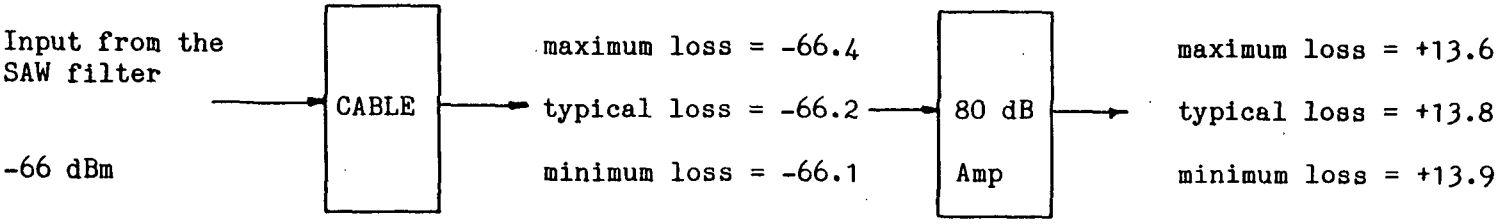

Integrator Switch:

The equivalent model for the integrator switch when it is in the "on" state is shown below.

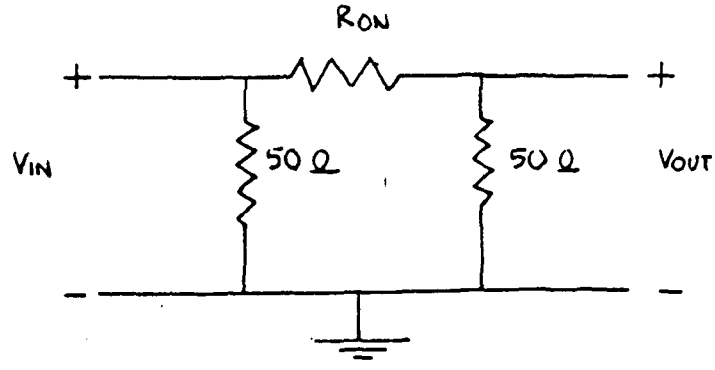

The "on" resistance of the integrator is specified to have the value of 20 Ohms minimum, 35 Ohms typically, and 50 Ohms maximum. The transfer function of the output/input can be found to be:

$$\frac{V_{OUT}}{V_{IN}} = 1 - \frac{R_{ON}}{50 + R_{ON}} \qquad \text{(B-1)}$$

The input level to the integrator is in the range of a minimum of 0.5 Volts to a maximum of 0.78 Volts. The voltage coming into the switch circuitry can be calculated from equation (8-1). The result is that the maximum voltage is 1.1 Volts and the minimum is 1.0 Volts. This voltage level will not place the switch in saturation.

Input from the
80 dB amplifier

maximum loss = 13.6 dBm

typical loss = 13.8 dBm

minimum loss = 13.9 dBm

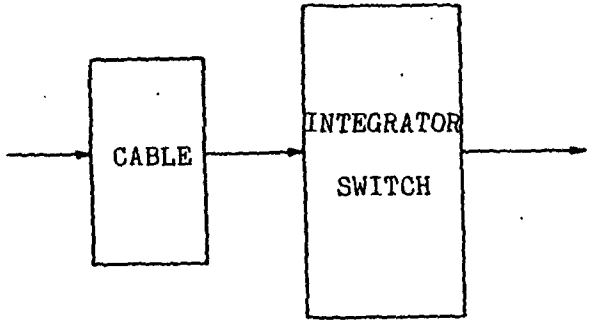

Output from the integrator circuit

maximum loss = +7.2 dBm = +0.5 V

typical loss = +9.0 dBm = +0.63 V

minimum loss =+10.9 dBm = +0.78 V

SAW FILTER:

Input level from
the 35 dB amplifier

Maximum loss = -20.9 dBm

typical loss = -20.8 dBm

minimum loss = -20.6 dBm

Output level to the 80 dB amplifier

The desired level is

about -66 dBm

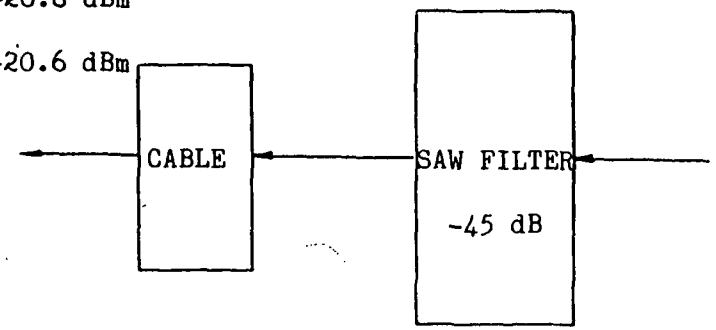

35 dB amplifier:

From the specifications for the 35 dB amplifier, the maximum output level is +5 dBm with a 35 dB of gain. This means that the maximum input level is -30 dBm. As shown in this calculation, the 35 dBm amplifier will not go into saturation under the worst case condition.

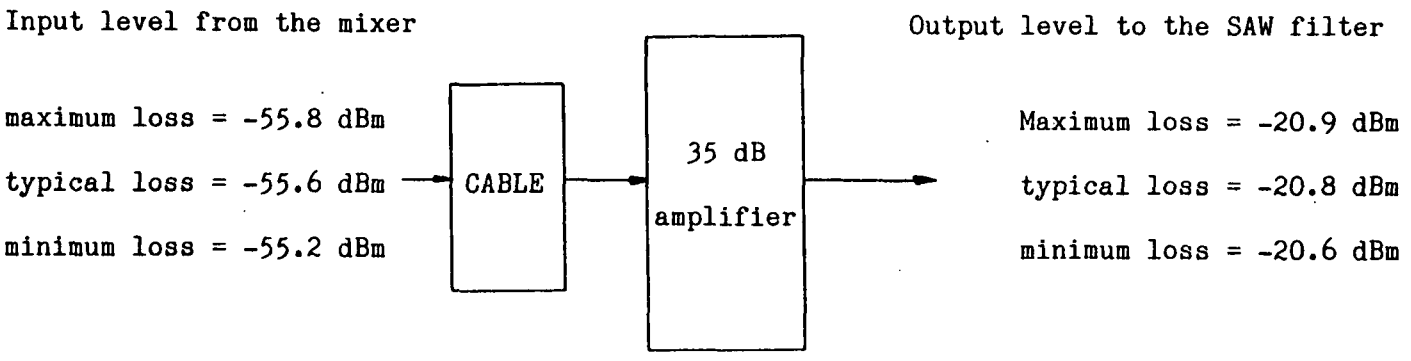

Mixer:

With the maximum input level specified to be at +1 dBm, there is no danger of the mixer operating in the saturation region.

From the 30 dB amplifier

maximum loss = -49.4 dBm

typical loss = -49.3 dBm

minimum loss = -46.3 dBm

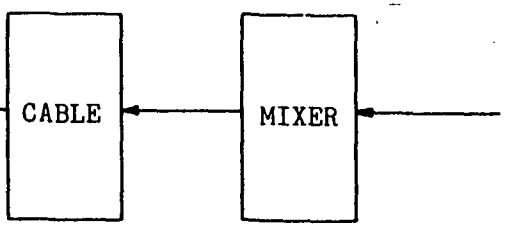

from the 35 dB amplifier

maximum loss = -55.8 dBm

typical loss = -55.6 dBm

minimum loss = -55.2 dBm

Note that the mixer has a conversion loss of -8.5 dBm for maximum value and -6.5 dBm for minimum value.

30 dB amplifier:

From the specification for the 30 dB amplifier, the maximum output level is 0 dBm with a 30 dB of gain. The maximum input level can be calculated by subtracting the maximum output level by the gain. The maximum input level calculated is then -31 dBm. As seen from the calculation, there is no danger of saturating the amplifier.

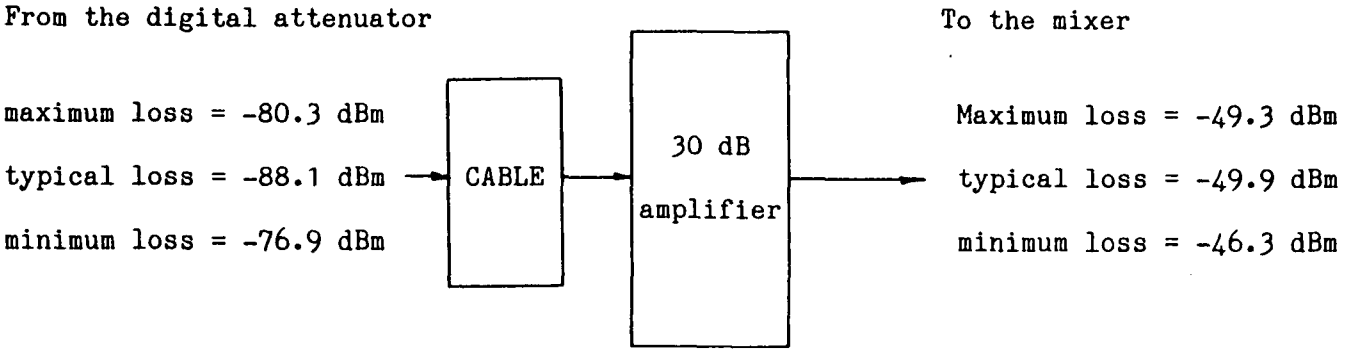

De-multiplexer switch:

The de-multiplexer switch is made up of two single pole double throw (SPDT) transfer switches connected as shown in the next page.

Input level at the receiver section

maximum loss = -80 dBm

typical loss = -49 dBm

minimum loss = -18 dBm

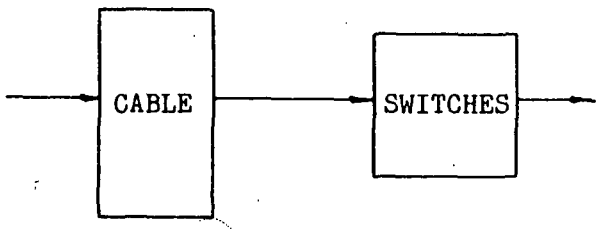

Output level to the attenuator

maximum loss = -81.2 dBm

typical loss = -49.6 dBm

minimum loss = -18.3 dBm

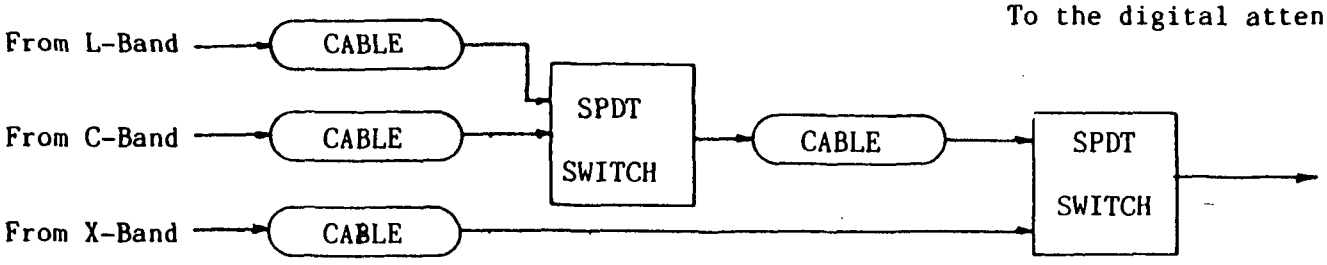

Figure B2- The connection diagram for making the de-multiplexer switch from the two SPDT transfer switch

APPENDIX C

EXPLANATION OF NOISE FIGURE AND THE SIGNAL TO NOISE RATIO CALCULATION FOR THE IF SECTION IN THE RPS

This appendix provides an explanation of the noise figure concept. From the noise figure, a calculation of the signal-to-noise ratio (SNR) in the IF sub-assembly of the RPS may be performed.

The signal level required to produce a satisfactory output from a detection system is limited by the amount of noise that is generated within the system. This noise energy might be produced by active and passive system components. Some noise that exist in the environment could not be controlled. However, noise produced in the detection and amplification process can be minimized by proper design and component selection.

The random motion of electrons in conductors constituting the circuitry of the detection system produces small voltage and current fluctuations within all system components. These fluctuations are commonly referred to as thermal or "Johnson" noise. The overall effect of various noise sources in a receiver system is commonly specified in terms of a noise figure. The noise figure is a figure of merit of the receiver at room temperature, taking into account the available power ratio and the available noise ratio. The noise figure which is usually denoted by F, is defined as the ratio of the available SNR at the input

to the available SNR at the output. If the receiver or amplifier did not introduce additional noise into the system, the expression for F will become unity.

The determination of the SNR of the receiver section in the RPS will be based upon the specifications of the individual components. The following examples will show the procedures by which the analysis of the SNR in the receiver section will be performed.

Given two amplifiers which are cascaded, a total noise figure can be calculated. From this, the SNR could be obtained.

Define:

F = noise factor (linear)

NF= noise figure

= 10 x log (F)

G = gain of the amplifier

For calculation purposes, let Fx = 4.2, Fy = 4.0, and Gx = 8.0 The total noise factor of a cascaded amplifier system may be written as:

$$Fxy = Fx + \frac{Fy - 1}{Gx} \qquad (C\text{-}1)$$

$$= 4.575$$

To get the noise figure expression,

$$NF = 10 \times \log Fxy \qquad (C\text{-}2)$$

$$= 6.6 \text{ dB}$$

If the input at stage x had a power of 10 Watts, and the operating bandwith and temperature is 1 MHz and 290 K, the SNR of the system can

be calculated as follows.

$$\text{Power of input noise} = k \times T \times f \qquad \text{(C-3)}$$

where : k = the Boltzmann's constant

T = operating temperature

f = operating bandwidth

So, the power of input noise = $1.38 \times 10^{-8} \times 290 \times 10^{6}$

$= 4 \times 10$ Watts

The ratio of the output signal to the power of input noise is

$$\frac{\text{Psignal out}}{\text{Pnoise out}} = \frac{\text{Psignal in}}{\text{FxPnoise in}} \qquad \text{(C-4)}$$

$$= 5464.5$$

$$\text{The SNR} = 10 \times \log (5464.5) \qquad \text{(C-5)}$$

$$= 37.4 \text{ dB.}$$

For the integrator circuit in the IF sub-assembly, the dominating noise factor will be the thermal noise. The thermal noise can be calculated as

$$\text{Noise} = E^2 = 4 \times R \times k \times T \times B \qquad \text{(C-6)}$$

where R is the resistive component of the system

k is the Boltzmann's constant = 1.38×10^{-23}

T is the operating temperature in degrees Kelvin

B is the bandwidth of the system

The expression of noise figure and SNR as discussed previously are in terms of power in decibel. To convert a voltage expression into a power expression, it is done as follow.

$$P \text{ (milli Watts)} = V / 0.05 \qquad \text{(C-7)}$$

The SNR Analysis

The performance of the IF section will be determined by its SNR. SNR is defined to be the ratio of the signal amplitude to the noise amplitude that exists in a system. The ratio will be obtained based on the given noise figure of the components in the IF section. By definition, noise figure is the ratio of the noise power output of the system to the noise power output which would be obtained in the same bandwidth if the only source of noise were the thermal noise in the internal resistance of the signal source. Thus, the noise figure is a quantity which compares the noise in an actual amplifier with that in an ideal or noiseless amplifier.

The components considered in the analysis are listed in Table C-1. The mixer is assumed to have a noise figure of 9. The following will present the mathematical steps leading to the SNR of the system.

After the attenuation step, (see the block diagram in Figure C-2), the input is assumed to be -85 dBm signal to be the worst case. The expected average value is -77 dBm typically. From the 30 dB amplifier through the mixer, the noise figure is calculated as follows:

From equation (C-1), F total $= 1.58 + \frac{7.94-1}{1000}$

$= 1.5918$

From equation (C-2), NF $= 10 \log (1.5918)$

$= 2.02$ dB

Continuing the path to the 35 dB amplifier,

$$F \text{ total} = 1.59 + \frac{1.98-1}{1000} = 1.591, \quad NF = 2.02 \text{ dB}$$

PARTS	GAIN (dB)	GAIN (W/W)	N.F. (dB)	N.F. (W/W)
30 dB amplifier RHG ICFT 6040	30	1000	2.0	1.585
35 dB amplifier Amplica AVD714201	35	3162.27	1.7	1.479
80 dB amplifier RHG EVT60G11DM	80	1 x 10	2.0	1.585
Mixer Mini Circuit ZLW13			9.0	7.943

The mixer has a conversion loss that is being cosidered which is more dominant that that of the Noise Figure (NF). The quantity of gains that are presented are of power gain.

Figure C-1. Specifications of the Parts in the Receiver Section Considered in the Noise Analysis

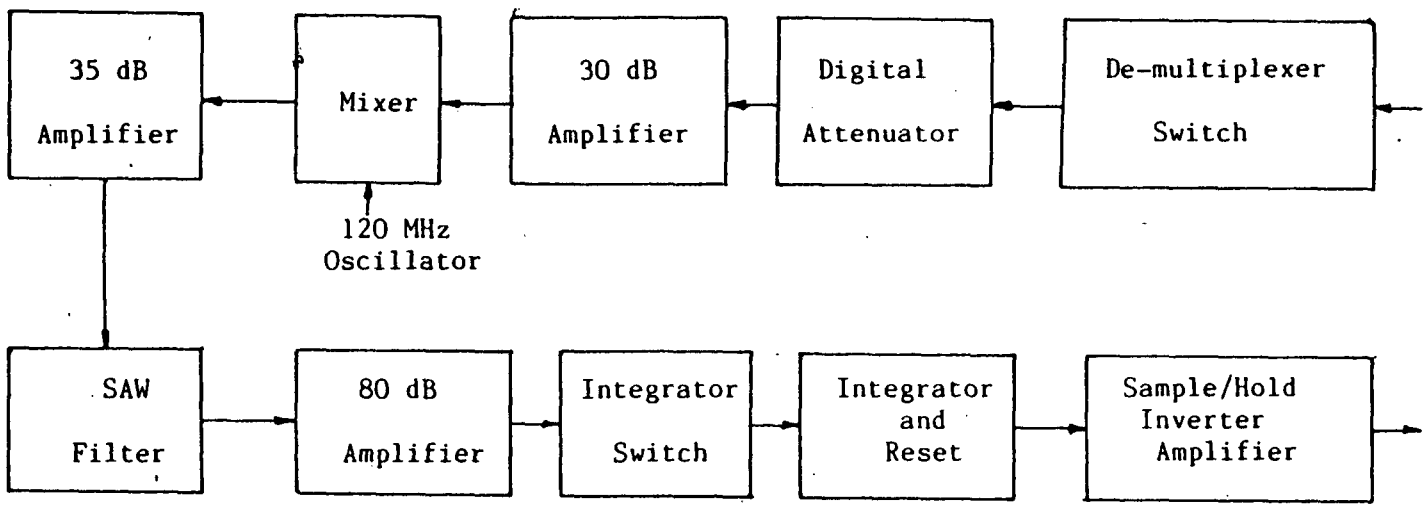

Figure C2 - The block diagram of the receiver section

The noise figure is unchanged as signals are passed through the Surface Acoustic Wave (SAW) filters. From the SAW filter to the 80 dB amplifier,

$$F_{total} = 1.591 + \frac{1.58-1}{100}$$

$$= 1.587$$

$$NF = 2.033 \text{ dB}$$

The integrator circuitry can be modeled as shown in Figure C-3. The resistive component is the 50 Ohms that is seen looking into the circuit. The dominating noise in the circuit is the thermal noise. Thus, from equation (6-6), the generated noise is:

$$E = 4 \times 50 \times k \times 40 \times 10$$

$$= -81.8 \text{ dBm}$$

At this point, the signal power is -1.1 dBm as calculated from the power analysis. A -81.8 dBm noise is negligible compared to -1.1 dBm. Thus the total noise figure of the receiver section is calculated to be 2.033 dB. The input power noise to the system can be calculated using equation (C-3) as follows:

$$P_{input\ noise} = 1.242 \times 10 \text{ Watts}$$

By using equations (C-4) and (C-5), the SNR of the receiver section can be calculated at different input signal levels.

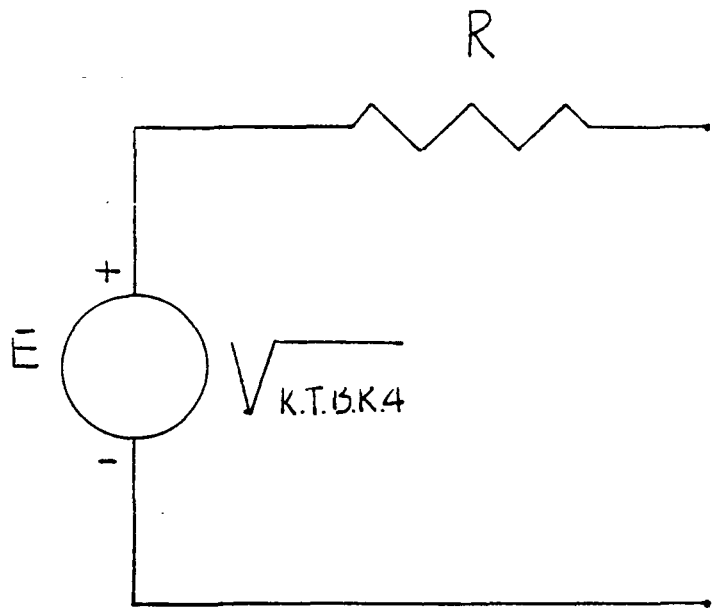

Figure C3- The Model of the Integrator Circuit

For a -80 dBm input signal, the SNR = 17.03 dB

For a -85.2 dBm input signal, the SNR = 11.8 dB

For a -76.9 dBm input signal, the SNR = 20.04 dB

For the worst input signal condition, the SNR of the receiver section is 11.8 dB. Referring to the design specification of the RPS, the SNR at those signal levels is within acceptable values.

APPENDIX D

FLOW CHART OF THE COMPUTER ALGORITHM FOR DATA REDUCTION

This appendix contains the algorithm of computing the average values of incoming radar cross section readings utilizing both methods of linear and logarithmic averaging.

As indicated in the flow-chart, data that are to be reduced must be in a form of a file that is previously determined as to how large it is, and how the data is written in the file. Referring to the sub-process that is termed the acquisition of data point, this process involves the computer to read numbers in in such fashion that they can be placed in the equation of radar cross section as given in equations 3-9a and 3-9b.

Such numbers are the attenuator setting when in calibration mode, and when in operation mode, along with system constants. These are the numbers that are being stored temporarily on a file for which the algorithm will then reduce into cross section values. A scheme will have to be obtained to manipulate the readings of these numbers such that the algorithm could be implemented.

After the process of the reduction, the algorithm then continues with the averaging process. This could be done linearly or logarithmically.

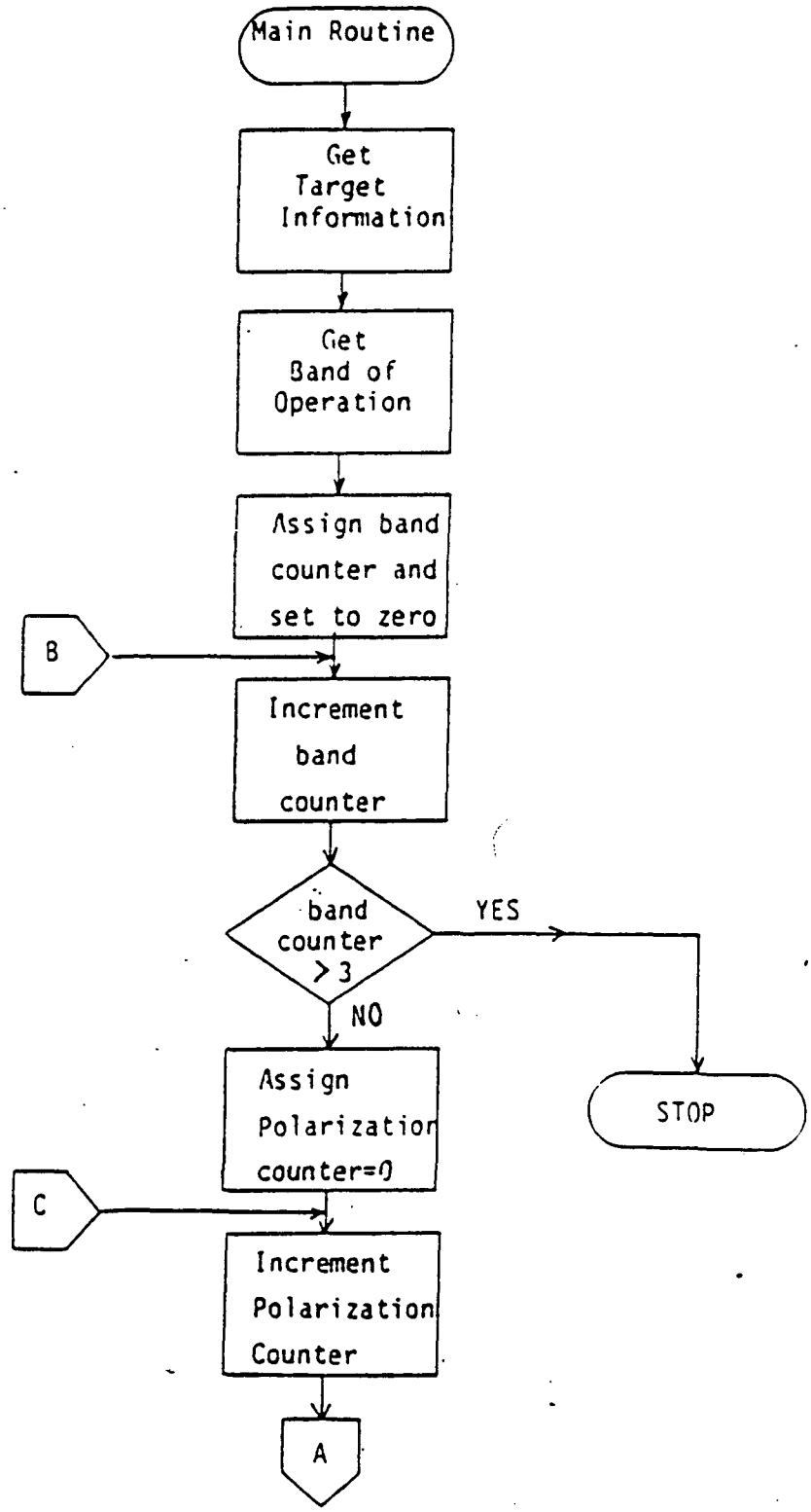
Main Routine
Get Target Information
Get Band of Operation
Assign band counter and set to zero
B
Increment band counter
band counter > 3
YES
NO
STOP
Assign Polarization counter=0
C
Increment Polarization Counter
A

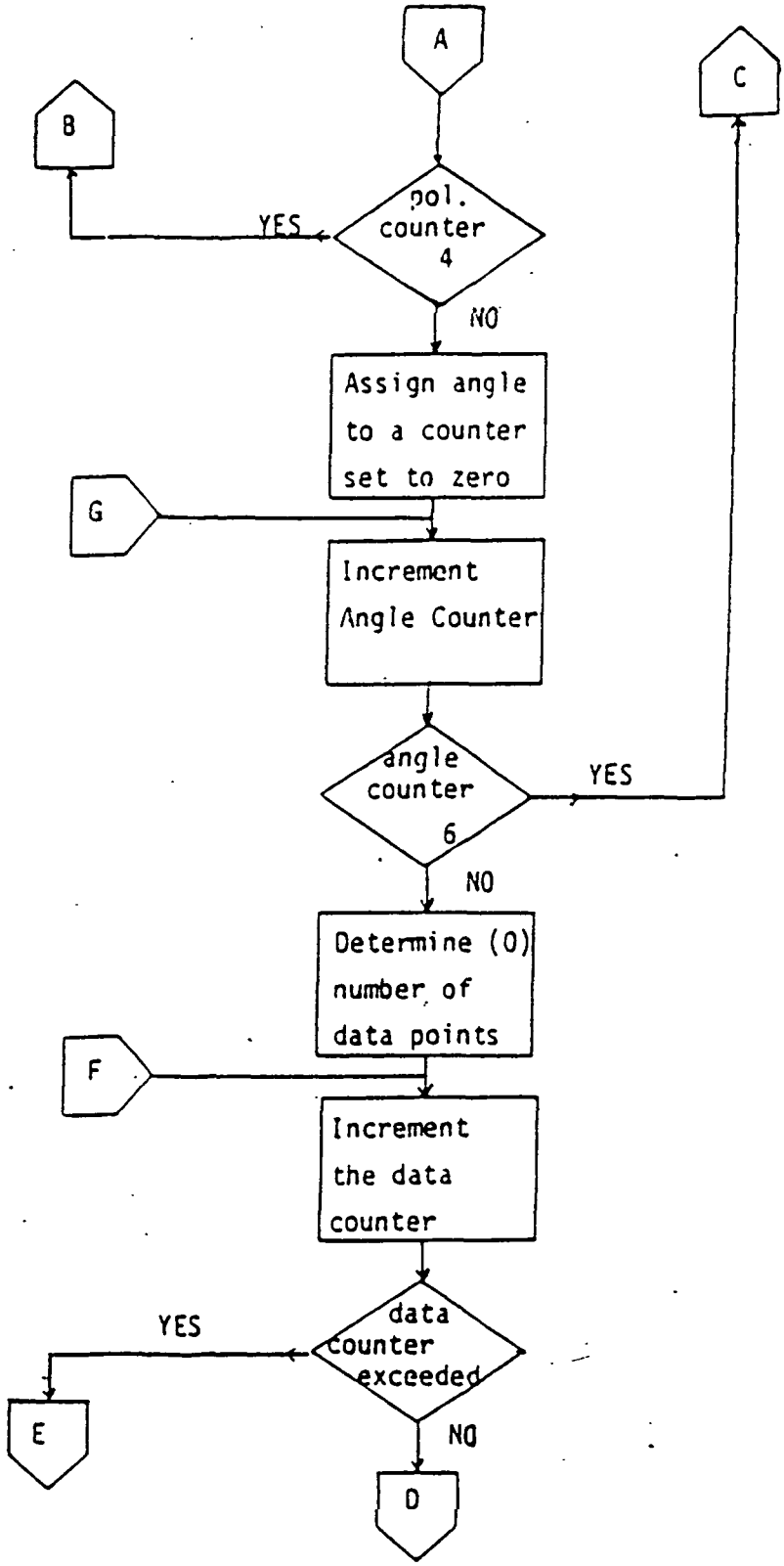
A
B
C
pol. counter 4
YES
NO
Assign angle to a counter set to zero
G
Increment Angle Counter
angle counter 6
YES
NO
Determine (0) number of data points
F
Increment the data counter
data counter exceeded
YES
NO
E
D

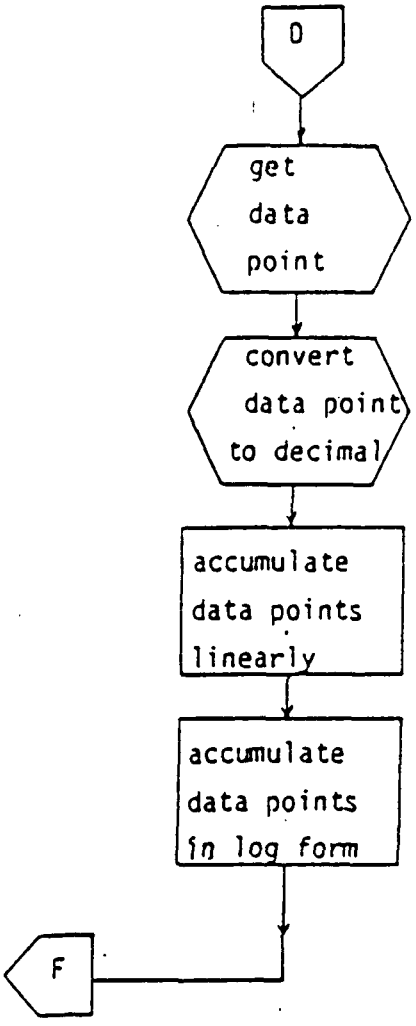
D
get
data
point
convert
data point
to decimal
accumulate
data points
linearly
accumulate
data points
in log form
F

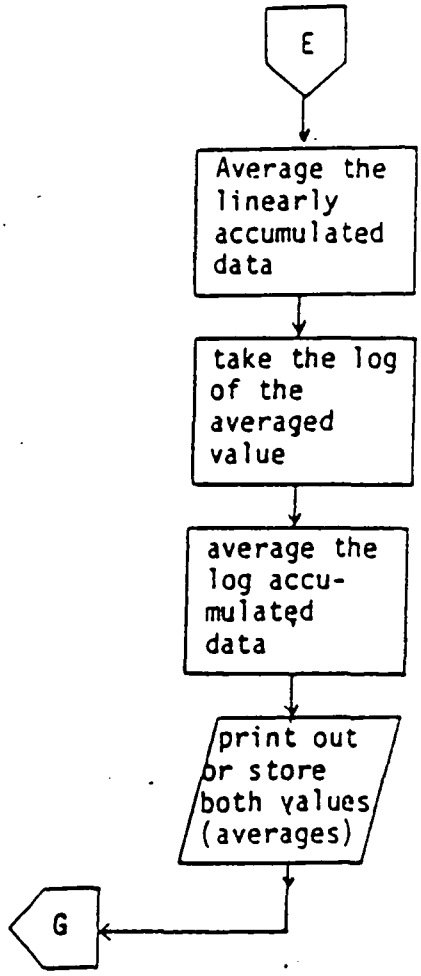
E
Average the linearly accumulated data
take the log of the averaged value
average the log accu-mulated data
print out or store both values (averages)
G

The REMOTE SENSING CENTER was established by authority of the Board of Directors of the Texas A&M University System on February 27, 1968. The CENTER is a consortium of four colleges of the University; Agriculture, Engineering, Geosciences, and Science. This unique organization concentrates on the development and utilization of remote sensing techniques and technology for a broad range of applications to the betterment of mankind.